

ELECTRON DONATING PROPERTIES AND CATALYTIC ACTIVITY OF RARE EARTH OXIDES

THESIS SUBMITTED TO THE
COCHIN UNIVERSITY OF SCIENCE AND TECHNOLOGY
IN PARTIAL FULFILMENT OF THE REQUIREMENTS
FOR THE DEGREE OF
DOCTOR OF PHILOSOPHY
IN
CHEMISTRY

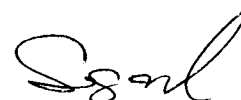
By
K. B. SHERLY

DEPARTMENT OF APPLIED CHEMISTRY
COCHIN UNIVERSITY OF SCIENCE AND TECHNOLOGY
KOCHI - 682 022, INDIA

AUGUST 1993

CERTIFICATE

This is to certify that the thesis is bound herewith is the authentic record of research work carried out by the author under my supervision in partial fulfilment of the degree of Doctor of Philosophy and no part thereof has been presented before for any other degree.



Dr.S.SUGUNAN
(Supervising Teacher)
Professor in Physical Chemistry
Department of Applied Chemistry
CUSAT

Kochi-22
16th August 1993

DECLARATION

I hereby declare that the work presented in this thesis is based on the original work done by me under the guidance of Dr.Sugunan, Professor in Physical Chemistry, Dept. of Applied Chemistry, CUSAT, Kochi-22 and no part of this thesis has been included in any other thesis submitted previously for the award of any degree.



K.B.SHERLY

Kochi-22
16th August 1993

CONTENTS

| | Page No. |
|--|------------|
| CHAPTER 1 INTRODUCTION | 1 |
| References | 14 |
| CHAPTER 2 SURFACE ELECTRON PROPERTIES | 18 |
| Electron donor-acceptor properties | 19 |
| Solid acids and bases | 24 |
| Catalytic activity & acid-base properties | 29 |
| References | 37 |
| CHAPTER 3 EXPERIMENTAL | 44 |
| Materials | 45 |
| Methods | 51 |
| References | 54 |
| CHAPTER 4 RESULTS AND DISCUSSION | 56 |
| References | 148 |
| CONCLUSION | 150 |
| LIST OF PUBLICATIONS | 152 |

INTRODUCTION

The rare earth group of elements, also called the lanthanides refers to the 14 elements following lanthanum in the periodic table, but as normally used also includes lanthanum itself [1]. From lanthanum ($Z=57$) to lutetium ($Z=71$) we go from a $[\text{Xe}]4f^0$ to $[\text{Xe}]4f^{14}$ configuration. Since the 4f electrons are relatively uninvolved in bonding, these highly electropositive elements have as their prime oxidation number +3 and, closely resemble one another chemically and physically. They generally occur together in nature.

The element yttrium, Y, ($Z=39$), which lies above La, has atomic and ionic radii close to those for terbium and dysprosium. It therefore resembles them closely in its chemistry and is generally found in nature with the lanthanides. The lanthanides plus yttrium are commonly called the rare earths, although many of them are relatively abundant. Lanthanum, cerium and neodymium are all more abundant than lead.

The use of rare earths as promoters or supports in catalytic reaction has grown extensively in the past few years, due to interesting properties encountered in automotive pollution control by catalysis or syngas conversion [2,3]. In catalysis by automotive pollution control, the reducibility of some of the rare earth oxides (eg. CeO_2) have been put forward to explain the increase in performance of rare earth modified catalysts [4]. In fact it seems that the easy reduction of ceria dispersed on such catalysts is favoured by the presence of a transition metal and increases the oxygen storage capacity of the catalyst [5]. Thus the rare earth oxides can store the oxygen

during the oxidative step of the exhaust cycle and remove it during the reductive step, thereby broadening the acceptance window of the air to fuel ratio. In syngas conversion, the situation is more complicated as both the reducibility and basicity properties of the rare earth oxides have been invoked.

Recent studies have demonstrated that several of the lanthanide sesquioxides (M_2O_3) are effective catalysts for the oxidative coupling of methane to ethane and ethylene [6]. Lanthanum oxide, for example, is capable of activating CH_4 by hydrogen atom abstraction, and the resulting CH_3 radicals enter the gas phase where they may undergo subsequent coupling reactions [7]. In an attempt to identify the active site for this hydrogen atom abstraction, the catalyst was quenched from 650 to -196°C , and the presence of superoxide ions were detected by EPR spectroscopy. These ions are believed to be formed by the reaction of O_2 either with thermally generated electron-hole pairs or with surface peroxide ions.

The rare earth oxides exhibit activity as oxidation catalysts [8] and have low work functions (approximately 2.7 eV) [9]. Thus they have both of the required attributes as negative surface ionisers (NSI). NSI is the process where a negative ion is sublimed from a solid surface and is efficient when the work function of the surface is close to or less than the electron affinity of the subliming negative ion. An additional requirement is that the chemistry on the surface of the ionizer be capable of preforming the chemical species that has the high electron affinity (atom or molecule). This preformed species may actually reside on the surface in an ionic state, although this is not well understood. Thus, systems which chemisorb a high electron affinity atom or molecule prior to desorption are in general more efficient ionizers for

that particular species. If an atomic or molecular species with a suitable electron affinity strikes a low work function surface, then no chemical reaction is required to produce the negative ion, and NSI (basically charge exchange) can proceed with a single collision, provided the thermodynamics are favourable.

Rare earth oxides can function as catalytic oxidizers to produce oxide species that have relatively high electron affinities and they can provide a low work function surface which helps to ionize the subliming molecules or perhaps, to allow the preformed ions to escape more easily from the surface as ions. Rare earth oxides are also refractory materials. This combination of properties presents an opportunity to study the oxidation of metallic rhenium, using rare earth oxides as catalysts, by observation of the rhenium oxide negative ions.

Fundamental catalytic and surface properties of alkali, alkaline earth and other basic oxides have been extensively studied and documented [10]. Equivalent information about the series of basic rare earth oxides is fragmentary. This family of refractories resembles the alkaline earth oxides in many respects, but offers a unique opportunity to study the effect of smoothly varying periodic trends on catalytic behaviour. In particular, the gradual decrease in trivalent ionic radius, and consequent increase in ionic charge density, in going from La^{3+} (1.06 Å) to Lu^{3+} (0.85 Å) results in a corresponding decrease in basicity of the sesquioxides (M_2O_3) across the series [11]. Furthermore, with only few irregularities, the effect of this basicity trend on catalytic properties can be assessed independently of other electronic and solid-state parameters, such as d-electron configuration, crystal structure and preferred stoichiometry, which are largely invariant through out the oxide series. All Ln^{3+} ions, for example, lack 5d electrons and differ

from each other electronically only in respective configuration of highly shielded 4f electrons. Systematic correlations, however, between surface basicity and catalytic properties among the rare earth oxides have been explored to only a limited extent.

Catalytic behaviour of rare earth oxides have been explored for many reactions and a wide variety of catalytic properties have been known [12]. Empirical studies have demonstrated that, following appropriate pretreatment, rare earth sesquioxides are active catalysts for a variety of reactions, including *ortho/para* hydrogen conversion [13], deuterium exchange reactions of hydrocarbons [14], H₂-D₂ equilibration [15], alcohol dehydration [16], olefin isomerization [17], decomposition of N₂O and NO [18,19] and oxidation reactions of hydrogen [20], carbon monoxide [21] and hydrocarbons [22,23].

By measuring the activities for the low temperature hydrogenation of ethylene for the entire lanthanum series of rare-earth oxides it is possible to estimate the role of pretreatment on the catalyst and it revealed a connection between catalytic activity and basicity of the oxide [24].

In the last several years, however, it has been found in a series of the catalytic oxidations that the catalytic activity of the lanthanide oxides significantly differ from each other. Sazonov and co-workers [25] measured the activation energies of the isotopic exchange of oxygen and of the desorption of carbon dioxide in the oxidation of carbon monoxide and found that the dependence of the activation energies on the atomic number was similar to that of the magnetic moment. Minachev [26] compared the catalytic activity in the oxidation of hydrogen and propylene

with that in the isotopic exchange of oxygen and suggested that the catalytic activity depends on the binding energy of oxygen with the surface and on the values of the lanthanide ions. Bakumenko and Chashenikova [27] found in the oxidation of hydrogen that activity of neodymium and erbium oxides were lower than cerium, praseodymium and terbium oxides with the tetravalent ion, which was explained on the basis of the heat of formation of oxide. Lazukin and co-workers [28] found a good correlation between the activation energy of the oxidation of propylene and that of the electrical conductivity and concluded that the electron transfer from the reactant or the intermediate to the catalyst surface is involved in the rate determining step. Some of the authors [25,26] suggested from these results that the catalytic activity of the lanthanide oxides depend on the electronic configuration of the inner 4f subshell.

The catalytic oxidation of butane was studied over a series of lanthanide oxides in order to investigate the effect of the electronic configuration on the catalytic activity [29]. Lanthanum oxide was one of the least active catalysts. Cerium oxide was the most active one and the activity decreased with an increase in the atomic number from cerium to gadolinium. The activity of terbium oxide was the second highest, and again the activity decreased from terbium to lutetium. Such a dependence of the activity on the atomic number was in good agreement with the electrical conductivity, and in fair agreement with the heat of formation of oxide. The dependence of the electrical conductivity and the heat of formation could be related to the stability of the tetravalent ion, to which the catalytic activity also could be related by assuming that the rate determining step is the oxidation of the trivalent ion to the tetravalent ion. A good correlation was obtained between the catalytic activity and the fourth ionization potential as a measure of the stability of the tetravalent ion relative to the trivalent ion. On referring to the correlation,

the dependence of the catalytic activity on the atomic number was interpreted in terms of two factors based on the electronic configuration of the 4f subshell, ie, the coulomb attraction energy between Xe shell and the 4f electron and the exchange energy between the 4f electrons.

The catalytic activity of rare earth oxides for simple reactions show patterns which broadly resemble each other and also reactions in which the number of 4f electrons changes [30]. If simple concepts of electron transfer are augmented, it emerges that any rate controlling step which involves the adsorption of a species by electron transfer to it, leads to an activity pattern with maxima for f^0 , f^7 and f^{14} structures. Rare earth oxides are hardly reducible. La_2O_3 and Ce_2O_3 , for example, remain trivalent oxides after treatment in hydrogen at 673K and Lu_2O_3 generates divalent ions even at 823-973 K by treatment in hydrogen. This character is suited for the catalyst support which is applied under reducing atmosphere. The addition of Dy_2O_3 , Nd_2O_3 , Yb_2O_3 , La_2O_3 or Gd_2O_3 to the $\text{Rh-Al}_2\text{O}_3$ catalyst enhanced the activity of the hydrogenation of CO to methane. There was the linear relationship between the carbon skeleton propagation of the hydrocarbons formed and the basicity of the rare earth oxides [31].

Because of their high melting points, rare earth oxides are superior in thermal stability to catalysts containing low melting metal oxides/salts for the methane coupling process [32].

Otsuka *et al.* [33,34] observed that among the rare earth oxides, Sm_2O_3 shows highest activity and selectivity for C_2 - hydrocarbons in the oxidative coupling of methane. Whereas Campbell *et al.* [35] have found that for hydrothermally treated rare earth oxides, La_2O_3 shows

much higher activity than Sm_2O_3 in catalytic production of gas-phase methyl radicals from methane and also in oxidative coupling of methane. However, in both the studies, CeO_2 showed very low activity/selectivity in the methane coupling process. It was pointed out that the relative activities of rare earth metal oxides parallel their basicities [36]. It is, therefore, very interesting to know quantitatively the surface basicity and base strength distribution on rare earth oxides.

Oxygen (site and isotope) exchange reactions over well outgassed and partially reduced cerium oxide were examined in the temperature range 200-373 K by means of FT-IR spectroscopy [37]. Isotopic exchange between gaseous O_2 and lattice oxygen of the cerium oxide does not occur at the temperature below 373 K. Site exchange via gaseous O_2 with adsorbed superoxide (O_2 ads) species was found to be very fast on both the outgassed and partially reduced surfaces even at 200K, but site exchange between gaseous O_2 and adsorbed peroxide (O_2 -ads) species does not take place in the temperature range 200-373K. Here the isotope exchange reaction proceeds via adsorbed superoxide species and the exchange reaction is presumed to involve a tetraoxygen intermediate as a result of the reaction of gaseous O_2 with adsorbed superoxide species.

The reduction of methyl benzoate and benzoic acid on a Y_2O_3 catalyst under hydrogen has been examined by using an infrared spectroscopic flow reactor at 250 -450°C [38]. The formation and reduction of surface benzoate was monitored by infrared spectroscopy. Surface methoxide formation was also observed during the methyl benzoate reaction. The experimental evidence indicates that the benzoic acid and benzoate esters are reduced to benzaldehyde via the surface benzoate. Hydrogen is transferred from the gas phase to the final product by surface hydroxyl groups.

Temperature programmed desorption (TPD) and ^{18}O -tracer techniques have been adopted to examine the contribution of the lattice oxygen atoms (oxide ions) of praseodymium oxide, Pr_6O_{11} , to the oxidation of carbon monoxide [39]. The TPD measurements revealed that some of the lattice oxygen atoms could be removed (reduced) by CO forming CO_2 . However; the oxygen vacancies formed by the reduction were continuously filled with oxide ions, if oxygen were coexisted in the gaseous phase. Most of the carbon dioxide formed during the reaction of CO with $^{18}\text{O}_2$ over Pr_6O_{11} catalyst was composed of $\text{C}^{16}\text{O}^{16}\text{O}$. These results showed that the lattice oxygen atoms of the praseodymium oxide play an important role in the catalytic oxidation of carbon monoxide. Surface parameters and thermal dehydration/rehydration behaviour of the $\text{La}(\text{OH})_3/\text{La}_2\text{O}_3$ system have been examined with a view toward establishing suitable methods for preparing and characterizing catalytic forms of the rare earth oxides [40]. Relatively nonporous $\text{La}(\text{OH})_3$, prepared by hydrolysis of the pure oxide, undergoes thermal dehydration in two distinct stages. A well defined oxyhydroxide (LaOOH) intermediate, formed by dehydration of the hydroxide at 200°C , decomposes in a second step at 300°C to generate the sesquioxide. A surface carbonate layer on the resulting oxide is only removed completely by subsequent thermal treatment at $700 - 800^\circ\text{C}$. Exposure of the oxide to water vapour at temperatures $< 200^\circ\text{C}$ causes complete rehydration to the trihydroxide, rather than mere formation of surface hydroxyl groups, and results in complete recovery of surface area lost by high temperature sintering. Spectroscopic studies reveal the existence of two structurally dissimilar kinds of bulk hydroxide ions in $\text{La}(\text{OH})_3$, differing in their relative extent of hydrogen bonding and giving rise to infrared bands at 3610 and 3590 cm^{-1} . The latter band corresponds to the less numerous and more strongly bound type of OH^- that is removed during second stage dehydration of the oxyhydroxide. Lanthanum sesquioxide, when properly activated, is an extremely active catalyst for double bond migration and cis/trans rotation in n-butene [41].

This reaction because of its often highly specific structural requirements when occurring on oxide catalysts, affords an opportunity to probe geometric restrictions and limitations on the behaviour of the active sites.

Lanthanum oxide-promoted MgO catalysts show a very high activity, C₂-selectivity and C₂-space time yield and no deactivation in oxidative coupling of methane [42]

The multi-pathway (dehydration/dehydrogenation) conversion of ethanol has been used to investigate the nature and behaviour of catalytically active sites on lanthanum and neodymium sesquioxides [43]. Catalytic reaction data, coupled with infrared spectroscopic characterizations of adsorbed species, indicate that at least two different types of catalytically active sites are generated on activated La₂O₃ and Nd₂O₃ surfaces that are prepared by thermal dehydration of the corresponding trihydroxides. One kind of site (designated Type I) is much less numerous than the other (designated Type II) but is more strongly basic and has a much higher initial activity for alcohol dehydration via a probable ethoxide intermediate, at 300-400°C. The parallel alcohol dehydrogenation pathway, on the other hand, occurs only on Type II sites which also have moderate dehydration activity. The resulting aldehyde product readsorbs exclusively on the more strongly basic Type I sites, where it undergoes a series of secondary condensation reaction that causes a decrease in the overall rate of alcohol dehydration. The comparative behavioural features of the two kinds of sites may be due to differing surface environments, with Type I sites being in structurally more defective and/or more energetic surface locations than are Type II sites. Increase in pretreatment temperature of the oxides cause thermally induced transformations of Type I sites into Type II sites by a surface annealing or restructuring process, with corresponding modifications in the observed catalytic

behaviour for the two alcohol conversion pathways.

Aldol addition of acetone was studied over alkaline earth oxides, La_2O_3 , ZrO_2 , $\text{SiO}_2\text{-Al}_2\text{O}_3$ and Nb_2O_5 at 0°C to elucidate the nature of active sites [44]. The activities of catalysts on a unit surface area basis were in the order; $\text{BaO} > \text{SrO} > \text{CaO} > \text{MgO} > \text{La}_2\text{O}_3 > \text{ZrO}_2 \gg \text{SiO}_2\text{-Al}_2\text{O}_3 > \text{Nb}_2\text{O}_5$. The reaction is base catalyzed and the oxides of stronger basic sites promote the reaction effectively. The active sites were suggested to be basic hydroxyl groups, either retained on the surface or originating from dehydration of diacetone alcohol to mesityl oxide.

The catalytic properties of La_2O_3 have much in common with those of ThO_2 and MgO not only for hydrogenation but also for other reactions such as double bond isomerizations of olefins [45] and of unsaturated compounds containing nitrogen [46] or oxygen [47]. It should be recognized, however that certain of the results described may not be representative of the behaviour of other rare earth oxides since La_2O_3 although it is the commonest and most widely used basic member of the group and apart from Nd_2O_3 and Ce_2O_3 (which is prepared only with difficulty by reduction of CeO_2) is the only sesquioxide of the series that invariably exists in the type-A (hexagonal) crystal structure, the others being of the type-C (body centered cubic) structure at temperatures $< 900^\circ\text{C}$ [48]. Moreover the electronic and magnetic properties of La_2O_3 differ considerably from those of the other oxides in the series because La^{3+} is the only trivalent rare earth cation that lacks 4f electrons and has the simple [Xe] electronic structure.

Minachev [49] has summarized many of the catalytic properties of dysprosium oxide with particular reference to organic reactions. The activity of dysprosium oxide is very similar

to that of erbium oxide and it is especially active towards n-butane cracking and double bond migration in 1-butene. Many studies have been made of reactions involving hydrogen or oxygen on dysprosium oxide. Adsorption results [50] show that the amount of adsorption depends on temperature, with a maximum adsorption at about 600 K. Hydrogen is probably adsorbed nondissociatively but oxygen may be dissociatively adsorbed above 600 K. The hydrogen deuterium exchange reaction occurs above 250 K [51] and shows a temperature dependence similar to the parahydrogen conversion reaction, leading to the conclusion that both these reactions involve equivalent dissociative mechanisms at these temperatures. Selwood [52] studied the nondissociative mechanism in a magnetic field and observed an increase in activity towards parahydrogen conversion in a strong field but no change in activity, in a weak field. Oxygen exchange reactions indicate that activity increases with a rise in mobility of surface oxygen, with dysprosium oxide becoming active at about 600 K.

The lanthanide oxides are making the “history” of the catalyst very important. Read and Perkins reported that the hydrogen-oxygen reaction is catalysed by dysprosium oxide [53]. Hydrogen and oxygen are competitively and nondissociatively adsorbed on the surface and the rate determining step involves the interaction between $H_2(\text{ads})$ and $H_2O_2(\text{ads})$ with the latter species being considered as equivalent to two adjacent hydroxyl groups. Temperature is critical, with changes in activation energy and effects of excess gas occurring at about 430 K.

The catalytic activity of rare earth oxides has recently been reviewed in a book by Tanabe *et.al.* [54]. Hattori *et.al.* [55] investigated the isomerization of n-butene over rare earth oxides. With few exceptions, however, these studies have been primarily exploratory in

nature, with the aim of obtaining kinetic data for the reactions investigated and comparative activity levels for the various oxides. Information is sparse, for example, about the chemical nature and surface densities of both catalytic and adsorption sites on these materials and about the mode of interaction of such sites with adsorbed and or reacting species. There has been however, little attention paid to the strength and distribution of electron donor sites on rare earth oxide surfaces. So we have done an investigation of the strength and distribution of electron donor sites on the rare earth oxide surfaces (La_2O_3 & Dy_2O_3) by adsorption of some electron acceptors.

REFERENCES

1. F.A.Cotton and G.Wilkinson, "Advanced Inorganic Chemistry", John Wiley & sons, Inc. p. 955 (1988)
2. K.C.Taylor, "Catalysis Science and Technology", Springer verlag, Berlin, 5 p.119 (1984)
3. A.Wpeters and G.Kim, "Industrial Applications of Rare Earth Elements", ACS symposium series No 164, American Chemical Society, 7 p.117 (1964)
4. J.C.Summers and A.J.Ausen, *J.Catal.*, 58 131 (1979)
5. Y.F.F. Yao, *J.Catal.*, 87 152 (1984)
6. K.Otsuka, K.Jinno and A.Morikawa, *Chem.Lett.*, 499 (1985)
7. C.H.Lin, K.D.Campbell, J.X.Wang and J.H.Lunsford, *J.Phys.Chem.*, 90 534 (1986)
8. J.Goldwasser and W.K.Hall, *J.Catal.*, 75 63 (1981)
9. V.S.Fomenko, "Handbook of Thermionic Properties", Plenum, Newyork (1966)
10. K.Tanabe, " Solid Acids and Bases", Academic Press, New York (1970)
11. T.Moeller, "Chemistry of the Lanthanides", Peragamon, New York (1973)
12. M.P.Rosynek, *Catal.Rev.*, 16 111 (1977)
13. P.W.Selwood, *J.Catal.*, 22 123 (1971)
14. K.M.Minachev, E.G.Vakk, R.V.Dmitrier and E.A.Nasedkin, *Izv.Akad. nauk SSSR, ser khim*, 3 421 (1964)
15. D.R.Ashmead, D.D.Eley and R.Rudham, *J.Catal.*, 3 280, (1964)
16. K.M.Minachev, "Catalysis" J.W.High Tower, North Holland, p.219 (1973)

17. Y.S.Khodakov, V.K.Nosteror and K.M.Minachev, *Izv Akad Nauk. SSS Rser Khim* **9** 2012 (1975)
18. J.F. Read, *J.Catal.*, **28** 428 (1973)
19. E.R.S.Winter, *J.Catal.*, **22** 158 (1971)
20. J.F.Read and R.E.Conrad, *J.Phys.Chem.*, **76** 2199 (1972)
21. E.V.Artamonov and L.A.Sazonov, *Kinet.Katal.*, **8** 131 (1967)
22. K.M.Minachev, D.A.Kondrat'ev and G.V.Antoshin, *Kinet.Katal.*, **8** 131 (1967)
23. H.Hattori, J.Inoko and Y.Murukami., *J.Catal.*, **42** 60 (1976)
24. K.M.Minachev, Y.S.Khodakov and V.S.Nakhshunov, *J.Catal.*, **49** 207 (1977)
25. L.A.Sazonov, E.V.Artamonov and G.N.Mitrofanova, *Kinet.Katal.*, **12** 378 (1971)
26. K.M.Minachev, Proc.Int.Congr.Catal. 5th 219 (1973)
27. T.T.Bakumenko and I.T.Chachenokova, *Kinet.Katal.*, **10** 796 (1969)
28. V.I.Lazukin, K.M.Kholyavenko, M.Y.Rubanik and A.I.Khanik, *Katal.* 29 (1971)
29. T.Hattori, J.I.Inoko and Y.Murukami, *J.Catal.*, **42** 60 (1976)
30. P.Pomopnis, *React.Kinet.Catal.Lett.*, **18** 247 (1981)
31. Y.Takita, T.Yoko-o, N.Egashira and F.Hori, *Bull.Chem.Soc.Jpn.*, **55** 2653 (1982)
32. J.E.Delmore, *J.Phys.Chem.*, **91** 2883 (1987)
33. K.Otsuka, K.Jinno and A.Morikawa, *Chem.Lett.*, 499 (1985)
34. K.Otsuka, K.Jonno and A.Morikawa, *Chem.Lett.*, 483 (1987)
35. C.H.Lin, K.D.Compbell, J.X.Wang and J.H.Lunsford, *J.Phys.Chem.*, **90** 534 (1986)

36. K.D.Campbell,H.Zhang and J.H.Lunsford, *J.Phys.Chem.*, **92** 750 (1988)
37. C.Li.K.Domen, K.Maruya and T.Onishi, *J.Catal.*, **123** 436 (1990)
38. S.T.King and E.J.Strojny, *J.Catal.*, **274** (1982)
39. Y.Takasu, M.Matsui and Y.Matsuda, *J.Catal.*, **76** 61 (1982)
40. M.P.Rosynek and D.T.Magnuson, *J.Catal.*, **46** 402 (1977)
41. M.P.Rosynek and J.S.Fox, *J.Catal.*, **49** 285 (1977)
42. V.R.Choudhary, S.T.Chaudhary, A.M.Rajput and V.H.Rane, *J.Chem.Soc., Chem.Comm.*,
555 (1989)
43. M.P.Rosynek, R.J.Koprowski and G.N.Dellisante, *J.Catal.*, **122** 80 (1990)
44. G.Zhang, H.Hattori and K.Tanabe, *Applied Catal.*, **36** 189 (1988)
45. Y.Fukuda, H.Hattori and K.Tanabe, *Bull.Chem.Soc.Jpn.*, **51** 3150 (1978)
46. A.Hattori, H.Hattori and K.Tanabe, *J.Catal.*, **65** 245 (1980)
47. H.Matsushashi, H.Hattori and K.Tanabe, *Chem.Lett.*, 341 (1981)
48. I.Warshaw and R.J.Roy, *J.Phys.Chem.*, **65** 2048 (1961)
49. K.M.Minachev, *Int.Congr.Catal. 5th I* 219 (1973)
50. J.F.Read, *J.Catal.*, **50** 490 (1972)
51. D.R.Ashmead, D.D.Eley and R.Ruthan, *J.Catal.*, **3** 280 (1964)
52. P.W.Selwood, *J.Catal.*, **22** 123 (1971)
53. J.F.Read and E.W.Perkins, *J.Catal.*, **42** 443 (1976)

54. K.Tanabe, M.Misono, Y.Ono and H.Hattori, "New Solid Acids and Bases", Kodansha, Elsevier, New York, p.18-44-265 (1989)
55. H.Hattori, H.Kumai, K.Tanabe, G.Zhang and K.Tanaka, Proc. 8th National symp.Catal., India, Sindri, 243 (1987)

CHAPTER 2
SURFACE ELECTRON PROPERTIES

SURFACE ELECTRON PROPERTIES

ELECTRON DONOR-ACCEPTOR PROPERTIES

The formation of radical ions on surfaces by electron transfer processes is well established and several examples of the observation of positive ions on electron acceptor sites in silica-alumina and zeolite systems have been reported [1-9]. Chemisorption of oxygen on the surface of magnesium oxide, an insulating oxide, can be observed under conditions which involve different types of electron transfer processes either from electron donor centres formed by irradiation or by the addition of extrinsic impurity ions [10-14]. Carbon dioxide can also form CO_2^- ions by electron transfer from S centres in irradiated MgO [15].

It is also possible that an anionic species will be formed on an adsorbent of an electron donor if a strong electron acceptor is used as the adsorbate [16]. When strong electron acceptors (Lewis acids) or donors (Lewis bases) are adsorbed on metal oxides, the corresponding radicals are formed as a result of electron transfer between the adsorbate and the metal oxide surface [17-20]. Flockhart *et al.* attempted the adsorption of tetracyanoethylene (TCNE) for the estimation of the electron donor properties of alumina surface [21-24]. The adsorption of nitro compounds on the surface of MgO powder has been studied by ESR and reflectance spectrophotometry [25]. Meguro *et al.* studied the surface properties of alumina, titania, silica-alumina and silica-titania systems prepared by the co-hydrolysis of metal alkoxides [26-28].

The electron donor properties of metal oxides (magnesia, alumina, silica, titania, zinc oxide and nickel oxide) were investigated by means of TCNQ adsorption [29]. The order of radical forming activity, determined by ESR, was as follows: magnesia > zinc oxide > alumina > titania > silica > nickel oxide. The electron donor property of the metal oxide surfaces might be dependent on the nature of the semiconductor and the surface hydroxyl ion.

The radical ion of nitrogen heterocyclics and sulphur heterocyclics have been generated and studied on a variety of oxide surfaces including silica-alumina and molybdena-alumina by K.S.Seshadri and L.Petrakis [30-31]. The adsorption of a series of aromatic hydrocarbons from solution on hydroxylated and dehydroxylated silica surfaces have been investigated [32]. Dehydroxylation of silica surfaces sharply diminishes the adsorption of aromatic hydrocarbons. Che *et al* [33] carried out a systematic study of the adsorption of TCNE on the surface of titania and magnesia.

The reduction of iodine to iodide ions occurs readily on the surface of partially dehydrated catalytic aluminas and silica-aluminas [34]. An increase in the alumina content of the latter results in an increase in reducing activity. The electron donor property of silica-alumina, silica-titania and alumina-titania surfaces were investigated by means of TCNQ adsorption [35]. TCNQ was adsorbed from several aromatic solvents, aniline, mesitylene, *p*-xylene, toluene, bromobenzene and chlorobenzene whose ionization potentials vary from 8.32 to 9.60 eV onto the oxide surfaces [36].

The electron donor properties of several oxide powders (CaO, MgO, ZnO, Al₂O₃,

SiO₂-Al₂O₃), activated in vacuum at temperatures upto 1200 K, have been investigated using the ESR spectroscopy of adsorbed nitrobenzene radicals as a probe [37]. The results show the existence of a correlation between the electron donor activity of oxides and their Lewis base strength, indicating a direct connection between basic centres and donor surface sites.

Pigmentary samples of titanium dioxide react with electron acceptors such as quinones, tetracyanoethylene and TCNQ to give paramagnetic species [38]. Visible absorption spectral measurements confirmed these assignments. The electron donor properties of TiO₂ and MgO have been investigated by tetracyanoethylene and trinitrobenzene adsorption [39] and found that the electron donor centres are associated with OH⁻ groups present on the surfaces of the solids activated at low temperature (< 300°C)

The adsorptive characteristics of zirconium oxide have been investigated by studying the adsorption of nitrogen, argon and water [40]. Surface properties were found to depend primarily on the amount of irreversibly adsorbed water retained by the sample. Water was found to be irreversibly adsorbed on zirconium oxide in amounts far in excess of that required for a classical chemisorbed monolayer.

Electron donor and acceptor properties of γ -alumina, silica and silica supported palladium oxide have been reported [41]. It was observed that while γ -alumina had both electron acceptor and donor properties, silica had only electron acceptor characteristics. γ -alumina supported palladium oxide showed better acceptor properties than donor properties. Silica supported palladium oxide showed only electron acceptor properties.

The adsorption of electron acceptors with various electron affinity, on the surface of alumina and titania have been studied by measuring the adsorption isotherms, ESR and electronic spectra [42,43]. The limiting amount of electron acceptor adsorbed decreased with decreasing electron affinity of the electron acceptors. The electron donor property of the zirconia-titania system was investigated by means of the adsorption of TCNQ [44]. This system had a much lower electron donocity than TiO_2 .

The electron donor strength on a metal oxide can be defined as the conversion ratio of an electron acceptor adsorbed on the surface into its anion radical. The strength and distribution of electron donor sites on Al_2O_3 , TiO_2 and $\text{ZrO}_2\text{-TiO}_2$ by adsorption of some electron acceptors were measured by means of an ESR spectrometer [45].

The study of the adsorption of anion radical salts on metal oxides can provide useful information concerning the interaction between anion radical salts and metal oxide surfaces. Esumi and Meguro reported the adsorption of TCNQ anion radical salts such as Li^+TCNQ^- , Na^+TCNQ^- and K^+TCNQ^- on alumina from a solution in acetonitrile by measuring the adsorption isotherm, and the ESR and electronic spectra of these adsorbed TCNQ anion radical salts [46]. They found that TCNQ anion radicals were adsorbed at electron-deficient sites on the alumina surface.

The electron donor property of zirconia was investigated by means of the adsorption of TCNQ [47]. The radical concentration decreased with an increase in the calcining temperatures, reached a minimum value at 700°C and then increased. This behaviour was explained by a change

in the number of electron donor site and their strength.

Titanium dioxide catalyses the dehydration of formic acid. A comparative study of the variation of surface properties and the catalytic activity of TiO_2 samples preheated in vacuum has shown that the active sites in this reaction are electron donor centres, the number of which has been determined by the adsorption of tetracyanoethylene or trinitrobenzene and ESR analysis of the paramagnetic anions formed [48].

Esumi *et al.* have reported the solvent effect on the acid base interaction of electron acceptors with metal oxides (Al_2O_3 and TiO_2) [49,50]. Similarly the acid-base interaction at the solid-liquid interface has also been confirmed to be important for the adsorption of tetrachloro-*p*-benzoquinone from various solvents [51].

Acid-base interactions at interfaces have been studied extensively in colloidal systems also [52,53]. Fowkes *et al.* [54-56] in particular have studied the adsorption of acidic and basic molecules from neutral solvents on inorganic powders such as iron oxides, silica and titania. They found that the calorimetric heats of adsorption are actually the heats of acid-base interactions governed by the Drago equation [57] and that the Drago equation constants can be accurately determined for the surface sites of these inorganic solids. Furthermore Fowkes [58] has extended this acid-base interaction theory to polymer-powder interfaces.

The zeta potential of metal oxides Al_2O_3 and titania decreases with increasing concentration of TCNQ in acetonitrile and ethyl acetate indicating that TCNQ anion radicals

formed on the surface of these oxides contribute to the decrement in the zeta potential [59].

Recently plasma treatment has become attractive [60] as a method for surface treatment, probably because it is a dry process at low temperatures with a relatively low pressure gas. Esumi *et al.* have studied the surface modification of mesocarbon microbeads [61-63] by various plasma treatments and found that oxygen plasma treatment renders the surface more acidic owing to the formation of carbonyl groups, whereas nitrogen or ammonia plasma treatment renders the surface more basic owing to the formation of amino groups. Taking into consideration these plasma treatments for carbon, there is a possibility of modifying the electron donor properties of metal oxides by plasma treatment. The interaction of plasma treated metal oxides with TCNQ in acetonitrile solution was studied by measuring their adsorption intensity of TCNQ in acetonitrile solution[64]. The electron donocity is increased by the ammonia and nitrogen plasma treatments.

SOLID ACIDS AND BASES

It has been seen that a surprisingly large number of solids have surface acidic and/or basic properties. A number of solid acids and bases find applications as catalysts with novel activity and selectivity in petrochemical reactions, and as catalysts effective in organic synthesis. More recently, a number of new types of solid acids have been discovered and applied effectively as catalysts to a wide variety of chemical reactions.

Systematic study of the correlation between catalytic activity and selectively and the acidic properties of the catalyst surface (the amount, strength and type -Bronsted or Lewis-

of the acid sites) has to a greater or lesser extent, enabled identification of the optimum catalyst in terms of their acidic properties.

The acid strength of a solid is the ability of the surface to convert an adsorbed neutral base into its conjugate acid as described by Walling [65] and the basic strength of a solid surface is defined as the ability of the surface to convert an adsorbed electrically neutral acid to its conjugate base.

If the reaction proceeds by means of proton transfer from the surface to the adsorbate the acid strength is expressed by the Hammett acidity function H_0 [66]

$$H_0 = pK_a + \log[B]/[BH^+]$$

where $[B]$ & $[BH^+]$ are the concentrations of the neutral base and its conjugate acid respectively. There are many methods for the measurements of acid strength like visual colour change method [67], spectrophotometric method [68] and gaseous base adsorption method [69] and for basic strength, the method using indicators [70] and the phenol vapour adsorption method [71].

The amount of acid on a solid is usually expressed as the number of mmol of acid sites per unit weight or per unit surface area of the solid, and is obtained by measuring the amount of a base which reacts with the solid acid. It is also called "acidity".

Amine titration method, one of the several methods used to determine acidity,

was reported first by Benesi [72] and is based on O. Johnson's experiment [73] and has been subsequently modified [74,75]. The amine titration method is obviously limited to white or light coloured surfaces. Titrations of dark coloured solids can be carried out, however, by adding a small known amount of a white solid acid [76]. The end point of the titration is taken when the colour change is observed on the white solid and a correction is made for the amount of butylamine used for the added white material. Using this method, both acid amount and acid strength have been measured for titanium trichloride by employing silica alumina as the white material.

The amount of a base which a solid acid can adsorb chemically from the gaseous phase is a measure of the amount of acid on its surface [77]. The bases used as adsorbates include quinoline, pyridine, piperidine, trimethylamine, n-butylamine, pyrrole and ammonia [78-81]. The differential thermal analysis method is also available for the estimation of the acid amount together with the acid strength of a solid (82). By DTA and thermal gravimetric analysis of silica-alumina on which pyridine, n-butylamine or acetone had been adsorbed, Shirasaki *et al.* obtained values for the amount of the base retained on the solid.

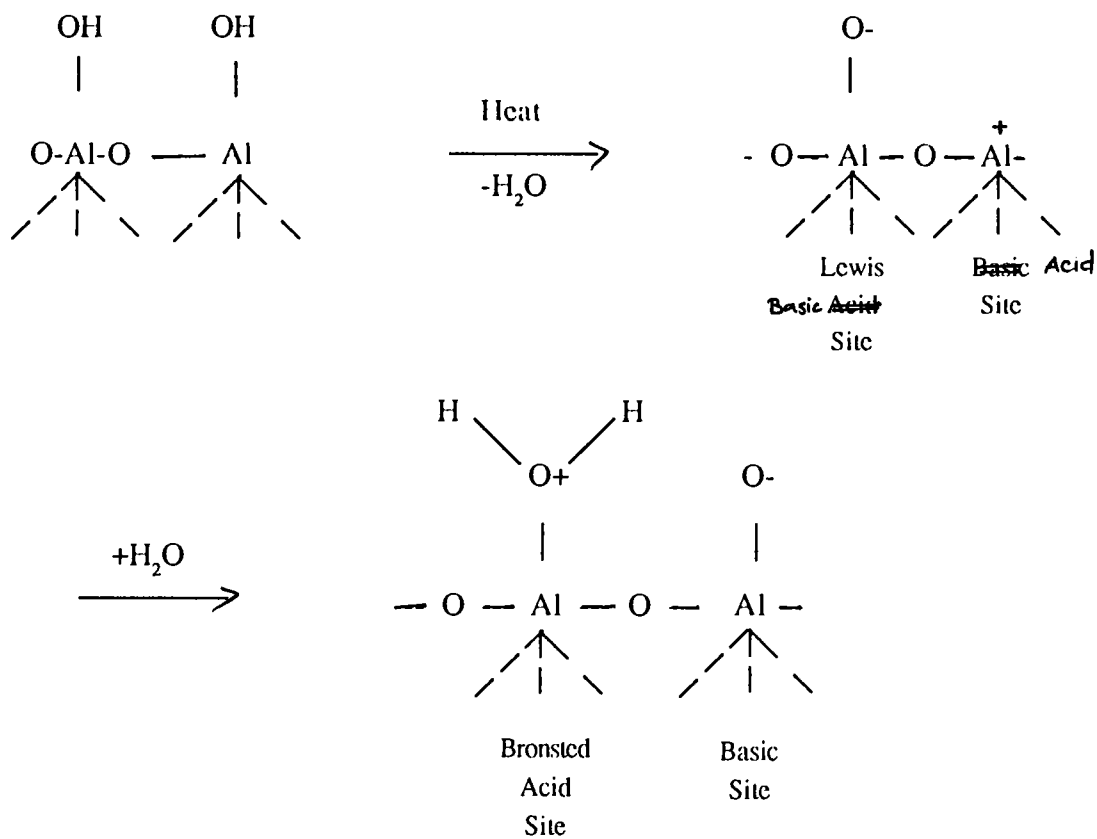
Infrared spectroscopic studies of ammonia and pyridine adsorbed on solid surfaces have made it possible to distinguish between Bronsted and Lewis acid sites and to assess the amount of Bronsted and Lewis acids independently. The original work was reported in a paper by Mapes and Eischens, who found that the IR spectra of ammonia adsorbed on silica-alumina show two kinds of absorption. One of which indicates NH_3 adsorbed on Lewis acid sites and the other NH_4^+ on Bronsted acid sites [83]. The spectrum of pyridine which is co-ordinately

bonded to the surface is very different from that of the pyridinium ion also permits differentiation between acid types on the surface of a solid acid [84].

The amount of base or basicity on a solid is usually expressed as the number (or mmol) of basic sites per unit weight or per unit surface area of the solid. Just as the acid amount is determined by n-butylamine titration, the amount of basic sites can be measured by titrating a suspension in benzene of a solid on which an indicator has been adsorbed in its conjugate basic form, with benzoic acid or trichloroacetic acid dissolved in benzene [85-86]. Take *et al.* determined both the strength and the amount of base for several alkaline earth metal oxides [87].

The number of CO₂ molecules adsorbed per unit surface area also can be considered as a measure of the amount of basic sites on the surface [88]. The base amount can be determined by observing the rise in temperature due to the heat of reaction between solid bases and acids in benzene [86].

Acid and basic sites on the surface of alumina can be pictured according to the scheme shown below [89].



The Lewis acid site is visualized as an incompletely coordinated aluminum atom formed by dehydration, and the weak Bronsted site as a Lewis site which has adsorbed moisture, while the basic site is considered to be a negatively charged oxygen atom.

Most of the alkaline earth metal oxides show surface basicity. According to the phenol vapour adsorption method, the basic strength of beryllium oxide and magnesium oxide may be classified as moderate, and that of calcium oxide as strong [90]. Silica-alumina is a very well known solid acid and the acidic properties and the nature of the acid site have been extensively studied. Several reviews dealing with the subject of surface acidity of solid catalysts

have been published [91-93].

CATALYTIC ACTIVITY & ACID-BASE PROPERTIES

Good correlation has been found in many cases between the total amount of acid (Bronsted plus Lewis types usually measured by the amine titration method) and the catalytic activities of solid acids [93]. For example the rates of both the catalytic decomposition of cumene and the polymerization of propylene over SiO_2 , Al_2O_3 catalysts were found to increase with increasing acid amount [73].

The acidic properties of alumina remarkably change with the degree of dehydration. Catalytic activities of alumina in a range of reaction such as the isomerization of hydrocarbons, the polymerizations of olefins *etc* have been attributed to the acidic properties of the surface [94-95]. Certain reactions catalyzed by sulphates and phosphates have revealed good correlation between the acidity measured by amine titration and the catalytic activity. For example there is an excellent correlation between the acidity of nickel sulfates and their catalytic activity for the depolymerization of paraldehyde [96].

The influence of the acid strength of solid catalysts on their activity per unit amount of acid in the dimerization of propylene, isobutylene and the dehydration of isopropyl alcohol has been studied by Dzisko [97].

As may be seen from Table 1 the rate of three reactions do change with the

acid strength of the catalysts. The precise character of the dependence of reaction rate on acid strength varies from reaction to reaction. The dependence of the dimerization rate of propylene on acid strength is for instance, much more marked than that for the dimerization of isobutylene.

| Table 1. Correlation of activity with acid strength | | | | |
|---|------|--|---------------------------|-----------------------------|
| Composition of Catalyst | pKa | (Logarithm of reaction rate constants in l.mmol ⁻¹ .h ⁻¹) | | |
| | | Dehydration of Isopropyl Alcohol | Dimerization of Propylene | Dimerization of Isobutylene |
| ZrO ₂ .SiO ₂ | -8.2 | 2.25 | 2.75 | 4.0 |
| Phosphorous acid on silica gel | -5.6 | 1.47 | 1.6 | 3.6 |
| MgO.SiO ₂ | -3.0 | 1.25 | - | - |
| Meta phosphorous acid on silica gel | -3.0 | 0.55 | 0.0 | 3.3 |

For each of the three reactions in Table 1, however, the dependence of the catalytic activity, on the acid strength is less pronounced than for homogeneous acid-catalyzed reactions.

The isomerization of n-butene on alumina is reported to be catalysed by Lewis acid sites [98]. In the case of $\text{SiO}_2\text{-Al}_2\text{O}_3$ and NiO-SiO_2 , Ozaki and Kimura suggested that the Lewis acid sites could be effective for isomerization, a proton being donated by the olefin molecule chemisorbed on the Lewis acid site [99].

The selectivity of a solid acid catalyst is influenced by its acidic properties and many other factors such as its geometric structure (particularly pore structures), the distribution of basic sites if present, the polarity of the surface *etc* [93].

Usually the reactions which are catalyzed by solid bases are polymerization, isomerization, alkylation, condensation, addition and dehydrohalogenation. The oxides, carbonates and hydroxides of alkali metals and alkaline earth metals (MgO , CaO , SrO , Na_2CO_3 , K_2CO_3 , CaCO_3 , SrCO_3 , NaOH , Ca(OH)_2) have been found active in the high polymerization of formaldehyde, ethylene oxide, propylene oxide, and β -propiolactone [100-103].

The first order rate constant for the formation of benzyl benzoate from benzaldehyde over calcium oxides calcined at various temperatures is found to change in parallel with the change in catalyst basicity. There is a good correlation between the catalytic activity and the amount of base per unit surface area [104].

The cis-trans isomerization of crotonitrile has been investigated using various catalysts including Al_2O_3 , MgO , CaO , Na_2CO_3 and NaOH supported on silica gel and some solid organic compounds [105]. Inorganic and organic compounds such as Al_2O_3 , potassium 2-naphthol-

3-carboxylate, sodium salicylate *etc* which have both acidic and basic groups are found to be catalytically active. On the other hand unmounted NaOH and Na₂CO₃, silica and potassium biphthalate, each of which possess either only basic or only acidic properties are inactive. These observations indicate that this isomerization undergoes by acid-base bifunctional catalysis.

The dehydration of various types of alcohols with alumina catalysts has been the subject of intensive studies, and the reaction mechanism and the nature of the alumina have been discussed by Pines and Manassen [106]. They regard the dehydration of most alcohols (menthols, neomenthols, alkylcyclohexanols, decalols, bornanols) as taking the form of a trans elimination, requiring the participation of both acid and basic sites on alumina.

The elimination of hydrogen halide from alkyl halides in many cases is thought to proceed by a concerted mechanism with acid-base bifunctional catalysis similar to that for the alcohol water elimination reactions [107].

The mixed metal oxide TiO₂-ZnO was prepared by coprecipitation and its acidic property was measured by *n*-butylamine titration and by observation of infrared spectra of adsorbed pyridine [108]. It was found that TiO₂-ZnO containing about 7 or 57% of ZnO shows a very large acid amount of 0.5-0.9 mmol/g and a fairly high acid strength of Ho < -3. The catalytic activity and selectivity of TiO₂-ZnO were found to be very high for the hydration reaction of ethylene.

The concentration of surface hydroxyl groups and catalytic properties of alumina-

silica catalysts in the decomposition of isopropanol were studied [109] and found that the dehydration of isopropanol is independent of the amount of the acid or basic sites but depends on the ratio of former to the latter.

The decomposition of 4-hydroxy-4-methyl-2-pentanone and the isomerization of 1-butene were carried out over La_2O_3 , Y_2O_3 and CeO_2 [110]. The activities for both types of reactions were in the following order. $\text{La}_2\text{O}_3 > \text{Y}_2\text{O}_3 > \text{CeO}_2$. With La_2O_3 , the change in the activity for the decomposition with the pretreatment temperature of the catalyst correlated well with the change in basicity. The activity and basicity maxima were observed when the catalyst was pretreated at 500°C. Y_2O_3 showed a maximum activity for the decomposition when pretreated at 700°C. For the isomerizations of 1-butene and cis-2-butene, La_2O_3 exhibited activity maxima when pretreated at 700°C. The number of basic sites on La_2O_3 was measured by titrating the sample suspended in dry benzene with a benzene solution of 0.1 mol.dm⁻³ benzoic acid, 2,4,6 trinitroaniline (pKa = 12.2) being used as an indicator.

The acid-base properties of various adsorbents (magnesia, silica, silica-alumina $\epsilon\text{-Al}_2\text{O}_3$, $\gamma\text{-Al}_2\text{O}_3$ with 0.5% initial Na content, fluorine, magnesium and alkali treated γ -alumina, thorium oxide) have been investigated by the infrared study of the adsorption of probe molecules [111]. Based on the adsorption of benzene surface hydroxyls were classified into four categories. Adsorption of nitrile and pyridine reveals that the average strength of the nonprotonic acid sites increases in the order $\text{HgO} < \text{Mg-Al}_2\text{O}_3 < \text{Al}_2\text{O}_3 < \text{F-Al}_2\text{O}_3$. Adsorption of pyrrole indicates that the average strength of basic sites increases in the order $\text{MgO} < \text{Mg-Al}_2\text{O}_3 < \text{Al}_2\text{O}_3 < \text{ThO}_2 < \text{Na \& K-Al}_2\text{O}_3$ and no basic site is detected on silica, silica-alumina and fluorine treated alumina.

Esumi *et al.* measured the basicity of alumina and titania by titration method [112] and found that the distribution of sites having different basicity were similar on these two metal oxides with respect to Lewis and Bronsted sites.

The acidity function, H_0 of silica supported heteropoly compounds (HPC) such as $H_3PMO_{12}O_{40}$, $H_3PW_{12}O_{40}$ and their sodium, potassium, ammonium, cesium and bismuth oxide salts have been examined in connection with their catalytic activity for the dehydration of t-butyl alcohol (TBA) [113]. The value of H_0 for the respective catalysts have been determined spectrophotometrically utilizing adsorbed dicinnamylideneacetone as a probe molecule. A linear relationship has been established between the amount of HPC supported and its H_0 . Also, for the dehydration of TBA in the liquid-phase all plots of $\log k$, vs H_0 (k is the apparent rate constant of the dehydration of liquid TBA) fall on a straight line with a slope of -1 independent of the kind of catalyst. On the other hand, for the gas-phase dehydration of TBA the plots yield straight lines with different slopes, depending on the type of catalyst. The dependence of catalytic activity on H_0 value indicate that the dehydration of liquid and gaseous TBA proceeds through pseudo-liquid and outer surface mechanisms respectively.

The catalytic isomerization of butenes over samarium oxide has been investigated in view of acid-base catalysis [114]. The ratio cis/trans-2-butene, formed from 1-butene isomerization was 22.2. The reaction profile of butene isomerization obtained from the relative rate constants was of the cis-convex type. The basic sites on the oxide surface have been revealed by the benzoic acid titration method.

Hydrous zirconium oxide is an amorphous solid and has several catalytic activities [115]. The oxide was changed to crystalline zirconia by calcination at a high temperature, and the catalytic activities were lowered. The correlation between the surface property and the catalytic activity was investigated on hydrous zirconium oxide calcined at several temperatures; the best activity was obtained in the oxide calcined at 300°C. The quantity of surface acid or basic sites was measured by the butylamine or trichloroacetic acid titration method respectively, using various Hammett indicators.

Alumina prepared from different aluminum hydroxides (boehmite, bayerite, and gibbsite) and containing controlled amounts of impurities (sodium or sulphate) introduced in different ways (by impregnation or residual ions from the preparation) were characterised with respect to their acidic properties (*n*-butylamine adsorption at 373 K, gravimetric method), basic properties (sulphur dioxide chemisorption at 373 K, volumetric method) and textural properties (surface area and pore size distribution) [116]. Their activity in the hydrogen sulphide and in sulphur dioxide reaction was measured in a tubular flow microreactor at 523 K. The effect of the nature and mode of introduction of the impurities on the acid-base properties of alumina established that, besides the basicity, the pore size distribution of the alumina strongly influences its catalytic performance, probably due to capillary condensation of sulphur in small pores.

Rare earth oxides (viz. La_2O_3 , CeO_2 , Sm_2O_3 , Eu_2O_3 and Yb_2O_3) have been compared for their acid and basic strength distribution (measured by stepwise thermal desorption of CO_2 from 323 to 1173 K and TPD of NH_3 from 323 to 1223K, respectively) and their catalytic activity/selectivity in oxidative coupling of methane to C_2 -hydrocarbons at 973-1123 K [117]. The catalytic

activity and selectivity showed dependence on both the surface acidity and basicity. However the relationship of the catalytic activity or selectivity with the surface acidity or basicity is not straight forward; it is quite complex.

Investigations are carried out to have a systematic comparison of the acidic properties and catalytic activities of single oxide TiO_2 , SiO_2 , Al_2O_3 , their binary oxides and the ternary oxide $\text{TiO}_2\text{-SiO}_2\text{-Al}_2\text{O}_3$ [118]. The acidity distribution is measured by using butylamine titration technique and the test reactions selected for the catalytic activity measurements are alkylation of toluene with 2-propanol and the dehydration of 2-propanol.

The ternary oxide system $\text{MOO}_3\text{-SiO}_2\text{-Al}_2\text{O}_3$ was prepared by coprecipitation method [119]. The pH of coprecipitation has been varied from 2 to 8 and its effect on the acidic properties of the ternary oxide were studied by butylamine titration. The catalytic activity of $\text{MOO}_3\text{-SiO}_2\text{-Al}_2\text{O}_3$ was found to be very high for the alkylation of toluene with 2-propanol.

Both Lewis and Bronsted acid sites were found on the surface of $\text{TiO}_2\text{-SiO}_2$ mixed oxide [120] though no Bronsted acid sites were detected on the surface of pure TiO_2 and SiO_2 while on the surface of $\text{TiO}_2\text{-Al}_2\text{O}_3$ mixed oxide, no Bronsted acid sites were generated. The rate of isomerization of 1-butene was found to be enhanced on the Bronsted acid sites formed on the $\text{TiO}_2\text{-SiO}_2$ mixed oxide.

REFERENCES

1. D.M.Bronwer, *Chem.Ind.*, 177 (1961)
2. J.J.Rooney and R.C.Pink, *Proc.Chem.Soc.*, 70 (1961)
3. W.K.Hall, *J.Catal.*, 1 53 (1962)
4. H.P.Leftin and M.C.Hobson, *Advan.Catal.*, 14 372 (1963)
5. A.Terenin, *J.Catal.*, 15 256 (1964)
6. R.P.Porter and W.K.Hall, *J.Catal.*, 5 366 (1966)
7. J.J.Rooney and R.C.Pink, *Trans.Faraday Soc.*, 58 1632 (1962)
8. J.A.N Scott, B.D.Folckhart and R.C.Pink, *Proc.Chem.Soc.*, 139 (1964)
9. D.N.Stamires and J.Trkevich, *J.Am.Chem.Soc.*, 86 749 (1964)
10. R.L.Nelson and A.J.Tench, *J.Chem.Phys.*, 40 2736 (1964)
11. R.L.Nelson, A.J.Tench and R.W.Wilkinson, *Proc.Brit.Ceram Soc.*, 5 181 (1965)
12. A.J.Tench and R.L.Nelson, *J.Chem.Phys.* 44 1714 (1966)
13. R.L.Nelson, A.J.Tench and B.J.Harmsworth, *Trans.Faraday Soc.*, 63 1427 (1967)
14. J.H.Lunsford and J.P.Jayne, *J.Chem.Phys.*, 44 1487 (1966)
15. J.H.Lunsford and J.P.Jayne, *J.Phys.Chem.*, 69 2182 (1965)
16. T.H.Wolkenstein, "Advances in Catalysis", vol.12, Academic press, New York (1960)
17. M.Okuda and T.Tachibana, *Bull.Chem.Soc.Jpn.*, 33 863 (1960)
18. B.D.Flockhart, J.A.N.Scott and R.C.Pink, *Trans.Faraday Soc.*, 62 730 (1966)

19. A.J.Tench and R.L.Nelson, *Trans.Faraday Soc.*, **63** 2254 (1967)
20. H.Hosaka, T.Fujiwara and K.Meguro, *Bull.Chem.Soc.Jpn.*, **44** 2616 (1971)
21. B.D.Flockhart, G.Naccache, J.A.N.Scott and R.C.Pink., *Chem.Comm.*, **11** 238 (1965)
22. B.D.Flockhart, J.A.N.Scott and R.C.Pink,*Trans.Faraday Soc.*, **62** 730 (1966)
23. B.D.Flockhart, I.R.Leith and R.C.Pink, *Trans.Faraday Soc.*, **66** 469 (1970)
24. B.D.Flockhart, I.R.Leith and R.C.Pink, *Trans.Faraday Soc.* **65** 542 (1969)
25. A.J.Tench and R.L.Nelson, *Trans.Faraday Soc.*, **63** 2254 (1967)
26. H.Murayama, K.Kobayashi,M.Koishi and K.Meguro, *J.Colloid Interface Sci.*, **32** 470 (1970)
27. H.Murayama and K.Meguro, *Bull.Chem.Soc.Jpn.*, **43** 2386 (1970)
28. H.Hosaka and K.Meguro, *Bull.Chem.Soc.Jpn.*, **44** 1252 (1971)
29. H.Hosaka, T.Fujiwara and K.Meguro, *Bull.Chem.Soc.Jpn.*,**44** 2616 (1971)
30. K.S.Seshadri and L.Petrakis, *Bull.Chem.Soc.Jpn.*, **43** 1317 (1970)
31. L.Petrakis and K.S.Seshadri, *J.Phys.Chem.*, **76** 1443 (1972)
32. Y.A.Eltekov, V.V.Khopina and A.V.Kiselev, *Faraday Trans.* **68** 889 (1972)
33. M.Che, C.Naccache and B.Imelik, *J.Catal.* **24** 328 (1972)
34. B.D.Flockhart, K.Y.Liew and R.C.Pink, *J.Catal.*, **32** 20 (1974)
35. H.Hosaka, N.Kawashima and K.Megoro, *Bull.Chem.Soc.Jpn.*, **45** 3371 (1972)
36. H.Hosaka and K.Megura, *Colloid Polymer Sci.*, **252** 322 (1974)
37. D.Cordischi and V.Indovina, *Bull.Chem.Soc.Jpn.*, **49** 2341 (1976)
38. R.S.Davidson and R.M.Slater, *Bull.Chem.Soc.Jpn.*, **48** 2416 (1975)

39. M.Che, C.Naccache and B.Imelik, *J.Catal.*, **24** 328 (1972)
40. H.F.Holmes, E.L.Fuller and R.A.Beh, *J.Colloid Interface.Sci.*, **47** 365 (1974)
41. I.Bodrikov, K.C.Khulbe and R.S.Mann, *J.Catal.*,**43** 339 (1976)
42. K.Meguro and K.Esumi, *J.Colloid Interface Sci.*,**59** 93 (1977)
43. K.Esumi and K.Meguro, *Bull.Chem.Soc.Jpn.*, **55** 1647 (1982)
44. K.Esumi, H.Shimada and K.Meguro, *Bull.Chem.Soc.Jpn.*, **50** 2795 (1977)
45. K.Esumi and K.Meguro, *J.Colloid Interface Sci.*, **66** 192 (1978)
46. K.Esumi and K.Meguro, *J.Colloid Interface Sci.*, **61** 192 (1977)
47. K.Esumi and K.Meguro, *Bull.Chem.Soc.Jpn.*, **55** 315 (1982)
48. M.A.Enriquez and J.P.Fraissard, *J.Catal.*, **74** 77 (1982)
49. K.Esumi, K.Miyata and K.Meguro, *Bull.Chem.Soc.Jpn.*, **58** 3524 (1985)
50. K.Esumi, K.Miyata, F.Waki and K.Meguro, *Colloids Surf.* **20** 81 (1986)
51. K.Esumi, K.Miyata, F.Waki and K.Meguro, *Bull.Chem.Soc.Jpn.*, **59** 3363 (1986)
52. W.B.Jensen "The Lewis Acid-Base Concepts" Wiley, New York (1980)
53. P.Sorensen, *J.Paint.Tech.*, **47** 31 (1975)
54. S.T.Joslin and F.M.Fowkes, *Ind.Eng.Chem., Prod.Res.Dev.* **24** 369 (1985)
55. F.M.Fowkes, D.C.Mccarthy and J.A.Wolfe, *J.Polym.Sci.*, **22** 547 (1984)
56. F.M.Fowkes, Y.C.Huang, B.A.Shab, M.J.Kulp and T.B.Lloyd, *Colloids Surf.*, **29** 243 (1988)
57. R.S.Drago, L.B.Parr and C.S.Chamerlain, *J.Am.Chem.Soc.*, **99** 3203 (1977)
58. F.M.Fowkes,"Physico Chemical Aspects of Polymer Surfaces", K.L.Mittal, Plenum Press,

- New York **2** 583 (1983)
59. K.Esumi, K.Meguro and K.Magara, *J.Colloid Interface Sci.*, **141** 578 (1991)
 60. J.R.Hollaban and A.T.Bell, "Techniques & Applications of Plasma Chemistry", Wiley, New York (1974)
 61. M.Sugiura, K.Esumi, K.Meguro and H.Honda, *Bull.Chem.Soc. Jpn.*, **58** 2638 (1985)
 62. K.Esumi, M.Sugiura, T.Mori, K.Meguro and H.Honda, *Colloids Surf.* **19** 331 (1986)
 63. K.Esumi, S.Nishina, S.Sakurada, K.Meguro and H.Honda *Carbon*, **25** 821 (1987)
 64. K.Esumi, N.Nishiuchi and K.Meguro, *J.Surf.Sci.Tech.*, **4** 207 (1988)
 65. C.Walling, *J.Am.Chem.Soc.*, **72** 1164 (1950)
 66. L.P.Hammett and A.J.Deyrup, *J.Am.Chem.Soc.*, **54** 2721 (1932)
 67. A.E.Hirschler, *J.Catal.*, **2** 428 (1963)
 68. H.P.Lefstin and M.C.Hobson, "Advances in Catalysis", Vol 14 p.115 Academic press (1963)
 69. A.N.Webb, *Ind.Eng.Chem.*, **49** 261 (1957)
 70. S.Malinowski and S.Szczepanska, *J.Catal.*, **2** 310 (1963)
 71. C.Naccache, Y.Kodratoff, R.C.Pink and B.Imelik, *J.Chem.Phys.*, **63** 341 (1966)
 72. H.A.Benesi, *J.Am.Chem.Soc.*, **78** 5490 (1956)
 73. O.Johnson, *J.Phys.Chem.*, **59** 827 (1955)
 74. H.A.Benesi, *J.Phys.Chem.*, **61** 970 (1957)
 75. A.E.Hirschler and A.Schneider, *J.Chem.Eng.Data* **6** 313 (1961)
 76. K.Tanabe and Y.Watanabe, *J.Res.Inst.Catal.*, **11** 65 (1963)

77. G.A.Mills, E.R.Boedecker and A.G.Oblad, *J.Am.Chem.Soc.*, **72** 1554 (1950)
78. T.H.Milliken,G.H.Mills andA.G.Oblad,*Discussions Faraday Soc.*,**8** 279 (1950)
79. Y.Tezuka and T.Takeuchi, *Bull.Chem.Soc.Jpn.*, **38** 485 (1965)
80. Y.Kubokawa, *J.Phys Chem.*, **67** 769 (1963)
81. R.L.Stone and H.F.Rase, *Anal.Chem.*, **29** 1273 (1957)
82. T.Shirasaki,M.Minura and K.Mukaida,Bunsekikiki(Japanese)., **5** 59 (1968)
83. J.E.Mapes and R.R.Eishens, *J.Phys.Chem.*, **58** 809 (1954)
84. E.P.Parry, *J.Catal.*, **2** 371 (1963)
85. K.Tanabe and M.Katayamma, *J.Res.Inst.Catal.*, **7** 106 (1959)
86. K.Tanabe and T.Yamaguchi, *J.Res.Inst.Catal.*, **14** 93 (1966)
87. J.Take,N.Kikuchi and Y.Youeda, *J.Catal.*, **21** 164 (1971)
88. S.Malinowski, S.Szczepanska and J.Sloczynski, *J. Catal* **7** 67 (1964)
89. S.G.Hondin and S.W.Weller, *J.Phys.Chem.*, **60** 1501 (1956)
90. E.B.Cornelius, T.H.Milliken, G.A.Mills and A.G.Oblad, *J.Phys.Chem.*, **59** 809 (1955)
91. K.Tanabe, "Solid Acids and Bases" Kodansha, New York 1970
92. F.Forni, *Catal.Rev.*, **8** 69 (1977)
93. K.Tanabe, M.Misono, Y.Ono and H.Hattori,"New solid Acids & Bases", Kodansha New York (1989)
94. H.Pines and J.Ravoire, *J.Phys.Chem.*,**65** 1859 (1961)
95. J.B.Peri, *J.Phys.Chem.*, **69** 231 (1965)

96. K.Tanabe and R.Ohnishi, *J.Res.Inst.Catal.*, **10** 229 (1962)
97. V.A.Dzisko, Proc.Intern.Congr, Catalysis 3rd, Amsterdam (1964)
98. J.B.Peri, *J.Catal.*, **31** 65 (1961).
99. A.Ozaki and K.Kimura, *J.Catal.*, **3** 395 (1964)
100. F.N.Hill, F.E.Bailey and J.T.Fitzpatrick, *Ind.Eng.Chem.*, **50** 5 (1958)
101. O.Vkrylov, M.J.Kushnerev, Z.A.Markova and E.A.Fokina, Proc.Intern.Congr.Catal. Amsterdam (1964)
102. Japan.pat. Showa 18-1048 (1943)
103. R.N.Goyce, *J.Polym.Sci.*, **3** 169 (1948)
104. K.Saito and K.Tanabe, *J.Polym.Sci.*, **11** 206 (1969)
105. M.Ichikawa, M.Soma, T.Ohnishi and K.Tamaru, *Trans.Faraday Soc.*, **63** 2012 (1967)
106. H.Pines and J.Manasen, *Advan.Catal.*, **16** 49 (1966)
107. H.Noller, P.Andren, E.Schmitz, S.Serain, Intern.Congr.Catal.4th, Moscow 81 (1968)
108. K.Tanabe, C.Ishiya, I.Matsuzaki, I.Ichikawa and H.Hattori, *Bull.Chem.Soc.Jpn.*, **45** 47 (1972)
109. I.Ahmed, *J.Colloid Interface Sci.*, **69** 469 (1979)
110. Y.Fukuda, H.Hattori and K.Tanabe, *Bull.Chem.Soc.Jpn.*, **51** 3150 (1978)
111. P.O.Scokart and P.G.Rouxhet, *J.Colloid Interface Sci.*, **86** 96 (1982)
112. K.Esumi and K.Meguro, *J.Colour Material.*, **58** 9 (1985)
113. R.F.Ohtsuka, Y.Morioka and J.Kobayashi, *Bull.Chem.Soc.Jpn.*, **63** 2071 (1990)
114. Y.Nakashima, Y.Sakata, H.Imamura and S.Tsuchiya, *Bull.Chem.Soc.Jpn.*, **63** 3313 (1990)

115. M.Shibagaki, K.Takahashi, H.Kuno and H.Matsushita, *Bull. Chem.Soc.Jpn.*, **63** 258 (1990)
116. J.L.Zotin and A.C.Faro Jr. *Applied Catal.*, **75** 57 (1991)
117. V.R.Choudhary and V.H.Rane, *J.Catal.*, **130** 411 (1991)
118. K.R.Sabu, K.V.C.Rao and C.G.R.Nair, *Bull.Chem.Soc.Jpn.*, **64** 1920 (1991)
119. K.R.Sabu, K.V.C.Rao and C.G.R.Nair, *Bull.Chem.Soc.Jpn.*, **64** 1926 (1991)
120. H.Nakabayashi, *Bull.Chem.Soc.Jpn.*, **65** 914 (1992)

CHAPTER 3
EXPERIMENTAL

MATERIALS

Single Oxides

The rare earth oxides La_2O_3 & Dy_2O_3 (99.9% pure) were obtained from Indian Rare Earths Ltd., Udyogamandal, Kerala. Since the oxides were already heat treated at higher temperature, they were regenerated by the hydroxide method [1] from the nitrate solution.

Hydroxide method

Nitrate solution of the sample (250 ml) containing 0.5g of rare earth oxide was heated to boiling and 1:1 ammonium hydroxide solution was added dropwise, with stirring, until the precipitation was complete. Concentrated ammonium hydroxide solution (an amount equal to one tenth of volume of solution) was then added with stirring. It was then allowed to digest on a steam bath until the precipitate was flocculated and settled. The precipitate was filtered on a Whatman No:41 filter paper and washed with small portions of an aqueous solution containing 1g of ammonium nitrate and 10 ml of concentrated ammonium hydroxide in 100 ml, until the precipitate was free from NO_3^- . The precipitate was kept in an air oven at 100°C for overnight and was ignited in a china dish at $300-400^\circ\text{C}$ for 2 hrs.

Mixed Oxides

Mixed oxides of rare earths and aluminum were prepared by co-precipitation method [2]

from their nitrate solutions[3].

10 % mixed oxide

Rare earth oxide (1g) was dissolved in concentrated nitric acid and was crystallised by repeated evaporation with nitric acid. Aqueous ammonia (5%) solution was added to an aqueous solution containing rare earth nitrate and aluminum nitrate [prepared by dissolving 66.15g of aluminum nitrate, (SQ grade, obtained from Qualigens Fine chemicals) in 250 ml distilled water], until the precipitation was complete. The precipitate was washed with distilled water, dried by keeping overnight at 110°C and then calcined at 500°C for 3 hrs.

Using the same method, mixed oxides of rare earths (20,45,60 and 75% by wt. of rare earth oxide) with aluminum were prepared from the required amounts of aluminum nitrate and rare earth oxide.

Electron acceptors:

Electron acceptors used for the study are 7,7,8,8-tetracyanoquinodimethane (TCNQ), 2,3,5,6-tetrachloro-*p*-benzoquinone (chloranil), *p*-dinitrobenzene (PDNB) and *m*-dinitrobenzene (MDNB).

TCNQ was obtained from Merck-Schuchardt and was purified by repeated recrystallisation from acetonitrile [4].

Chloranil was obtained from Sisco Research Laboratories Pvt. Ltd. and was purified by recrystallisation from benzene [5].

p-Dinitrobenzene was supplied by Koch-Light Laboratories Ltd. and was purified by recrystallisation from alcohol [6].

m-Dinitrobenzene was obtained from Loba-ChemicalIndoaustranal company and was purified by recrystallisation from rectified spirit [7].

Solvents

Acetonitrile

SQ grade acetonitrile obtained from Qualigens Fine Chemicals was first dried by passing through a column filled with silica gel (60-120 mesh) activated at 110°C for 2 hrs. It was then distilled with anhydrous phosphorous pentoxide and the fraction between 79-82°C was collected [8].

1,4-Dioxan

SQ grade 1-4 dioxan was obtained from Qualigens Fine Chemicals. It was dried by keeping over potassium hydroxide pellets for 2-3 days, filtered and refluxed with sodium metal for 6-7 hrs till the surface of sodium metal got the shining appearance. The refluxed solvent

was then distilled and the fraction at 101°C was collected [9].

Ethyl acetate

SQ grade ethyl acetate was obtained from Qualigens Fine Chemicals. A mixture of 1 litre of ethyl acetate, 100 ml of acetic anhydride and 10 drops of conc. sulphuric acid was heated under reflux for 4 hrs and was then fractionated using an efficient column. The distillate was then shaken with 20-30 g of anhydrous potassium carbonate, filtered and redistilled. The fraction boiling at 77°C was collected [10].

Benzene

Benzene used for the acidity and basicity measurements was purified by the following procedure [11].

Pure benzene obtained from Merck was shaken repeatedly with about 15% of its volume of conc. sulphuric acid in a stoppered separating funnel until the acid layer was colourless on standing. After shaking, the mixture was allowed to settle and lower layer was drawn off. It was then washed with water and 10% sodium carbonate solution and finally dried with anhydrous CaCl_2 . It was filtered and distilled, and the distillate was kept over sodium wire for 1 day and again distilled and the fraction boiling at 80°C was collected.

Hammett Indicators

Hammett indicators used for the study are the following:

1. Methyl red [E.Merck (India) Pvt Ltd]
2. Dimethyl yellow (Loba Chemie Industrial Company)
3. Crystal violet (Romali)
4. Neutral red (Romali)
5. Bromothymol blue (Qualigens Fine Chemicals)
6. Thymol blue (Qualigens Fine Chemicals)
7. 4-nitroaniline (Indian Drugs & Pharmaceuticals Ltd)

Trichloroacetic acid (SQ grade obtained from Qualigens Fine Chemicals) and n-butylamine (Sd-Fine Chemicals Pvt Ltd.) were used without further purification.

Cyclohexanone

Commercial cyclohexanone obtained from BDH was purified through the bisulphite method [12]. A saturated solution of sodium bisulphite was prepared from 40 g of finely powdered sodium bisulphite. The volume of the resulting solution was measured and it was treated with 70% of its volume of rectified spirit. Sufficient water was added to dissolve the precipitate which separated. 20g of commercial cyclohexanone was introduced into the aqueous

alcoholic bisulphite solution with stirring and the mixture was allowed to stand for 30 minutes. The crystalline bisulphite compound was filtered off at the pump and washed it with a little rectified spirit.

The bisulphite compound was transferred to a separating funnel and decomposed with 80ml of 10% NaOH solution. The liberated cyclohexanone was removed, saturated the aqueous layer with salt and extracted it with 30ml of ether. The ether extract was combined with the ketone layer and dried with 5g of anhydrous magnesium sulphate. The dried ethereal solution was filtered into a 50ml distilling flask, attached with a condenser and distilled off the ether using a water bath. The residual cyclohexanone was distilled and the fraction at 153°C was collected.

2-Propanol

LR grade reagent obtained from Merck was further purified by adding about 200g of quicklime to one litre of 2-propanol. It was kept for 3-4 days, refluxed for 4 hrs and distilled. The fraction distilling at 82°C was collected [13].

Xylene : Extra pure quality xylene obtained from Merck was used as such.

METHODS

Adsorption studies [14]

The oxides were activated at a particular temperature for 2 hrs, prior to each experiment and 0.5g was then placed in a 25ml test tube and outgassed at 10^{-5} Torr for 1 hr. Into the test tube which was fitted with a mercury sealed stirrer 20ml of a solution of an electron acceptor in organic solvent was then poured in. After the solution had subsequently been stirred for 4 hrs at 28°C in a thermostated bath, the oxide was collected by centrifuging the solution and dried at room temperature in vacuum. The reflectance spectra of the dried samples were recorded in a Hitachi 200-20 UV-visible spectrophotometer with a 200-0531 reflectance attachment.

The ESR spectra were measured at room temperature using Varian E-112 X/Q band ESR Spectrophotometer. Radical concentrations were calculated by comparison of areas obtained by double integration of the first derivative curves for the sample and standard solutions of 2,2-diphenyl-2-picrylhydrazyl in benzene. The amount of electron acceptor adsorbed was determined from the difference in concentration of the electron acceptor before and after adsorption. The absorbance of electron acceptor was measured by means of a UV-visible spectrophotometer (Hitachi 200-20) at the λ_{\max} of the electron acceptor in the solvent. The λ_{\max} of chloranil was 288 nm in acetonitrile, 287 nm in ethyl acetate and 286 nm in 1-4 dioxan, while the λ_{\max} for TCNQ was 393.5 nm in acetonitrile, 393nm in ethyl acetate and 403 nm in 1-4 dioxan. The λ_{\max} of PDNB and MDNB in acetonitrile were 262 nm and 237 nm and in 1-4 dioxan 261

and 218 nm respectively.

Surface areas of oxides were determined by BET method using Carlo Erba Strumentazione Sorptomatic Series 1800.

Acidity/Basicity measurements

The oxides were sieved to prepare powders of 100 to 200 mesh size and then activated at a particular temperature for 2 hrs. prior to each experiment.

The acidity at various acid strengths of a solid was measured by titrating 0.1g of solid suspended in 3ml of benzene with a 0.1N solution of n-butylamine in benzene. At the end point, the basic colour of indicators appeared [15].

The basicity was measured by titrating 0.1g of solid suspended in 3ml of benzene with a 0.1N solution of trichloroacetic acid in benzene using the same indicators as those used for acidity measurement. The colours of indicators on the surface at the end point of the titration were the same as the colours which appeared by adsorption of respective indicators on the acid sites. The colour of the benzene solution was the basic colour of the indicator at the end point but it turned to be the acidic colour by adding an excess of the acid. As the results for a titration lasting 1 hr. were the same as those for a titration lasting 20 hr, 1 hr was taken for titration.

Magnetic Susceptibility Measurements

Magnetic moments of the oxides before and after the adsorption of electron acceptors were determined by magnetic susceptibility measurements.

The Magnetic susceptibility measurements were done at room temperature on a simple Guoy type balance. The Guoy tube was standardised using $[\text{Hg}(\text{Co}(\text{CNS})_4)]$ as recommended by Figgis and Nyboln [16]. The effective magnetic moment μ_{eff} was calculated using the equation

$$\mu_{\text{eff}} = 2.8 (\chi_m T)^{1/2}$$

where T is the absolute temperature and χ_m is the molar susceptibility [17].

Catalytic activity measurements

1g of the catalyst was placed in a 25 cm³ round-bottom flask equipped with a reflux condenser. 5 mmol of cyclohexanone, 10 cm³ of 2-propanol and 0.5 mmol of xylene as an internal standard were added. The contents were heated under gentle reflux. The reaction was followed by product analysis by means of a Hewlett packard 5730 A gas chromatograph by comparison of its retention time with that of authentic samples. From the peak area of the product, the concentration of cyclohexanol formed was calculated with reference to that of the internal standard, xylene [18].

REFERENCES

1. "Encyclopaedia of Industrial Chemical Analysis", F.D.Snell and L.S.Ettre. Vol.17 Interscience, New York p.473 (1973)
2. "Encyclopaedia of Industrial Chemical Analysis", F.D.Snell and L.S.Ettre. Vol.17 Interscience, New York p.475 (1973)
3. T.Arai, K.Maruya, K.C.Domen and T.Omishi, *Bull.Chem.Soc.Jpn.*, **62** 349 (1989).
4. D.S.Acker and W.R.Hertler, *J.Am.Chem.Soc.*, **84** 3370 (1962).
5. L.F.Fiesser and Mary Fiesser,"Reagents for Organic Synthesis", John Wiley, New York p.125 (1967)
6. B.S.Furness, A.J. Hannaford, V. Rogers, P.W.G. Smith and A.R.Tatchell, "Vogel's Text Book of Practical Organic Chemistry", 4th ed. ELBS London p.526 (1978)
7. B.S.Furness, A.J.Hannaford, V.Rogers, P.W.G. Smith and A.R.Tatchell,"Vogel'sText Book of Practical Organic Chemistry," 4th ed. ELBS London p.613 (1978).
8. A.I.Vogel, "A Text Book of Practical Organic Chemistry" 3rd ed. ELBS London p.407 (1973).
12. A.I.Vogel, "A Text Book of Practical Organic Chemistry" 3rd ed. ELBS London p.342 (1973)
13. A.I.Vogel,"A Text Book of Practical Organic Chemistry" 3rd ed. ELBS London p.886 (1973).
14. K.Èsumi, K.Miyata, F.Waki and K.Meguro, *Bull.Chem. Soc.Jpn.*, **59** 3363 (1986).

15. T.Yamanaka and K.Tanabe, *J.Phys.Chem.*, **79** 2409 (1978).
16. B.N.Figgis and R.S.Nyholm, *J.Am.Chem.Soc.*, 4190 (1958).
17. B.N.Figgis and J.Lewis,"Modern Co-ordination Chemistry" Interscience New York (1960).
18. M.Shibagaki, K.Takahashi, H.Kuno and H.Matsushita, *Bull.Chem.Soc.Jpn.*, **63** 258 (1990).

CHAPTER 4
RESULTS AND DISCUSSION

RESULTS AND DISCUSSION

Although investigations of the catalytic properties of rare earth sesquioxides have multiplied in recent years, the primary mode of surface interaction on these materials remain largely undefined. Details of adsorption/desorption processes, for example, and of the nature of adsorbed species on these oxide surfaces are very little. There has been, however, little attention paid to the strength and distribution of electron donor sites on rare earth oxide surfaces apart from the studies on oxides of Y, Pr and Nd [1-5]. In this thesis, the strength and distribution of electron donor sites, surface acidity, and magnetic properties of some of the rare earth oxides (La_2O_3 & Dy_2O_3) have been reported. The surface electron donor properties were studied by adsorption of electron acceptors having electron affinity varying from 1.24 eV to 2.84 eV. The electron affinity values have been reported earlier [K. Meguro and K. Esumi, Bull. Chem. Soc. Jpn., 55 1647 (1982)]. The data were correlated with catalytic activity of these oxides.

The electron acceptors used for adsorption study are given in Table 2.

| Table 2 - Electron acceptors used. | |
|---|------------------------|
| Electron acceptor | Electron affinity (eV) |
| 7,7,8,8 - tetracyanoquinodimethane (TCNQ) | 2.84 |
| 2,3,5,6 - tetrachloro- <i>p</i> -benzoquinone (chloranil) | 2.40 |
| <i>p</i> - dinitrobenzene (PDNB) | 1.77 |
| <i>m</i> - dinitrobenzene (MDNB) | 1.26 |

Since the electron donating properties depend on the basicity of the medium, studies were carried out in three solvents, acetonitrile a very weak base, ethyl acetate a weak base and 1,4-dioxan a moderately weak base.

La_2O_3 and Dy_2O_3 used for adsorption study were prepared by the hydroxide method from the respective nitrate solutions. They were activated by heating in air for 2 hrs. at various temperatures viz. 300, 500 and 800°C. The specific surface area of these oxides were determined by BET method and were obtained as print from a Carlo Erba Strumentazione Sorptomatic Series 1800. The values are given in Table 3.

| Table 3 - Surface area of La_2O_3 and Dy_2O_3 activated at different temperatures. | | |
|---|---|---|
| Activation temperature (°C) | surface area (m²/g) | |
| | La_2O_3 | Dy_2O_3 |
| 300 | 39.80 | 24.35 |
| 500 | 38.28 | 24.41 |
| 800 | 29.75 | 29.53 |

In the case of PDNB and MDNB the adsorption was so negligible that the amount adsorbed was hardly estimated. The adsorption isotherms of TCNQ and chloranil from these solvents may be classified as Langmuir type. It was verified by the plot of C_{eq}/C_{ad} against C_{eq} , where C_{eq} is the equilibrium concentration of the electron acceptor in mol dm^{-3} and C_{ad} is the amount adsorbed in mol. m^{-2} . The plot was found to be linear (Fig.1). From the Langmuir plots of isotherms the limiting amounts of TCNQ and chloranil adsorbed on the rare earth oxides were obtained (Fig. 2 & 3). Data are given in Tables 4-30.

BET SURFACE AREA ANALYSIS

Kinetics & Catalysis Laboratory
Department of Chemistry
I.I.T. Madras - 600 036

Analysis done by: Dorothy Samuel
Sample ID : CUSAT NO: 22, Dr. S. Suganan.
Sample Weight : 1.17125 g.
Bulk Density : 0.69920 g/cc.
Sample outgas'd : 20 microns vacuum, 120°C
Data points :

| P/P_0 | $P/(P_0 - P) * N * 28$ |
|---------|------------------------|
| 0.035 | 4.351 |
| 0.113 | 12.185 |
| 0.174 | 17.012 |
| 0.223 | 20.629 |

SPECIFIC SURFACE AREA = 29.75 m²/g.

Pure Cu_2O . 800°C.

BET SURFACE AREA ANALYSIS

Kinetics & Catalysis Laboratory
Department of Chemistry
I.I.T. Madras _ 600 036

Analysis done by: Dorothy Samuel
Sample ID : CUSAT NO: 20, Dr. S. Suganan.
Sample Weight : 0.92885 g.
Bulk Density : 0.77558 g/cc.
Sample outgas'd : 20 microns vacuum, 120°C
Data points :

| P/P ₀ | P/(P ₀ -P)*N*28 |
|------------------|----------------------------|
| 0.034 | 4.093 |
| 0.112 | 11.841 |
| 0.167 | 15.969 |
| 0.218 | 19.089 |

SPECIFIC SURFACE AREA = 39.80 m²/g.

Pure La₂O₃ · 300°C

BET SURFACE AREA ANALYSIS

Kinetics & Catalysis Laboratory
Department of Chemistry
I.I.T. Madras _ 600 036

Analysis done by: Dorothy Samuel
Sample ID : CUSAT NO: 21, Dr. S. Suganan.
Sample Weight : 1.00215 g.
Bulk Density : 0.83675 g/cc.
Sample outgas'd : 20 microns vacuum, 120°C
Data points :

| P/P ₀ | P/(P ₀ -P)*N*28 |
|------------------|----------------------------|
| 0.035 | 3.837 |
| 0.130 | 11.948 |
| 0.201 | 17.097 |
| 0.257 | 21.011 |

SPECIFIC SURFACE AREA = 38.28 m²/g.

Pure La₂O₃ · 500°C


```

MMMMMMMMMMMMMMMMMMMMMMMMMMMMMMMMMMMMMMMMMMMMMMMMMMMMMMMMMMMMMMMMMMMMMMMMMMMMMMMMMMMMMMMMMMMMMMMMMMMMMMMMMMMM;
MMMMMMMMMMMMMMMMMMMMMMMMMMMMMMMMMMMMMMMMMMMMMMMMMMMMMMMMMMMMMMMMMMMMMMMMMMMMMMMMMMMMMMMMMMMMMMMMMMMMMMMMMMMM;
: Carlo Erba Strumentazione Microstructure Lab. : :
: MI. Le. S. TO. NE. 1 0 0 : :
MMMMMMMMMMMMMMMMMMMMMMMMMMMMMMMMMMMMMMMMMMMMMMMMMMMMMMMMMMMMMMMMMMMMMMMMMMMMMMMMMMMMMMMMMMMMMMMMMMMMMMMMMMMM<
:
: Calculation parameters of Sorptomatic :
:

```

```

le : CUSAT 10/CU10
ent : OUTGASSED AT 120 C
ator : DS
(mm/dd/yy) : 05-19-1992

```

```

layer thickness (a): 4.3 Total introduction : 11
r/limit pressure (torr): 760 Reduced introduction : 11
mass. gas ads. (g/mol): 28 Reduction factor : .25
ads. density (g/cm3): .808 Constant bur.(cm3/torr): .1163
tte temperature (c): -195.82 Sample weight (g): 1.12485
ating pressure (torr): 800 Sample Density (g/mm3): 1.63

```

```

MMMMMMMMMMMMMMMMMMMMMMMMMMMMMMMMMMMMMMMMMMMMMMMMMMMMMMMMMMMMMMMMMMMMMMMMMMMMMMMMMMMMMMMMMMMMMMMMMMMMMMMMMMMM<

```

```

l point (P/P0) for linear regression of B.E.T. region : 0
point (P/P0) for linear regression of B.E.T. region : .3
ation factor = .9992933
per Volume (CM3/G) = 5.574553
ic surface area (M2/G) = 24.35877

```

Pure Dy2O3 300°C

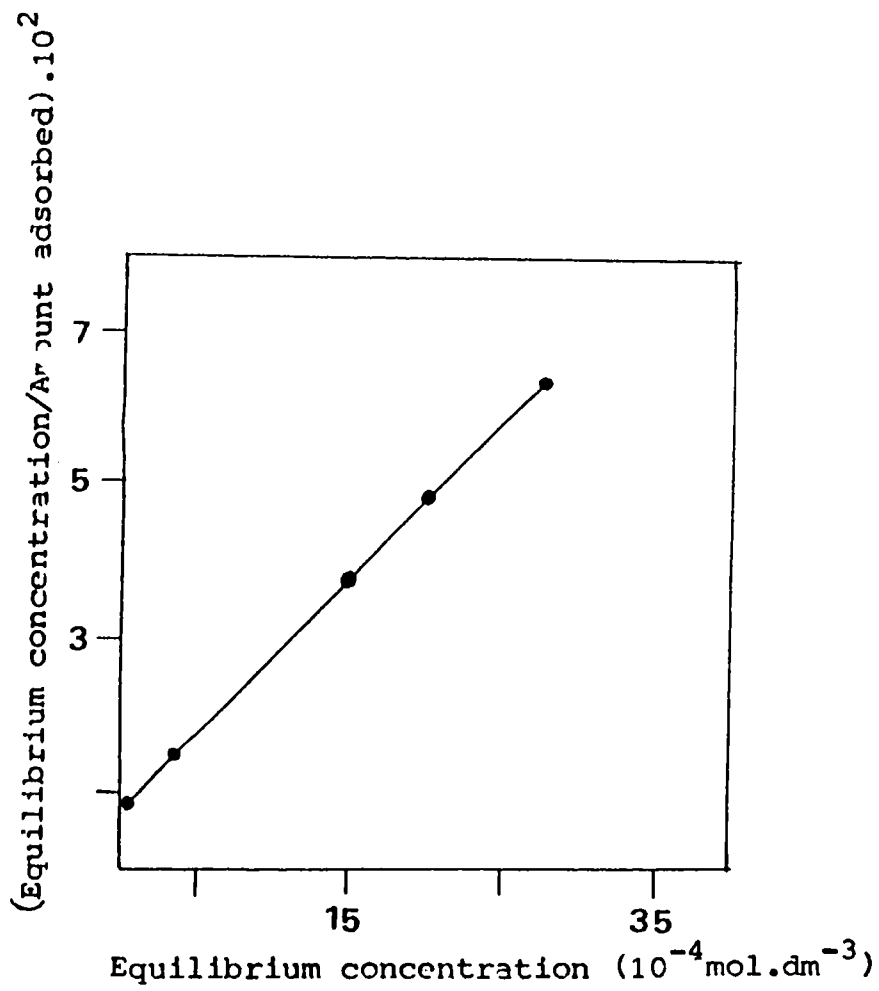


Fig.1 Linear form of Langmuir isotherm obtained for adsorption of chloranil on La_2O_3 (500°C)

| Table 4 - Adsorption of TCNQ in acetonitrile on La₂O₃ activated at 800°C | | |
|---|---|--|
| Initial concentration mol.dm ⁻³ | Equilibrium concentration mol. dm ⁻³ | Adsorbed amount mol. m ⁻² |
| 8.8646 x 10 ⁻⁵ | 3.0048 x 10 ⁻⁸ | 5.9644 x 10 ⁻⁶ |
| 4.4321 x 10 ⁻⁴ | 1.2019 x 10 ⁻⁷ | 2.9776 x 10 ⁻⁵ |
| 8.8643 x 10 ⁻⁴ | 3.7561 x 10 ⁻⁶ | 5.9328 x 10 ⁻⁵ |
| 2.2161 x 10 ⁻³ | 2.0283 x 10 ⁻⁴ | 1.3508 x 10 ⁻⁴ |
| 2.6593 x 10 ⁻³ | 4.0780 x 10 ⁻⁴ | 1.5133 x 10 ⁻⁴ |
| 4.4321 x 10 ⁻³ | 2.1635 x 10 ⁻³ | 1.5202 x 10 ⁻⁴ |

| Table 5 - Adsorption of TCNQ in ethyl acetate on La₂O₃ activated at 800°C | | |
|--|--|---|
| Initial concentration mol.dm ⁻³ | Equilibrium concentration mol.dm ⁻³ | Adsorbed amount mol.m ⁻² |
| 9.8634 x 10 ⁻⁵ | 4.9308 x 10 ⁻⁵ | 1.4136 x 10 ⁻⁶ |
| 4.9317 x 10 ⁻⁴ | 2.4886 x 10 ⁻⁴ | 6.9971 x 10 ⁻⁶ |
| 9.8634 x 10 ⁻⁴ | 5.0280 x 10 ⁻⁴ | 1.3854 x 10 ⁻⁵ |
| 1.9727 x 10 ⁻³ | 1.0046 x 10 ⁻³ | 2.7708 x 10 ⁻⁵ |
| 3.9453 x 10 ⁻³ | 2.3051 x 10 ⁻³ | 4.6958 x 10 ⁻⁵ |
| 4.9317 x 10 ⁻³ | 3.2809 x 10 ⁻³ | 4.7309 x 10 ⁻⁵ |

| Table 6 - Adsorption of TCNQ in dioxan on La₂O₃ activated at 800°C | | |
|---|--|---|
| Initial concentration mol.dm⁻³ | Equilibrium concentration mol.dm⁻³ | Adsorbed amount mol.m⁻² |
| 2.4879 x 10 ⁻⁴ | 2.4607 x 10 ⁻⁶ | 1.6507 x 10 ⁻⁵ |
| 4.9758 x 10 ⁻⁴ | 1.2694 x 10 ⁻⁴ | 2.4382 x 10 ⁻⁵ |
| 9.9516 x 10 ⁻⁴ | 5.4895 x 10 ⁻⁴ | 2.9931 x 10 ⁻⁵ |
| 1.2440 x 10 ⁻³ | 7.7444 x 10 ⁻⁴ | 3.1567 x 10 ⁻⁵ |
| 2.4879 x 10 ⁻³ | 1.9888 x 10 ⁻³ | 3.3488 x 10 ⁻⁵ |
| 2.8601 x 10 ⁻³ | 2.3554 x 10 ⁻³ | 3.3849 x 10 ⁻⁵ |

| Table 7 - Adsorption of chloranil in acetonitrile on La₂O₃ activated at 800°C | | |
|--|---|---|
| Initial concentration mol.dm⁻³ | Equilibrium/ concentration mol.dm⁻³ | Adsorbed amount mol.m⁻² |
| 8.0934 x 10 ⁻⁵ | 2.9865 x 10 ⁻⁷ | 5.4037 x 10 ⁻⁶ |
| 4.0467 x 10 ⁻⁴ | 3.9685 x 10 ⁻⁷ | 2.0744 x 10 ⁻⁵ |
| 8.0934 x 10 ⁻⁴ | 9.9550 x 10 ⁻⁷ | 5.4148 x 10 ⁻⁵ |
| 1.6187 x 10 ⁻³ | 1.4933 x 10 ⁻⁵ | 1.0769 x 10 ⁻⁴ |
| 2.0234 x 10 ⁻³ | 1.7297 x 10 ⁻⁴ | 1.2390 x 10 ⁻⁴ |
| 4.0467 x 10 ⁻³ | 2.1872 x 10 ⁻³ | 1.2456 x 10 ⁻⁴ |

| Table 8 - Adsorption of chloranil in ethyl acetate on La₂O₃ activated at 800°C | | |
|---|--|---|
| Initial concentration mol.dm⁻³ | Equilibrium concentration mol.dm⁻³ | Adsorbed amount mol.m⁻² |
| 4.9366 x 10 ⁻⁵ | 3.1913 x 10 ⁻⁷ | 1.1077 x 10 ⁻⁶ |
| 2.4683 x 10 ⁻⁴ | 6.1832 x 10 ⁻⁷ | 5.5617 x 10 ⁻⁶ |
| 4.9366 x 10 ⁻⁴ | 5.3255 x 10 ⁻⁶ | 1.1053 x 10 ⁻⁵ |
| 9.8732 x 10 ⁻⁴ | 3.2507 x 10 ⁻⁴ | 1.4975 x 10 ⁻⁵ |
| 1.9746 x 10 ⁻³ | 5.3105 x 10 ⁻⁴ | 3.2575 x 10 ⁻⁵ |
| 2.4683 x 10 ⁻³ | 8.5269 x 10 ⁻⁴ | 3.6436 x 10 ⁻⁵ |

| Table 9 - Adsorption of chloranil in dioxan on La₂O₃ activated at 800°C | | |
|--|--|---|
| Initial concentration mol.dm⁻³ | Equilibrium concentration mol.dm⁻³ | Adsorbed amount mol.m⁻² |
| 1.2038 x 10 ⁻⁵ | 1.6231 x 10 ⁻⁶ | 6.9795 x 10 ⁻⁷ |
| 6.0192 x 10 ⁻⁵ | 4.4810 x 10 ⁻⁶ | 3.7341 x 10 ⁻⁶ |
| 1.2038 x 10 ⁻⁴ | 1.3932 x 10 ⁻⁵ | 7.1378 x 10 ⁻⁶ |
| 3.0096 x 10 ⁻⁴ | 1.2038 x 10 ⁻⁴ | 1.2103 x 10 ⁻⁵ |
| 6.0192 x 10 ⁻⁴ | 4.1962 x 10 ⁻⁴ | 1.2207 x 10 ⁻⁵ |

| Table 10 - Adsorption of TCNQ in acetonitrile on La ₂ O ₃ activated at 500°C | | |
|--|---|--|
| Initial concentration mol.dm ⁻³ | Equilibrium concentration mol.dm ⁻³ | Adsorbed amount mol.m ⁻² |
| 1.9746 x 10 ⁻³ | 6.9748 x 10 ⁻⁴ | 6.6591 x 10 ⁻⁵ |
| 2.9619 x 10 ⁻³ | 1.3509 x 10 ⁻³ | 8.4169 x 10 ⁻⁵ |
| 3.4556 x 10 ⁻³ | 1.7539 x 10 ⁻³ | 8.8375 x 10 ⁻⁵ |
| 3.9493 x 10 ⁻³ | 2.0789 x 10 ⁻³ | 9.7139 x 10 ⁻⁵ |
| 4.9366 x 10 ⁻³ | 2.8814 x 10 ⁻³ | 1.0631 x 10 ⁻⁴ |
| 5.1423 x 10 ⁻³ | 3.0808 x 10 ⁻³ | 1.0771 x 10 ⁻⁴ |

| Table 11 - Adsorption of TCNQ in ethyl acetate on La ₂ O ₃ activated at 500°C | | |
|---|---|--|
| Initial concentration mol.dm ⁻³ | Equilibrium concentration mol.dm ⁻³ | Adsorbed amount mol.m ⁻² |
| 8.3550 x 10 ⁻⁵ | 1.0831 x 10 ⁻⁷ | 1.1529 x 10 ⁻⁶ |
| 4.1775 x 10 ⁻⁴ | 1.0985 x 10 ⁻⁶ | 5.7585 x 10 ⁻⁶ |
| 8.3550 x 10 ⁻⁴ | 3.8681 x 10 ⁻⁶ | 1.1494 x 10 ⁻⁵ |
| 1.8041 x 10 ⁻³ | 4.8269 x 10 ⁻⁶ | 1.8252 x 10 ⁻⁵ |
| 3.6083 x 10 ⁻³ | 1.7623 x 10 ⁻⁵ | 2.5518 x 10 ⁻⁵ |
| 4.5103 x 10 ⁻³ | 2.6105 x 10 ⁻⁵ | 2.6153 x 10 ⁻⁵ |

| Table 12 - Adsorption on TCNQ in dioxan on La₂O₃ activated at 500°C | | |
|--|--|---|
| Initial concentration mol.dm⁻³ | Equilibrium concentration mol.dm⁻³ | Adsorbed amount mol.m⁻² |
| 6.7094 x 10 ⁻⁵ | 5.3482 x 10 ⁻⁵ | 7.0946 x 10 ⁻⁷ |
| 1.3419 x 10 ⁻⁴ | 1.0658 x 10 ⁻⁴ | 1.4396 x 10 ⁻⁶ |
| 2.6838 x 10 ⁻⁴ | 2.1239 x 10 ⁻⁴ | 2.9188 x 10 ⁻⁶ |
| 3.3547 x 10 ⁻⁴ | 2.6693 x 10 ⁻⁴ | 3.5752 x 10 ⁻⁶ |
| 6.7094 x 10 ⁻⁴ | 5.7006 x 10 ⁻⁴ | 5.2664 x 10 ⁻⁶ |
| 7.5230 x 10 ⁻⁴ | 6.4603 x 10 ⁻⁴ | 5.5522 x 10 ⁻⁶ |

| Table 13 - Adsorption of chloranil in acetonitrile on La₂O₃ activated at 500°C | | |
|---|--|---|
| Initial concentration mol.dm⁻³ | Equilibrium concentration mol.dm⁻³ | Adsorbed amount mol.m⁻² |
| 8.1422 x 10 ⁻⁵ | 6.5894 x 10 ⁻⁵ | 8.0293 x 10 ⁻⁷ |
| 4.0712 x 10 ⁻⁴ | 3.6603 x 10 ⁻⁴ | 2.1281 x 10 ⁻⁶ |
| 8.1422 x 10 ⁻⁴ | 7.5750 x 10 ⁻⁴ | 2.9634 x 10 ⁻⁶ |
| 1.6284 x 10 ⁻³ | 1.5492 x 10 ⁻³ | 4.1345 x 10 ⁻⁶ |
| 2.0355 x 10 ⁻³ | 1.9511 x 10 ⁻³ | 4.4007 x 10 ⁻⁶ |
| 2.8601 x 10 ⁻³ | 2.7754 x 10 ⁻³ | 4.4232 x 10 ⁻⁶ |

| Table 14 - Adsorption of chloranil in ethyl acetate on La ₂ O ₃ activated at 500°C | | |
|--|---|--|
| Initial concentration mol.dm ⁻³ | Equilibrium concentration mol.dm ⁻³ | Adsorbed amount mol.m ⁻² |
| 1.5455 x 10 ⁻⁵ | 7.4280 x 10 ⁻⁶ | 4.1771 x 10 ⁻⁷ |
| 7.7273 x 10 ⁻⁵ | 4.8257 x 10 ⁻⁵ | 1.4980 x 10 ⁻⁶ |
| 1.5455 x 10 ⁻⁴ | 9.6130 x 10 ⁻⁵ | 3.0108 x 10 ⁻⁶ |
| 2.3182 x 10 ⁻⁴ | 1.6941 x 10 ⁻⁴ | 3.2479 x 10 ⁻⁶ |
| 3.0910 x 10 ⁻⁴ | 2.4389 x 10 ⁻⁴ | 3.3934 x 10 ⁻⁶ |
| 7.7273 x 10 ⁻⁴ | 7.0529 x 10 ⁻⁴ | 3.5026 x 10 ⁻⁶ |

| Table 15 - Adsorption of chloranil in dioxan on La ₂ O ₃ activated at 500°C | | |
|---|---|--|
| Initial concentration mol.dm ⁻³ | Equilibrium concentration mol.dm ⁻³ | Adsorbed amount mol.m ⁻² |
| 8.4024 x 10 ⁻⁵ | 9.8850 x 10 ⁻⁷ | 1.015 x 10 ⁻⁷ |
| 4.2012 x 10 ⁻⁴ | 2.467 x 10 ⁻⁶ | 5.1077 x 10 ⁻⁷ |
| 8.4024 x 10 ⁻⁴ | 3.642 x 10 ⁻⁶ | 1.0230 x 10 ⁻⁶ |
| 1.6805 x 10 ⁻³ | 5.464 x 10 ⁻⁶ | 1.3855 x 10 ⁻⁶ |
| 3.0248 x 10 ⁻³ | 1.897 x 10 ⁻⁵ | 1.3787 x 10 ⁻⁶ |

| Initial concentration mol.dm⁻³ | Equilibrium concentration mol.dm⁻³ | Adsorbed amount mol.m⁻² |
|--|--|---|
| 7.7105 x 10 ⁻⁴ | 6.4096 x 10 ⁻⁴ | 6.5241 x 10 ⁻⁶ |
| 1.1566 x 10 ⁻³ | 9.7027 x 10 ⁻⁴ | 9.3447 x 10 ⁻⁶ |
| 1.5421 x 10 ⁻³ | 1.3686 x 10 ⁻³ | 9.8417 x 10 ⁻⁶ |
| 3.8552 x 10 ⁻³ | 3.2522 x 10 ⁻³ | 3.0176 x 10 ⁻⁵ |
| 4.4958 x 10 ⁻³ | 3.8703 x 10 ⁻³ | 3.1306 x 10 ⁻⁵ |
| 5.9944 x 10 ⁻³ | 5.3494 x 10 ⁻³ | 3.2412 x 10 ⁻⁵ |

| Initial concentration mol.dm⁻³ | Equilibrium concentration mol.dm⁻³ | Adsorbed amount mol.m⁻² |
|--|--|---|
| 2.7622 x 10 ⁻⁵ | 1.4945 x 10 ⁻⁵ | 3.6330 x 10 ⁻⁷ |
| 1.3811 x 10 ⁻⁴ | 7.4853 x 10 ⁻⁵ | 1.8129 x 10 ⁻⁶ |
| 2.7622 x 10 ⁻⁴ | 1.4971 x 10 ⁻⁴ | 3.6256 x 10 ⁻⁶ |
| 5.5244 x 10 ⁻⁴ | 2.9819 x 10 ⁻⁴ | 7.2510 x 10 ⁻⁶ |
| 1.1049 x 10 ⁻³ | 7.0226 x 10 ⁻⁴ | 1.1504 x 10 ⁻⁵ |
| 1.3811 x 10 ⁻³ | 9.5605 x 10 ⁻⁴ | 1.2181 x 10 ⁻⁵ |

| Table 18 - Adsorption of TCNQ in dioxan on La₂O₃ activated at 300°C | | |
|--|--|---|
| Initial concentration mol.dm⁻³ | Equilibrium concentration mol.dm⁻³ | Adsorbed amount mol.m⁻² |
| 1.6651 x 10 ⁻⁵ | 1.8732 x 10 ⁻⁶ | 7.4261 x 10 ⁻⁷ |
| 8.3256 x 10 ⁻⁵ | 4.0000 x 10 ⁻⁵ | 2.1737 x 10 ⁻⁶ |
| 1.3321 x 10 ⁻⁴ | 8.6195 x 10 ⁻⁵ | 2.3578 x 10 ⁻⁶ |
| 1.6651 x 10 ⁻⁴ | 1.1405 x 10 ⁻⁴ | 2.6309 x 10 ⁻⁶ |
| 1.9981 x 10 ⁻⁴ | 1.3486 x 10 ⁻⁴ | 3.2572 x 10 ⁻⁶ |
| 3.3302 x 10 ⁻⁴ | 2.6750 x 10 ⁻⁴ | 3.2925 x 10 ⁻⁶ |

| Table 19 - Adsorption of TCNQ in acetonitrile on Dy₂O₃ activated at 800°C | | |
|--|--|---|
| Initial concentration mol.dm⁻³ | Equilibrium concentration mol.dm⁻³ | Adsorbed amount mol.m⁻² |
| 2.5858 x 10 ⁻⁴ | 1.2834 x 10 ⁻⁴ | 8.8053 x 10 ⁻⁶ |
| 5.1717 x 10 ⁻⁴ | 2.9553 x 10 ⁻⁴ | 1.5005 x 10 ⁻⁵ |
| 1.0343 x 10 ⁻³ | 3.8525 x 10 ⁻⁴ | 4.3959 x 10 ⁻⁵ |
| 2.0687 x 10 ⁻³ | 1.2310 x 10 ⁻³ | 5.6732 x 10 ⁻⁵ |
| 2.2530 x 10 ⁻³ | 1.2920 x 10 ⁻³ | 6.0229 x 10 ⁻⁵ |
| 2.5858 x 10 ⁻³ | 1.5461 x 10 ⁻³ | 6.0257 x 10 ⁻⁵ |

| Table 20 - Adsorption of TCNQ in ethyl acetate on Dy₂O₃ activated at 800°C | | |
|---|--|---|
| Initial concentration mol.dm⁻³ | Equilibrium concentration mol.dm⁻³ | Adsorbed amount mol.m⁻² |
| 3.6632 x 10 ⁵ | 6.9408 x 10 ⁶ | 3.9667 x 10 ⁷ |
| 1.8316 x 10 ⁴ | 3.1735 x 10 ⁵ | 2.0230 x 10 ⁶ |
| 3.6632 x 10 ⁴ | 3.3184 x 10 ⁵ | 4.4507 x 10 ⁶ |
| 7.3264 x 10 ⁴ | 1.3513 x 10 ⁴ | 9.7916 x 10 ⁶ |
| 1.4653 x 10 ³ | 1.5396 x 10 ⁴ | 1.9507 x 10 ⁵ |
| 1.8316 x 10 ³ | 1.7365 x 10 ⁴ | 2.2150 x 10 ⁵ |

| Table 21 - Adsorption of TCNQ in dioxan on Dy₂O₃ activated at 800°C | | |
|--|--|---|
| Initial concentration mol.dm⁻³ | Equilibrium concentration mol.dm⁻³ | Adsorbed amount mol.m⁻² |
| 9.8906 x 10 ⁻⁶ | 1.0091 x 10 ⁻⁷ | 6.6979 x 10 ⁻⁷ |
| 4.9953 x 10 ⁻⁵ | 3.0049 x 10 ⁻⁵ | 1.3480 x 10 ⁻⁶ |
| 9.8906 x 10 ⁻⁵ | 5.5004 x 10 ⁻⁵ | 3.0411 x 10 ⁻⁶ |
| 1.9981 x 10 ⁻⁴ | 1.3522 x 10 ⁻⁴ | 4.3576 x 10 ⁻⁵ |
| 3.9963 x 10 ⁻⁴ | 2.1999 x 10 ⁻⁴ | 1.2168 x 10 ⁻⁵ |
| 4.9953 x 10 ⁻⁴ | 2.9972 x 10 ⁻⁴ | 1.3525 x 10 ⁻⁵ |

| Table 22 - Adsorption of chloranil in ethyl acetate on Dy ₂ O ₃ activated at 800°C | | |
|--|---|--|
| Initial concentration mol.dm ⁻³ | Equilibrium concentration mol.dm ⁻³ | Adsorbed amount mol.m ⁻² |
| 5.0954 x 10 ⁻⁵ | 2.0614 x 10 ⁻⁶ | 3.3706 x 10 ⁻⁶ |
| 2.5297 x 10 ⁻⁴ | 5.3776 x 10 ⁻⁵ | 1.348 x 10 ⁻⁵ |
| 5.0954 x 10 ⁻⁴ | 5.6016 x 10 ⁻⁵ | 3.0411 x 10 ⁻⁵ |
| 1.0119 x 10 ⁻³ | 4.4212 x 10 ⁻⁴ | 4.1899 x 10 ⁻⁵ |
| 2.0238 x 10 ⁻³ | 1.3530 x 10 ⁻³ | 4.7432 x 10 ⁻⁵ |
| 2.5297 x 10 ⁻³ | 1.7948 x 10 ⁻³ | 4.9583 x 10 ⁻⁵ |

| Table 23 - Adsorption of chloranil in ethyl acetate on Dy ₂ O ₃ activated at 800°C | | |
|--|---|--|
| Initial concentration mol.dm ⁻³ | Equilibrium concentration mol.dm ⁻³ | Adsorbed amount mol.m ⁻² |
| 1.8546 x 10 ⁻⁵ | 8.3100 x 10 ⁻⁷ | 2.4491 x 10 ⁻⁷ |
| 9.2728 x 10 ⁻⁵ | 4.1388 x 10 ⁻⁶ | 1.2246 x 10 ⁻⁶ |
| 1.8546 x 10 ⁻⁴ | 1.0088 x 10 ⁻⁵ | 2.4247 x 10 ⁻⁶ |
| 3.7091 x 10 ⁻⁴ | 2.8861 x 10 ⁻⁵ | 4.7283 x 10 ⁻⁶ |
| 7.4182 x 10 ⁻⁴ | 1.5511 x 10 ⁻⁴ | 8.1134 x 10 ⁻⁶ |
| 9.2728 x 10 ⁻⁴ | 2.7987 x 10 ⁻⁴ | 8.9457 x 10 ⁻⁶ |

| Table 24 - Adsorption on chloranil in dioxan on Dy₂O₃ activated at 800°C | | |
|---|--|---|
| Initial concentration mol.dm⁻³ | Equilibrium concentration mol.dm⁻³ | Adsorbed amount mol.m⁻² |
| 1.0493 x 10 ⁻⁵ | 4.2130 x 10 ⁻⁶ | 4.2533 x 10 ⁻⁷ |
| 5.2465 x 10 ⁻⁵ | 4.0039 x 10 ⁻⁵ | 8.4158 x 10 ⁻⁷ |
| 2.0986 x 10 ⁻⁴ | 1.9290 x 10 ⁻⁴ | 1.1485 x 10 ⁻⁶ |
| 4.1972 x 10 ⁻⁴ | 3.9704 x 10 ⁻⁴ | 1.5328 x 10 ⁻⁶ |
| 5.2465 x 10 ⁻⁴ | 5.0170 x 10 ⁻⁴ | 1.5964 x 10 ⁻⁶ |

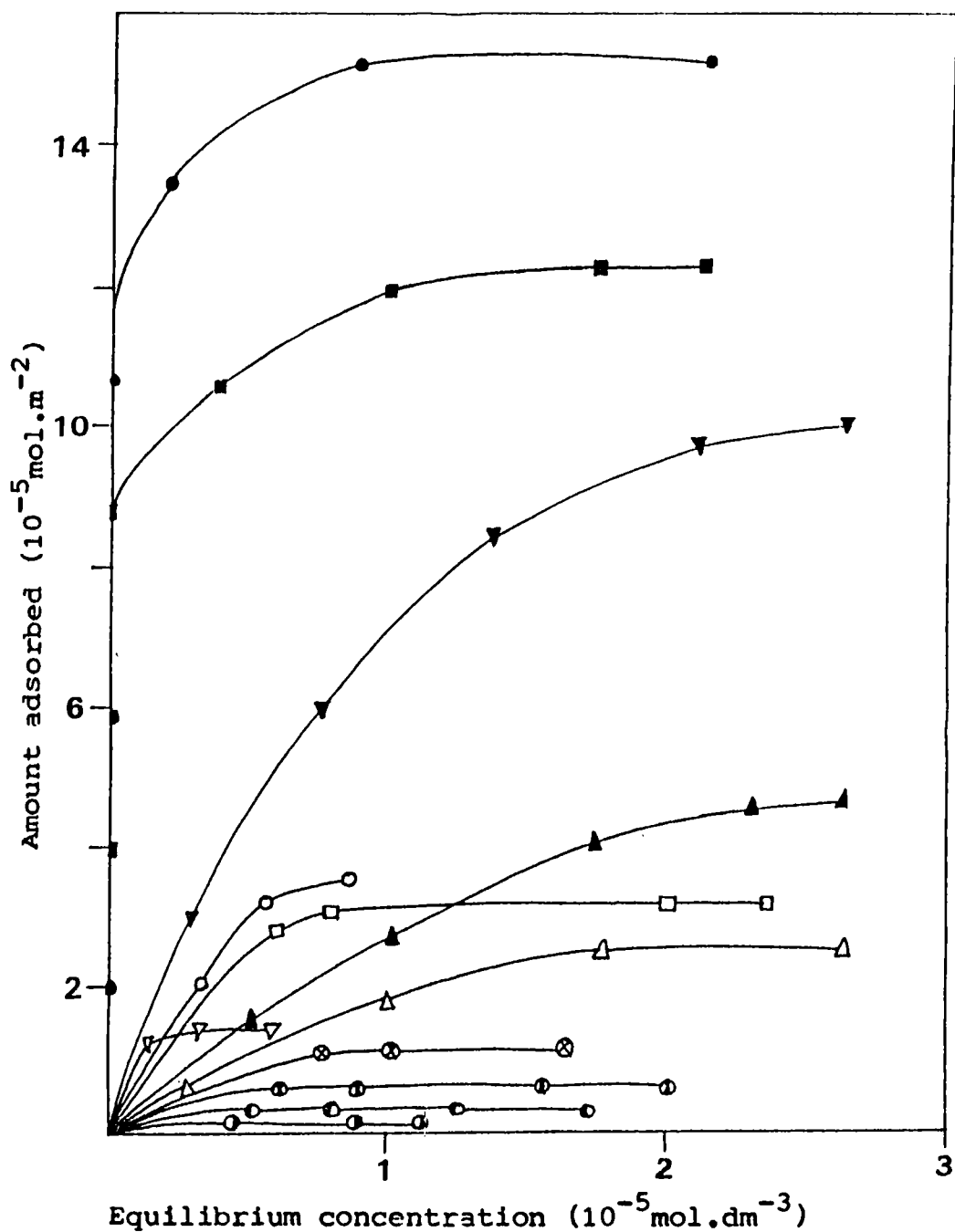
| Table 25 - Adsorption of TCNQ in acetonitrile on Dy₂O₃ activated at 500°C | | |
|--|--|---|
| Initial concentration mol.dm⁻³ | Equilibrium concentration mol.dm⁻³ | Adsorbed amount mol.m⁻² |
| 5.2304 x 10 ⁻⁵ | 2.3130 x 10 ⁻⁵ | 2.3841 x 10 ⁻⁶ |
| 2.6152 x 10 ⁻⁴ | 5.3269 x 10 ⁻⁵ | 1.7056 x 10 ⁻⁵ |
| 5.2304 x 10 ⁻⁴ | 9.3893 x 10 ⁻⁵ | 3.5176 x 10 ⁻⁵ |
| 1.8306 x 10 ⁻³ | 1.3396 x 10 ⁻³ | 4.0227 x 10 ⁻⁵ |
| 2.6152 x 10 ⁻³ | 2.0193 x 10 ⁻³ | 4.0775 x 10 ⁻⁵ |

| Table 26 - Adsorption of TCNQ in Ethyl acetate on Dy ₂ O ₃ activated at 500°C | | |
|---|---|--|
| Initial concentration mol.dm ⁻³ | Equilibrium concentration mol.dm ⁻³ | Adsorbed amount mol.m ⁻² |
| 2.0640 x 10 ⁻⁴ | 1.4150 x 10 ⁻⁵ | 2.1645 x 10 ⁻⁶ |
| 2.0640 x 10 ⁻³ | 8.6561 x 10 ⁻⁴ | 1.3496 x 10 ⁻⁵ |
| 5.1601 x 10 ⁻³ | 3.0036 x 10 ⁻³ | 2.4270 x 10 ⁻⁵ |
| 7.2243 x 10 ⁻³ | 5.0151 x 10 ⁻³ | 2.4869 x 10 ⁻⁵ |
| 8.3692 x 10 ⁻³ | 6.855 x 10 ⁻³ | 2.8334 x 10 ⁻⁵ |
| 9.8261 x 10 ⁻³ | 7.3027 x 10 ⁻³ | 2.8434 x 10 ⁻⁵ |

| Table 27 - Adsorption of TCNQ in dioxan on Dy ₂ O ₃ activated at 500°C | | |
|--|---|--|
| Initial concentration mol.dm ⁻³ | Equilibrium concentration mol.dm ⁻³ | Adsorbed amount mol.m ⁻² |
| 5.3284 x 10 ⁻⁶ | 1.0247 x 10 ⁻⁷ | 4.2814 x 10 ⁻⁷ |
| 1.3321 x 10 ⁻⁵ | 6.1576 x 10 ⁻⁸ | 1.0851 x 10 ⁻⁶ |
| 6.6605 x 10 ⁻⁵ | 4.9173 x 10 ⁻⁵ | 1.4283 x 10 ⁻⁶ |
| 1.3321 x 10 ⁻⁴ | 1.1486 x 10 ⁻⁴ | 1.5027 x 10 ⁻⁶ |
| 2.6642 x 10 ⁻⁴ | 2.4768 x 10 ⁻⁴ | 1.5347 x 10 ⁻⁶ |

| Table 28 - Adsorption of chloranil in acetonitrile on Dy₂O₃ activated at 500°C | | |
|---|--|---|
| Initial concentration mol.dm⁻³ | Equilibrium concentration mol.dm⁻³ | Adsorbed amount mol.m⁻² |
| 4.5551 x 10 ⁻⁵ | 6.6044 x 10 ⁻⁶ | 3.5206 x 10 ⁻⁶ |
| 2.2775 x 10 ⁻⁴ | 8.9837 x 10 ⁻⁵ | 1.1304 x 10 ⁻⁵ |
| 4.5551 x 10 ⁻⁴ | 2.6355 x 10 ⁻⁴ | 1.5728 x 10 ⁻⁵ |
| 6.8325 x 10 ⁻⁴ | 4.6028 x 10 ⁻⁴ | 1.8269 x 10 ⁻⁵ |
| 9.1101 x 10 ⁻⁴ | 6.7582 x 10 ⁻⁴ | 1.9270 x 10 ⁻⁵ |

| Table 29 - Adsorption on chloranil in ethyl acetate on Dy₂O₃ activated at 500°C | | |
|--|--|---|
| Initial concentration mol.dm⁻³ | Equilibrium concentration mol.dm⁻³ | Adsorbed amount mol.m⁻² |
| 8.4024 x 10 ⁻⁵ | 9.8850 x 10 ⁻⁷ | 1.0152 x 10 ⁻⁷ |
| 4.2012 x 10 ⁻⁴ | 2.4671 x 10 ⁻⁶ | 5.1077 x 10 ⁻⁷ |
| 8.4024 x 10 ⁻⁴ | 3.6423 x 10 ⁻⁶ | 1.0230 x 10 ⁻⁶ |
| 1.6805 x 10 ⁻³ | 5.4647 x 10 ⁻⁴ | 1.3855 x 10 ⁻⁶ |
| 3.0248 x 10 ⁻³ | 1.8968 x 10 ⁻³ | 1.3787 x 10 ⁻⁶ |



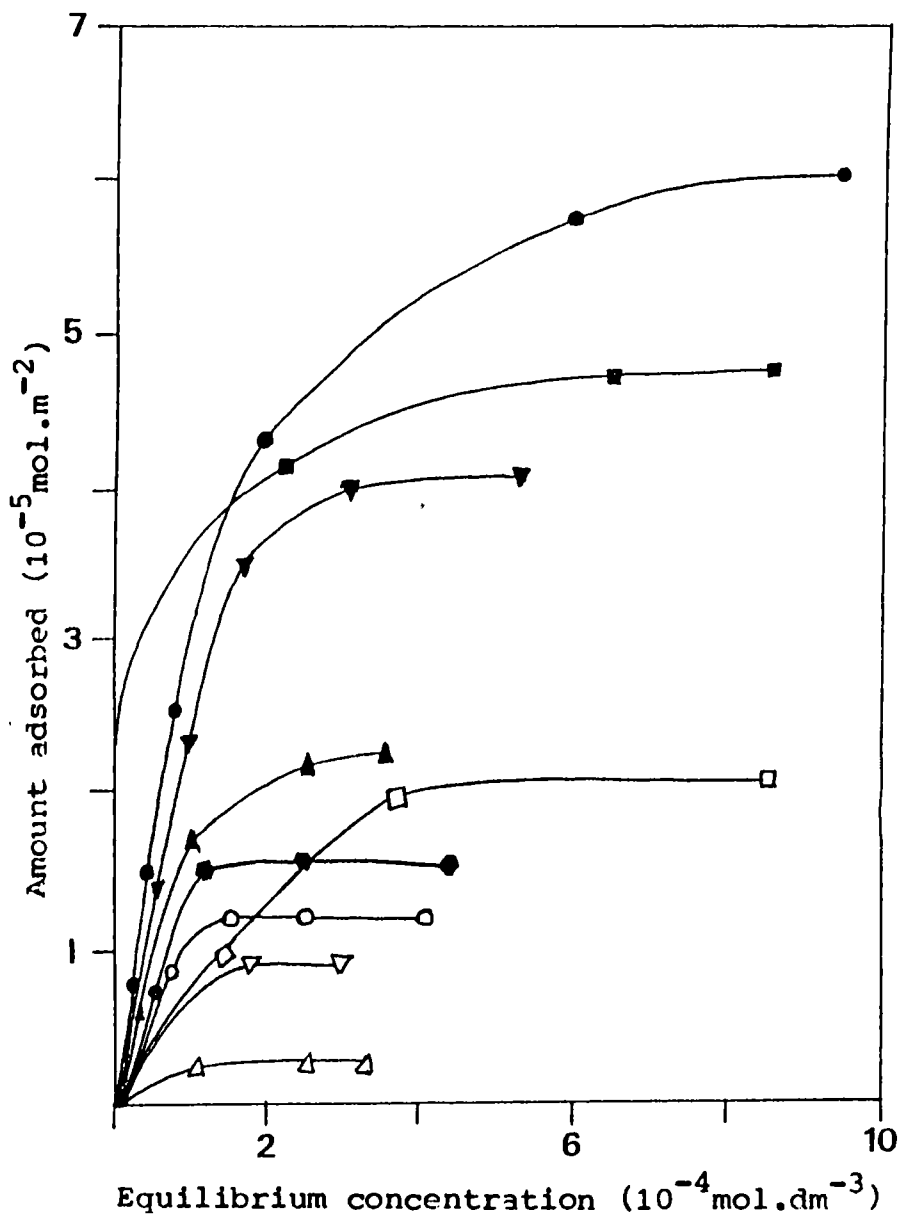
Electron acceptor/Solvent/Activation temperature(0°C)

(CA - Chloranil; AN - acetonitrile; TC - TCNQ;

EA - Ethyl acetate; D-1,4 dioxan)

| | | | |
|-------------|-------------|-------------|-------------|
| ■ CA/AN/800 | ● TC/AN/800 | ○ CA/EA/800 | ▲ TC/EA/800 |
| ▽ CA/D/800 | □ TC/D/800 | ⊙ CA/AN/500 | ▼ TC/AN/500 |
| ⊙ CA/EA/500 | △ TC/EA/500 | ⊙ TC/D/500 | ⊙ TC/AN/300 |

Fig.2 Adsorption isotherms of La_2O_3



Electron acceptor/Solvent/Activation temperature(0°C)

(CA - Chloranil; AN - acetonitrile; TC - TCNQ;

EA - Ethyl acetate; D-Dioxan)

- | | | |
|-------------|-------------|-------------|
| ● TC/AN/800 | □ TC/EA/800 | ○ TC/D/800 |
| ■ CA/AN/800 | ▽ CA/EA/800 | ▼ TC/AN/500 |
| ▲ CA/AN/500 | ◆ CA/D/800 | △ TC/AN/300 |

Fig.3 Adsorption isotherms of Dy_2O_3

| Table 30 - Adsorption of TCNQ in acetonitrile on Dy ₂ O ₃ activated at 300°C | | |
|--|---|--|
| Initial concentration mol.dm ⁻³ | Equilibrium concentration mol.dm ⁻³ | Adsorbed amount mol.m ⁻² |
| 3.3302 x 10 ⁻⁵ | 2.5570 x 10 ⁻⁵ | 6.4698 x 10 ⁻⁷ |
| 1.6651 x 10 ⁻⁴ | 1.5591 x 10 ⁻⁴ | 8.7018 x 10 ⁻⁷ |
| 3.3302 x 10 ⁻⁴ | 3.1695 x 10 ⁻⁴ | 1.3224 x 10 ⁻⁶ |
| 5.3280 x 10 ⁻⁴ | 5.1570 x 10 ⁻⁴ | 1.4045 x 10 ⁻⁶ |
| 6.6605 x 10 ⁻⁴ | 6.4763 x 10 ⁻⁴ | 1.5083 x 10 ⁻⁶ |

When TCNQ and chloranil were adsorbed from the solution on the surface of the oxides, the surface showed remarkable colouration characteristic for the kind of acceptors like bluish green for TCNQ and light pink for chloranil. These colourations are due to the interaction between the acceptor adsorbed and the oxide surface and new adsorbed species are formed on the surface [6].

The ESR spectrum of the samples coloured with adsorption of TCNQ and chloranil gave unresolved spectral line with a g value of 2.003 and 2.011 respectively, indicating the presence of anion radicals on the surface [7]. The g values were calculated using the standard method [F.K. Cneububl, J. Chem. Phys., 33 1074 (1960)] .

The radical concentration of TCNQ and chloranil formed on the oxide surfaces

2 in India

RECITER

3

ESR spectrum of $\text{FeO} \cdot \text{La}_2\text{O}_3$

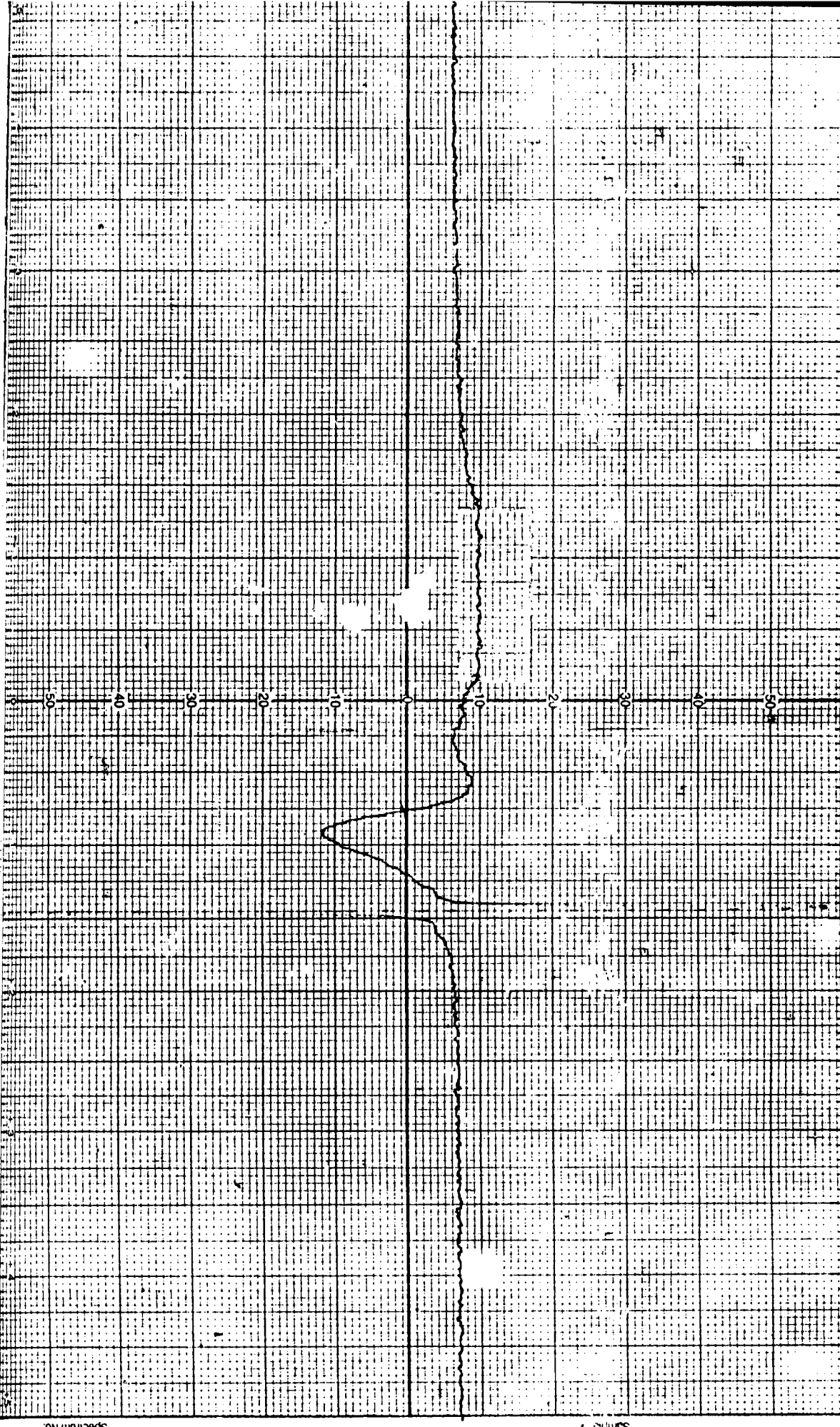
R.S.I.C. I.I.T. MADRAS-36.

Sample: FeO

Modulation Amplitude $\times 4.0$ G
 Receiver Gain RT
 Microwave Power $\times 0$ mW
 Microwave Frequency 9.451 GHz

Modulation Frequency 100 Hz
 Temperature RT

Operator: _____
 Date: _____
 Remarks: _____



ESR spectrum of Chloranil / $C_{6}O_3$

R.S.I.C. I.I.T. MADRAS-36.

Operator: *Bumble JI*

Microwave Power: 10 mW

Receiver Gain: 3

Modulation Amplitude: 4.0 G

Modulation Frequency: 100 kHz

Microwave Frequency: 9.451 GHz

Temperature: RT

Modulation Frequency: 100 kHz

Temperature: RT



Remarks

are given in Tables 31-34. The data were estimated by comparing the area under the peak for adsorbed sample and for standard solutions of 2,2-diphenyl-1-picrylhydrazyl in benzene. Fig. 4 & 5 show the radical concentration of electron acceptor formed on the oxide surface against the equilibrium concentration of electron acceptors in solution for lanthana and dysprosia. The isotherms obtained were also of Langmuir type. The limiting radical concentration were calculated from these plots.

| Table 31 - Adsorption of TCNQ in acetonitrile on La₂O₃ activated at 800°C | | |
|--|--|--|
| Initial concentration mol.dm⁻³ | Equilibrium concentration mol.dm⁻³ | Adsorbed amount 10¹⁸ spins m² |
| 8.8646 x 10 ⁻⁵ | 3.0048 x 10 ⁻⁸ | 0.2583 |
| 4.4321 x 10 ⁻⁴ | 1.2019 x 10 ⁻⁷ | 1.0330 |
| 8.8643 x 10 ⁻⁴ | 3.7561 x 10 ⁻⁶ | 2.5833 |
| 2.2161 x 10 ⁻³ | 2.0283 x 10 ⁻⁴ | 6.7160 |
| 2.6593 x 10 ⁻³ | 4.0780 x 10 ⁻⁴ | 7.7752 |
| 4.4321 x 10 ⁻³ | 2.1635 x 10 ⁻³ | 7.8551 |

| Table 32 - Adsorption of chloranil in acetonitrile on La₂O₃ activated at 800°C | | |
|---|--|---|
| Initial concentration mol.dm⁻³ | Equilibrium concentration mol.dm⁻³ | Adsorbed amount 10¹⁷ spins m⁻² |
| 8.0934 x 10 ⁻⁵ | 2.9865 x 10 ⁻⁷ | 0.1684 |
| 4.0467 x 10 ⁻⁴ | 3.9685 x 10 ⁻⁷ | 0.8424 |
| 8.0934 x 10 ⁻⁴ | 9.9550 x 10 ⁻⁷ | 1.6892 |
| 1.6187 x 10 ⁻³ | 1.4933 x 10 ⁻⁵ | 3.3338 |
| 2.0234 x 10 ⁻³ | 1.7297 x 10 ⁻⁴ | 3.8381 |
| 4.0467 x 10 ⁻³ | 2.1872 x 10 ⁻³ | 3.8446 |

| Table 33 - Adsorption of TCNQ in acetonitrile on Dy₂O₃ activated at 800°C | | |
|--|--|---|
| Initial concentration mol.dm⁻³ | Equilibrium concentration mol.dm⁻³ | Adsorbed amount 10¹⁸ spins m⁻² |
| 2.5858 x 10 ⁻⁴ | 1.2834 x 10 ⁻⁴ | 0.4546 |
| 5.1717 x 10 ⁻⁴ | 2.9553 x 10 ⁻⁴ | 0.7753 |
| 1.0343 x 10 ⁻³ | 3.8525 x 10 ⁻⁴ | 2.2712 |
| 2.0687 x 10 ⁻³ | 1.2310 x 10 ⁻³ | 2.8933 |
| 2.2530 x 10 ⁻³ | 1.2920 x 10 ⁻³ | 3.1103 |
| 2.5858 x 10 ⁻³ | 1.5461 x 10 ⁻³ | 3.1133 |

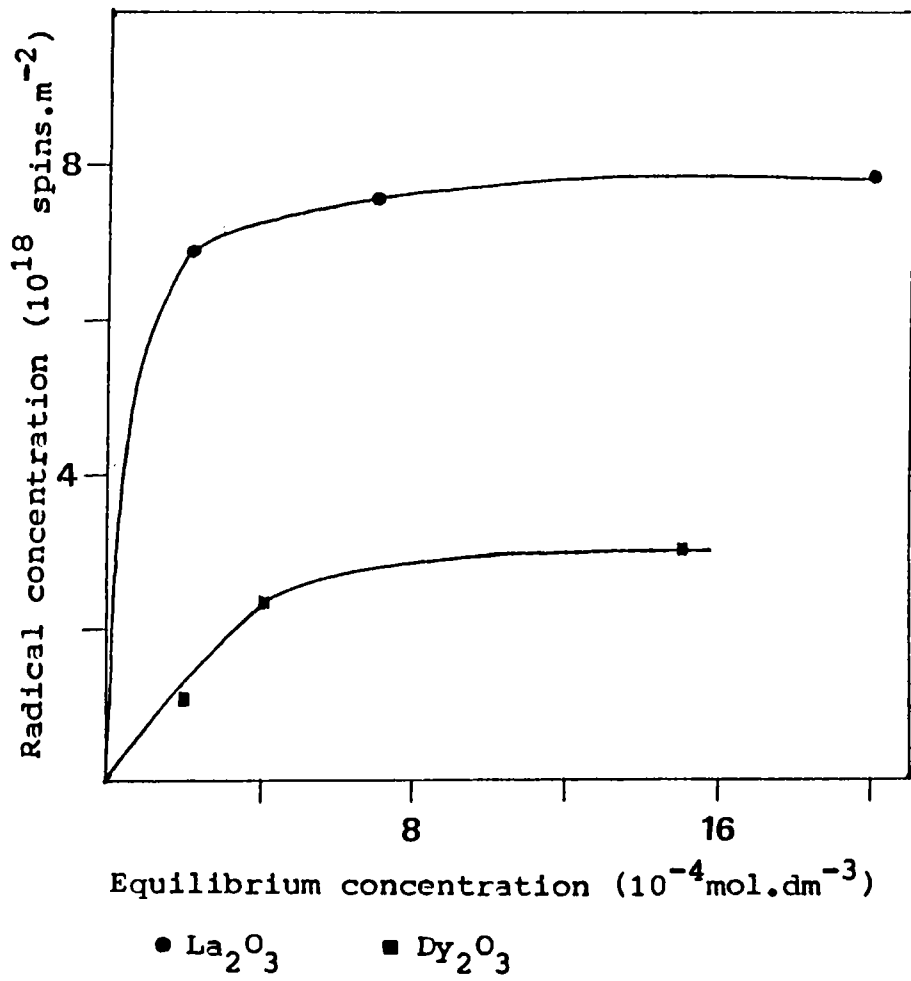


Fig.4 Radical concentration of TCNQ on La_2O_3 and Dy_2O_3 vs. equilibrium concentration of TCNQ.

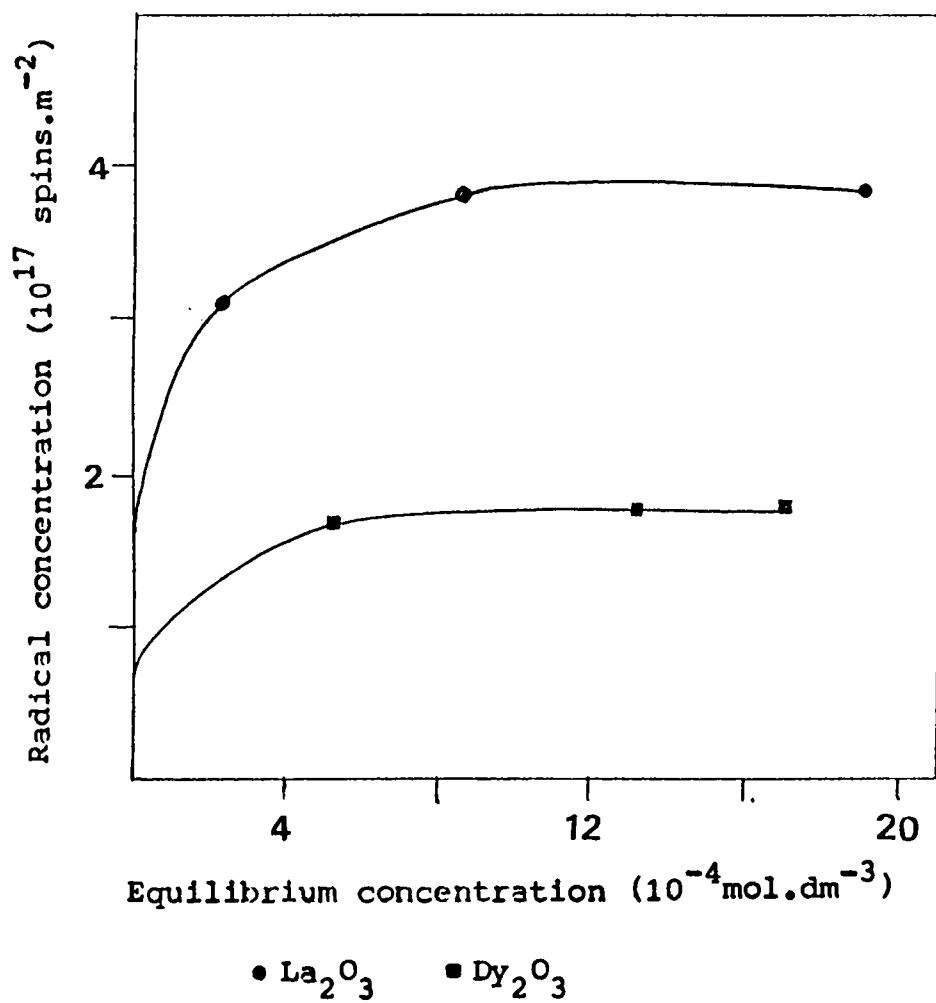


Fig.5 Radical concentration of chloranil on La_2O_3 and Dy_2O_3 vs. equilibrium concentration of chloranil

| Table 34 - Adsorption of chloranil in acetonitrile on Dy₂O₃ activated at 800°C | | |
|---|--|---|
| Initial concentration mol.dm⁻³ | Equilibrium concentration mol.dm⁻³ | Adsorbed amount 10¹⁷ spins m⁻² |
| 5.0594 x 10 ⁻⁵ | 2.0614 x 10 ⁻⁶ | 0.2745 |
| 2.5297 x 10 ⁻⁴ | 5.3776 x 10 ⁻⁵ | 0.4680 |
| 5.0594 x 10 ⁻⁴ | 5.6016 x 10 ⁻⁵ | 1.3697 |
| 1.0119 x 10 ⁻³ | 4.4212 x 10 ⁻⁴ | 1.7700 |
| 2.0238 x 10 ⁻³ | 1.3530 x 10 ⁻³ | 1.7690 |
| 2.5297 x 10 ⁻³ | 1.7948 x 10 ⁻³ | 1.8798 |

The electronic spectrum of the samples coloured by TCNQ adsorption are given in figure (4a). The bands near 400nm and 600nm were also reported by Meguro et al when they studied the electronic spectrum of TiO₂ coloured by TCNQ adsorption. [K.Meguro and K. Esumi, Bull Chem Soc. Jpn., 55 1647 (1982)]. The bands near 600 nm are related to the dimeric TCNQ anion radical, which absorbs light at 643nm [8]. This tentative attribution is supported by the characteristic features that neutral TCNQ absorbs only at 395 nm, that TCNQ has a high electron affinity, and that the TCNQ anion radical derivatives are stable even at room temperature [9-10]. In the case of rare earth oxides, these assignments do not hold completely, because rare earth oxides have characteristic bands in the same region. The ESR and electronic spectra provide evidence that anion radicals are formed as a result of electron transfer from the oxide surface to adsorbed electron acceptors.

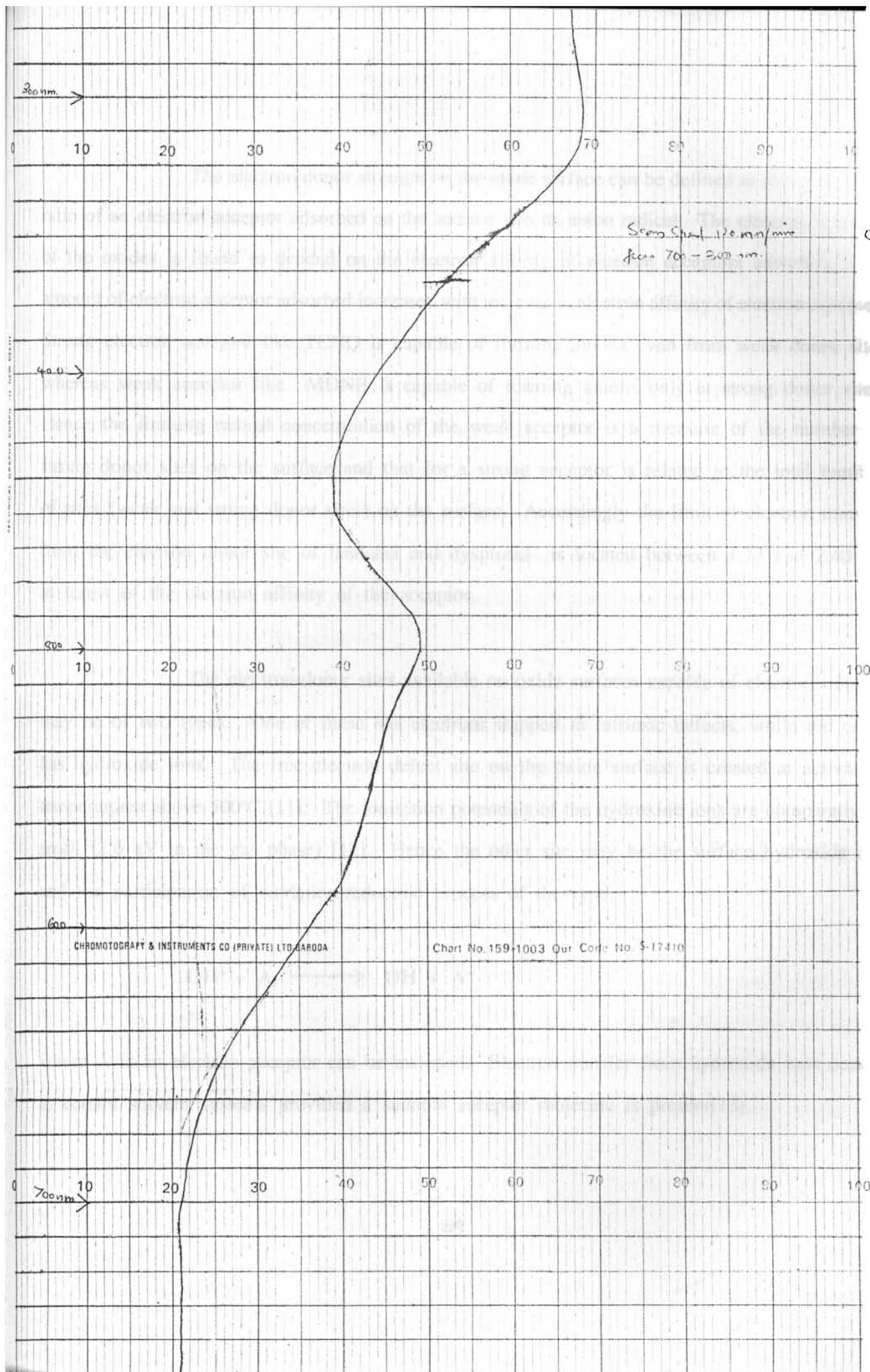
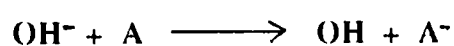


Figure 4a

The electron donor strength on the oxide surface can be defined as the conversion ratio of an electron acceptor adsorbed on the surface into its anion radical. The electron donocity of the oxides is found to depend on the electron affinity of elcetron acceptors adsorbed. The amount of electron acceptor adsorbed increased with increase in elcetron affinity of elcetron acceptor. Strong electron acceptor like TCNQ is capable of forming anions even from weak donor sites whereas weak acceptor like MDNB is capable of forming anions only at strong donor sites. Hence the limiting radical concentration of the weak acceptor is a measure of the number of strong donor sites on the surface and that for a strong acceptor is related to the total number of sites (weak and strong donor sites) on the surface. Accordingly the limit of electron transfer from the electron donor site of lanthana and dysprosia is located between 1.77 and 2.40 eV in terms of the electron affinity of the acceptor.

The electron-donor sites available on oxide surfaces capable of electron transfer may be of two types. One of these has electrons trapped in intrinsic defects, while the other has hydroxide ions. The free electron defect site on the oxide surface is created at activation temperatures above 500°C [11]. The ionisation potentials of the hydroxide ions are comparatively small (2.6 eV in the gas phase) [12]. Hence the other site may be the surface hydroxide ion and the participation of oxidation-reduction process of the type.



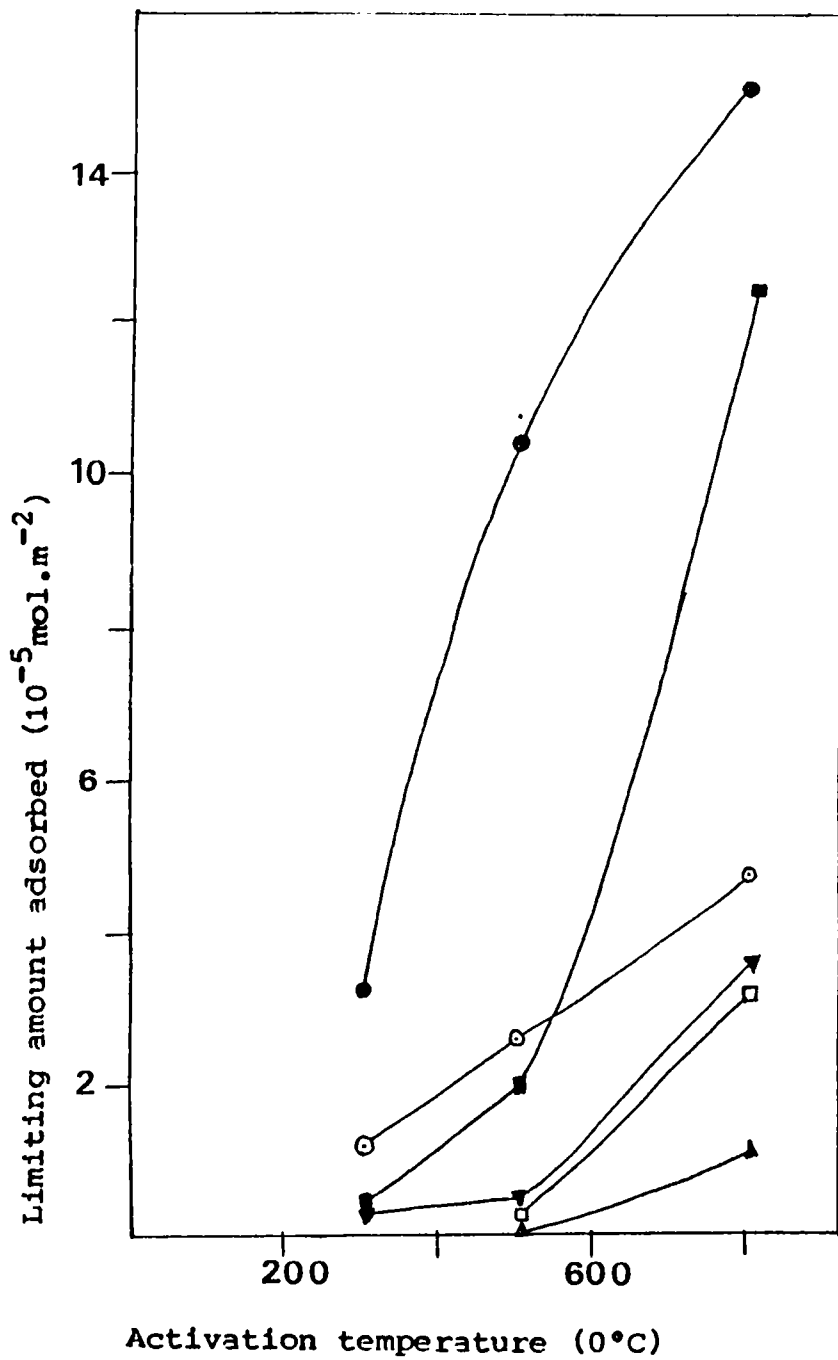
where A is an electron acceptor can be included. Electron transfer from hydroxide ions occurs in certain solvent systems provided a suitable acceptor molecule is present[13].

Fig. 6 & 7 show the increase in the limiting amount of electron acceptors adsorbed in acetonitrile and 1-4 dioxan ~~with the~~ increase of activation temperature of the oxides. Below 500°C, the increase in limiting amount of electron acceptors adsorbed is small and above 500°C, it increases appreciably with increasing activation temperature. This trend can be understood as the decrease in concentration of surface hydroxyl ions and the increase in concentration of trapped electron centres with increasing temperature. It might be expected that the trapped electron centres are solely responsible for the adsorption of electron acceptors on the surface of rare earth oxides activated at higher temperatures and they are stronger reducing agents than the surface hydroxyl ions. From the data it must be inferred that the effect of temperature is to increase the concentration of both weak and strong donor sites on the oxides because the amount of both TCNQ and chloranil adsorbed is large at high temperatures.

It may be seen that the amount of electron acceptors adsorbed decreases appreciably with an increase in the basicity of the solvent for both oxides. To interpret this result in terms of the acid-base theory, the Drago equation [14] was employed:

$$-\Delta H^{ab} = C_A C_B + E_A E_B.$$

where E and C are the Drago constants for the acidic compound (A) and the basic compound (B). Drago determined many E and C values for organic solvents from measurements of the heats of acid-base interaction made by his group and by others using calorimetric and spectroscopic methods [15]. These studies demonstrated that the Drago equation usually predicted

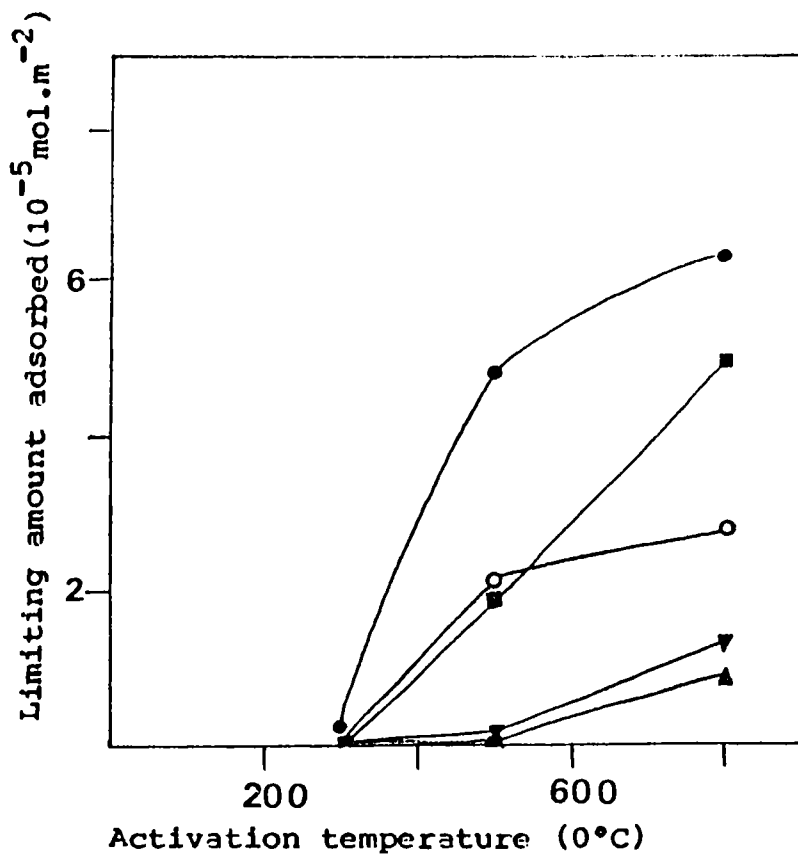


Electron acceptor/solvent

(CA - Chloranil; AN - acetonitrile; TC - TCNQ; EA - ethyl acetate; D - Dioxan)

● TC/AN ■ CA/AN ⊙ TC/EA
 □ CA/EA ▼ TC/D ▲ CA/D

Fig.6 Limiting amount of electron acceptors adsorbed on La_2O_3 as a function of activation temperature.



Electron acceptor/solvent

(CA - Chloranil; AN - acetonitrile; TC - TCNQ EA - Ethyl acetate; D - 1,4 Dioxan)

● TC/AN ■ CA/AN ○ TC/EA

▼ CA/EA ▲ TC/D

Fig.7 Limiting amount of electron acceptors adsorbed on Dy_2O_3 as a function of activation temperature.

ΔH^{ab} values within 3%. A very useful approach for relating the interfacial interactions quantitatively has been the Drago equation of enthalpy change in acid-base complexation. When the Drago equation is applied to this work, the basic compound corresponds to the solvents, such as acetonitrile, ethyl acetate and 1,4-dioxane and the acidic compound to electron acceptors. The E and C values for three basic solvents are available but not for TCNQ and chloranil. Therefore, in this study, the E and C values of tetracyanoethylene (TCNE) which is similar to TCNQ, are employed instead of those of TCNQ. These acid-base parameters are listed in Table 35. The E and C values of chloranil are not reported in the literature. However, from the enthalpy values [16,17] of chloranil and some electron donor solvents like acetone, the E and C values of chloranil can be calculated using the Drago equation. The Drago constants and their enthalpy values are listed in Table 36.

Fig. 8 & 9 show the limiting amount of electron acceptors adsorbed on La_2O_3

| Table 35 - Acid base Parameters | | | |
|--------------------------------------|-------|-------|--|
| Solvent | C_B | E_B | $-\Delta H^{ab}$ with TCNE (K cal mol ⁻¹) |
| Acetonitrile | 1.34 | 0.889 | 3.51 |
| Ethyl acetate | 1.74 | 0.975 | 4.27 |
| 1,4 Dioxan | 2.38 | 1.09 | 5.23 |
| TCNE ($C_A = 1.51$, $E_A = 1.68$) | | | |

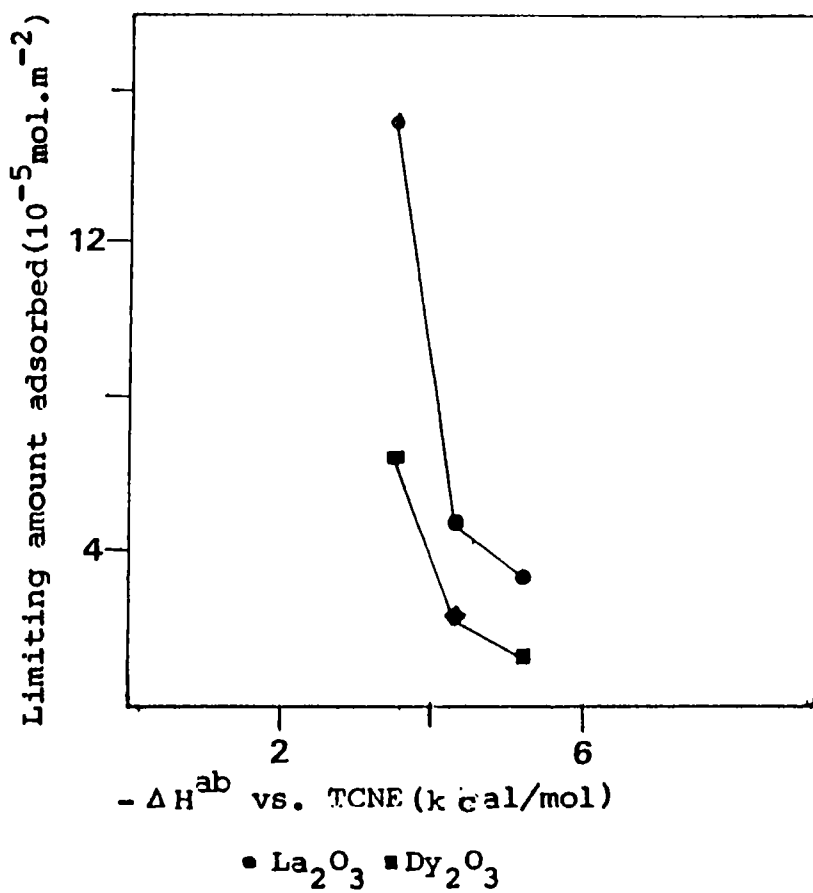


Fig.8 Limiting amount of TCNQ adsorbed on La_2O_3 and Dy_2O_3 (800°C) as a function of acid-base interaction enthalpy.

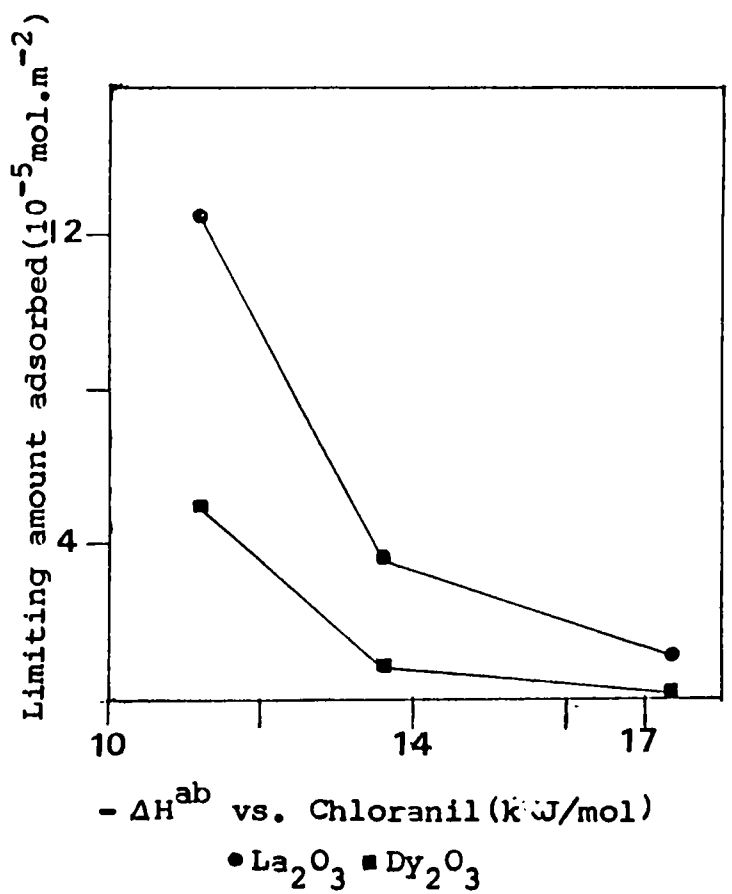


Fig.9 Limiting amount of chloranil adsorbed on La_2O_3 and Dy_2O_3 (800°C) as a function of acid-base interaction enthalpy

| Table 36 - Acid-Base Parameters | | | |
|---------------------------------|-------|-------|---|
| Solvent | C_B | E_B | $-\Delta H^{ab}$ with chloranil (k J mol ⁻¹) |
| Acetonitrile | 2.74 | 1.812 | 11.19 |
| Ethyl acetate | 3.56 | 1.994 | 13.61 |
| 1,4 Dioxan | 4.87 | 2.230 | 17.35 |

and Dy₂O₃ as a function of $-\Delta H^{ab}$. This amount decreases with an increase in the acid-base interaction (ΔH^{ab}) between the basic solvent and electron acceptors. For the three solvents the limiting amount decreased in the following order: acetonitrile > ethyl acetate > 1,4-dioxan; showing the competition between the basic solvents and basic sites (electron donor sites) of the oxides for electron acceptors.

ACID-BASE STRENGTH DISTRIBUTION.

Acidity and basicity at various acid-base strengths were measured [18] by titration with *n*-butylamine or trichloroacetic acid in benzene using the Hammett indicators listed in Table 37. Both the acidity and basicity were determined on a common H₀ scale, where the strength of basic sites were expressed by the H₀ of the conjugate acids. Visible colour change was obtained only for *p*-dimethylaminoazobenzene, methyl red, neutral red and bromothymol blue.

| Indicator | pKa | Colour | |
|-----------------------------------|------|--------|---------|
| | | Basic | Acidic. |
| Crystal violet | 0.8 | Blue | Yellow |
| <i>p</i> -dimethylaminoazobenzene | 3.3 | Yellow | Red |
| Methyl red | 4.8 | Yellow | Red |
| Neutral red | 6.8 | Yellow | Red |
| Bromothymol blue | 7.2 | Blue | Yellow |
| 4-nitroaniline | 18.4 | Orange | Yellow |

Tables 38 & 39 show the acidity and basicity at various acid-base strength of rare earth oxides (Fig.10 & 11). The acidity at an H_o value shows the number of acid sites whose acid strength is equal to or less than the H_o value and the basicity at an H_o value shows the number of basic sites whose base strength is equal to or greater than the H_o value.

| Activation Temperature | Basicity (10^{-4} meq. m^{-2}) | | | | H_o ,max. |
|------------------------|--------------------------------------|---------------------|---------------------|---------------------|-------------|
| | H_o ≥ 3.3 | H_o ≥ 4.8 | H_o ≥ 6.8 | H_o ≥ 7.2 | |
| 300 | 0.47 | 0.32 | 0.20 | 0.15 | 8.5 |
| 500 | 0.78 | 0.47 | 0.26 | 0.20 | 8.6 |
| 800 | 1.20 | 0.84 | 0.50 | 0.43 | 9.6 |

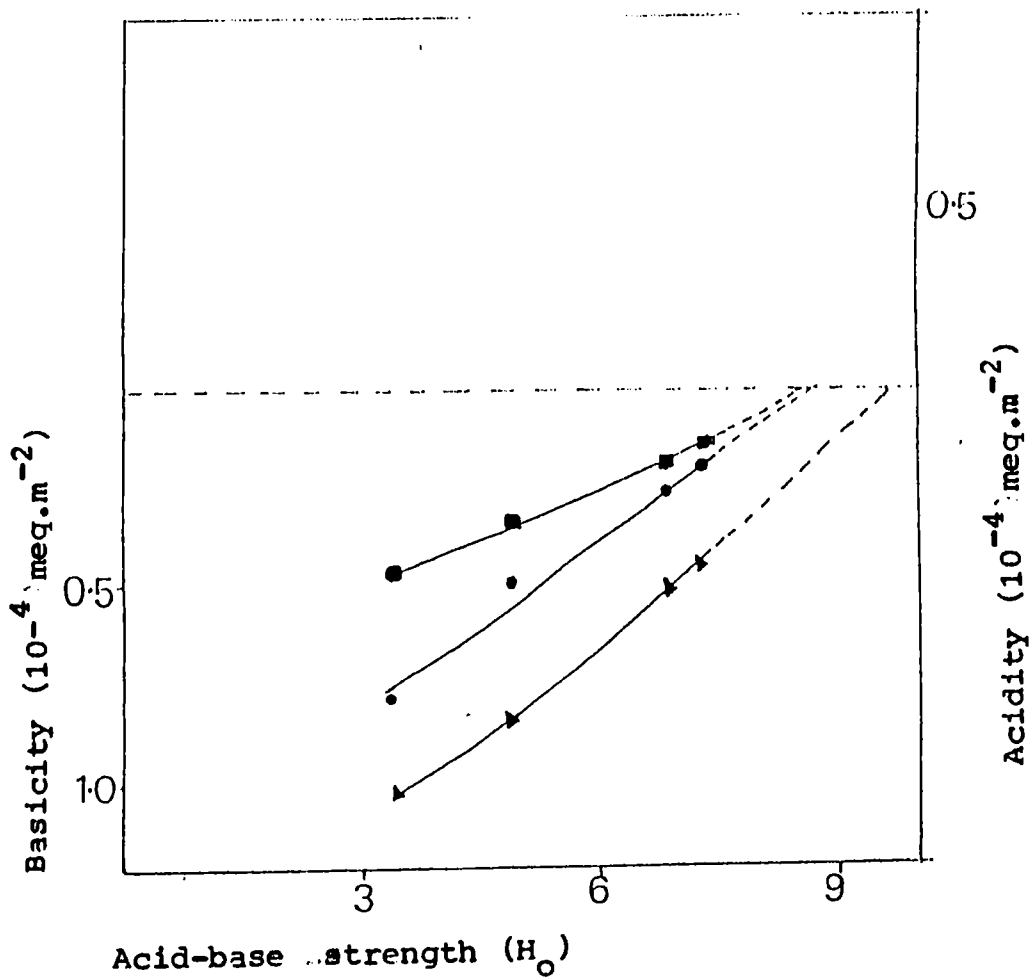


Fig.10 Acid-base strength distribution of La_2O_3

- G 5364 -

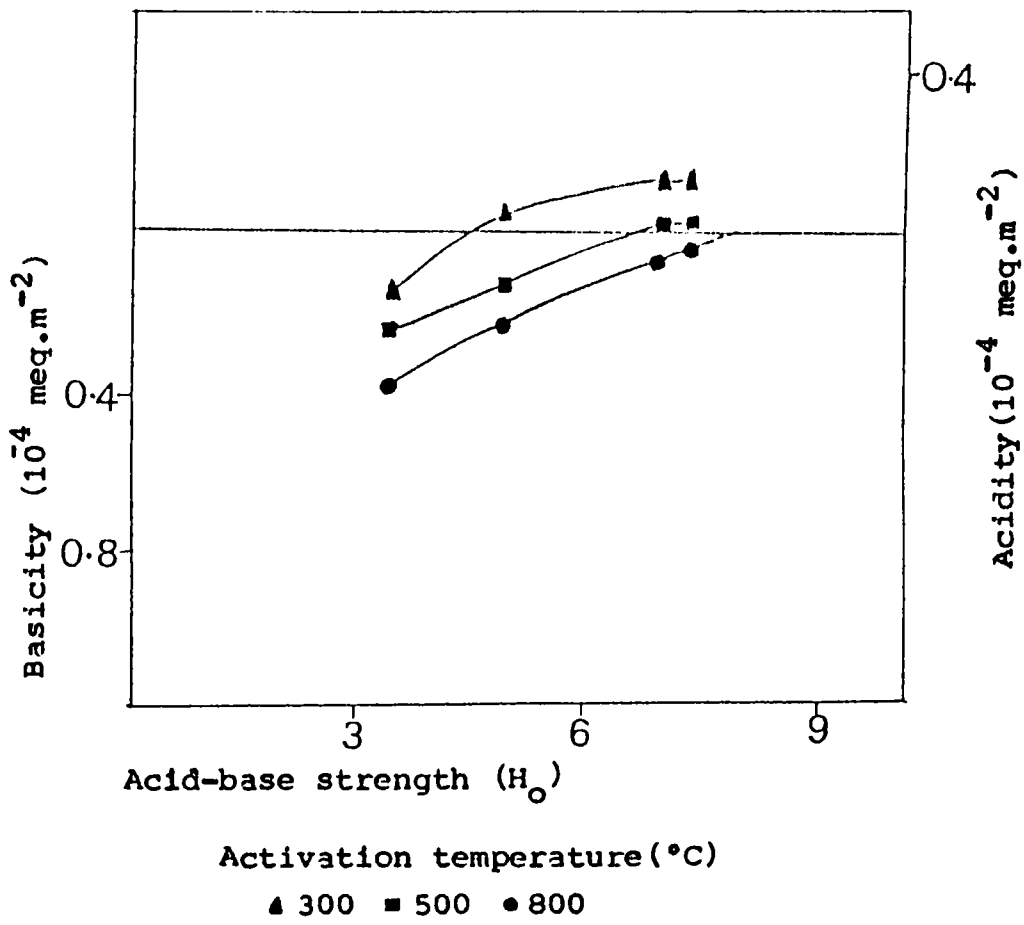


Fig.11 Acid-base strength distribution of Dy_2O_3

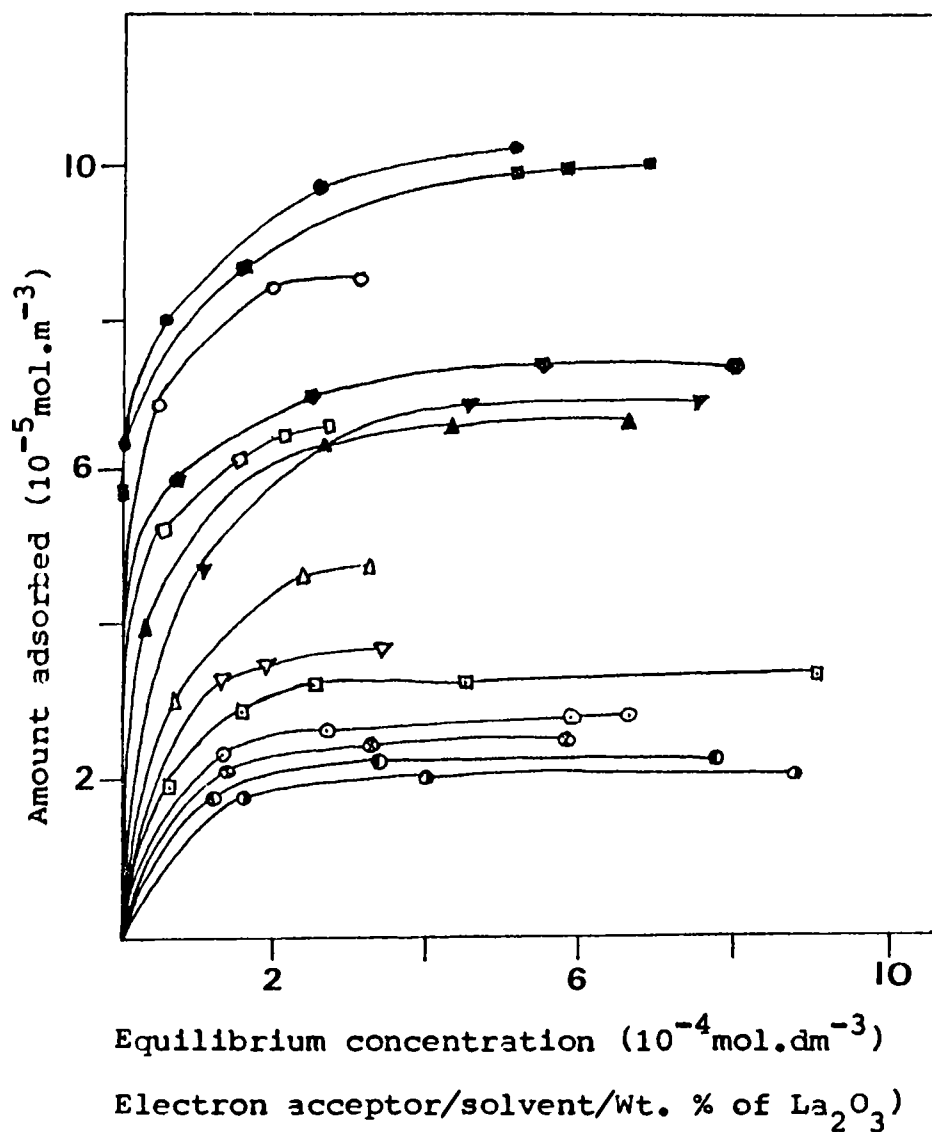
Table 39 - Acidity, Basicity and Ho,max of Dy₂O₃ at various activation temperatures

| Activa- tion Temp(°C) | Basicity(10 ⁻⁴ meq.m ⁻²) | | | Acidity(10 ⁻⁴ meq m ⁻²) | | | | Ho,max | |
|-----------------------------|---|------------|------------|--|------------|------------|------------|--------|------------|
| | Ho ≥3.3 | Ho ≥4.8 | Ho ≥6.8 | Ho ≥7.2 | Ho ≤3.3 | Ho ≤4.8 | Ho ≤6.8 | | Ho ≤7.2 |
| 300 | 0.15 | - | - | - | - | 0.05 | 0.14 | 0.14 | 4.5 |
| 500 | 0.25 | 0.15 | - | - | - | - | 0.02 | 0.02 | 6.5 |
| 800 | 0.40 | 0.24 | 0.07 | 0.05 | - | - | - | - | 7.9 |

The acid-base strength distribution curves intersect at a point on the abscissa ($H_{0,max}$) where acidity = basicity = 0 (Fig. 12 & 13). Hence the strongest H_0 value of the acid sites is equal to the strongest H_0 value of the basic sites. $H_{0,max}$ expresses the equal strongest H_0 value of both acid and basic sites [19]. Each $H_{0,max}$ value was determined from a point of intersection of acid-base strength distribution curve at the abscissa. $H_{0,max}$ can be regarded as a practical parameter to represent the acid-base properties of solids, which is sensitive to the surface structure. A solid with a large positive $H_{0,max}$ has strong basic sites and weak acid sites. On the other hand, a solid with a large negative $H_{0,max}$ has strong acid sites and weak basic sites.

The presence of acidic sites could not be detected in La_2O_3 activated at various temperatures. The results obtained from two different methods (ie. the adsorption and the titration method) gave a similar tendency towards the basicity of the rare earth oxides. However, the characteristics of basic sites estimated by the two methods are different: the basic sites estimated using the adsorption of electron acceptor are associated with Lewis sites resulting from the electron transfer, while the basic sites estimated by the titration are contributed by Lewis plus Bronsted sites.

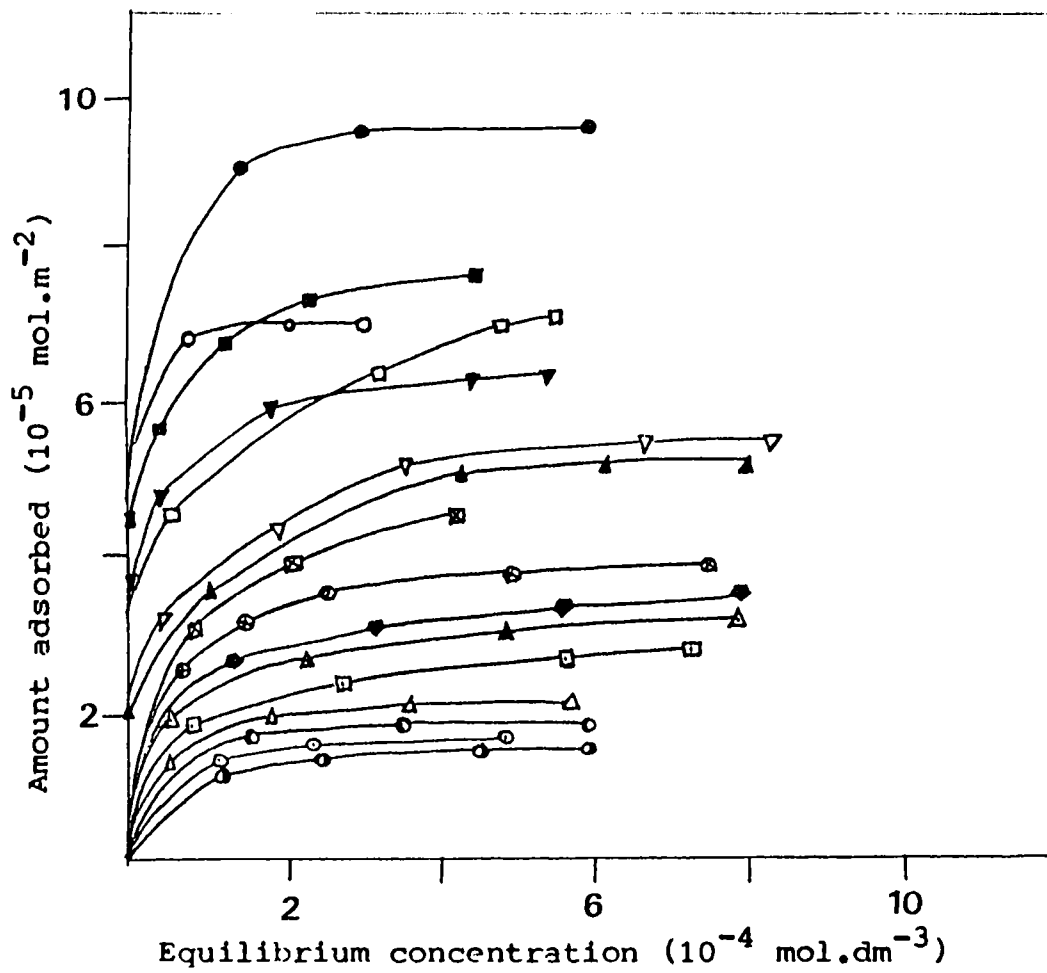
The magnetic susceptibility of these oxides were measured using a simple Guoy type balance before and after adsorption. Magnetic moment of Dy_2O_3 during adsorption decreases and reaches a minimum value at the concentration corresponding to limiting amount of electron acceptors adsorbed indicating the extent of electron transfer from the oxide surface to the electron acceptor (Fig.14). Data are in Tables 40-43. In the case of La_2O_3 because of its diamagnetism



(CA - Chloranil; AN - Acetonitrile; D - 1,4 dioxan; TC - TCNQ)

- | | | | |
|------------|------------|------------|------------|
| ○ TC/AN/10 | ◆ TC/D/10 | ⊙ CA/AN/10 | ■ TC/AN/20 |
| ⊞ CA/AN/20 | ⊙ CA/D/20 | ● TC/AN/75 | ▽ CA/AN/45 |
| ● C/D/75 | □ TC/AN/60 | ⊙ CA/AN/60 | ▲ TC/AN/75 |
| ● TC/D/75 | ⊙ CA/AN/75 | | |

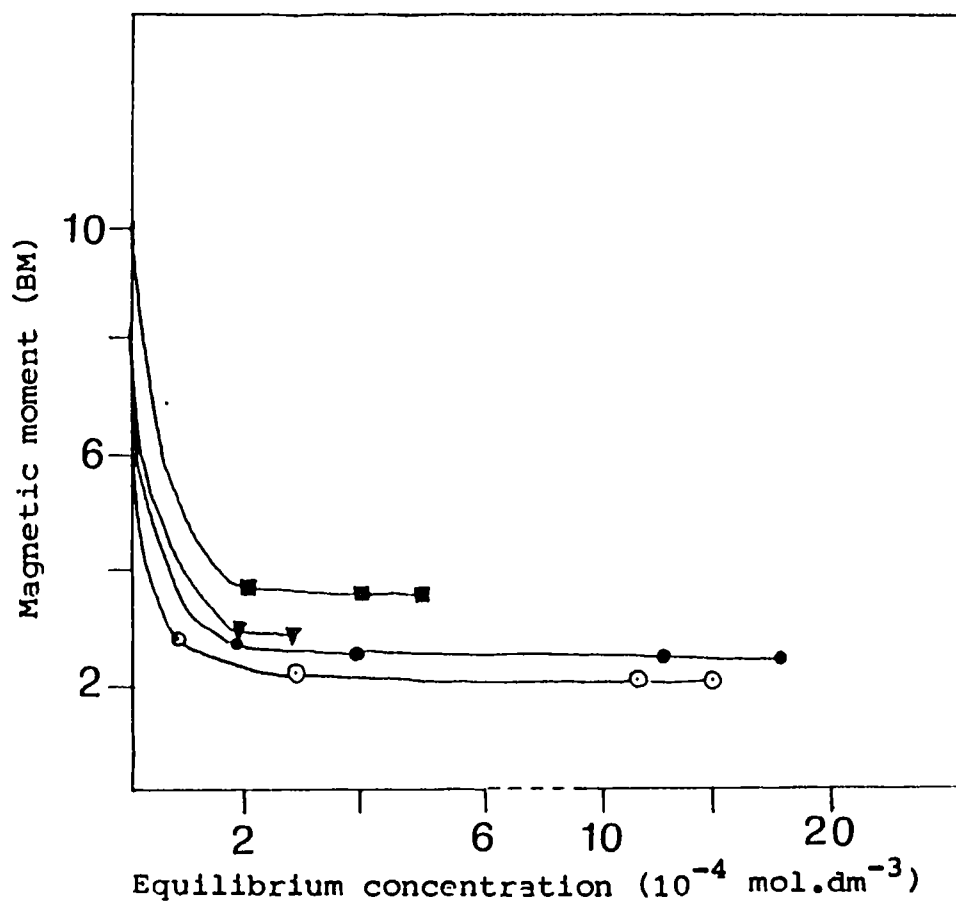
Fig.13¹² Adsorption isotherms of $\text{La}_2\text{O}_3/\text{Al}_2\text{O}_3$.



Electron acceptor/Solvent/Wt. % of Dy_2O_3

- | | | | |
|------------|------------|------------|-----------|
| ■ TC/AN/10 | ⊠ TC/D/10 | ▲ CA/AN/10 | ● CA/D/10 |
| ▼ TC/AN/20 | ▲ TC/D/20 | ● CA/AN/20 | ○ CA/D/20 |
| ● TC/AN/45 | ⊗ CA/D/45 | ⊙ TC/D/60 | ⊠ CA/D/60 |
| ○ TC/AN/65 | ● CA/AN/75 | ○ TC/D/75 | ● CA/D/75 |

Fig.14 Adsorption isotherms of Dy_2O_3/Al_2O_3



○ TCNQ in acetonitrile ● Chloranil in acetonitrile
 ▼ TCNQ in dioxan ■ Chloranil in dioxan.

Fig. ¹⁴12 Magnetic moment of Dy_2O_3 as a function of equilibrium concentration of the electron acceptor.

appreciable change in magnetic moment due to electron transfer could not be measured.

| Table 40 - Adsorption of TCNQ in acetonitrile on Dy₂O₃ activated at 800°C | | | |
|--|----------------------------------|---------------------------|------------------------|
| Initial concentration | Equilibrium Concentration | Amount adsorbed | Magnetic moment |
| mol.dm⁻³ | mol.dm⁻³ | mol.m⁻² | BM |
| 2.5858 x 10 ⁻⁴ | 1.2834 x 10 ⁻⁴ | 3.8063 x 10 ⁻⁶ | 4.52 |
| 5.1717 x 10 ⁻⁴ | 2.9553 x 10 ⁻⁴ | 1.5005 x 10 ⁻⁷ | 3.72 |
| 1.0343 x 10 ⁻³ | 3.8525 x 10 ⁻⁴ | 4.3959 x 10 ⁻⁵ | 3.02 |
| 2.0687 x 10 ⁻³ | 1.2310 x 10 ⁻³ | 5.6732 x 10 ⁻⁵ | 2.43 |
| 2.2530 x 10 ⁻³ | 1.2920 x 10 ⁻³ | 6.0229 x 10 ⁻⁵ | 2.10 |
| 2.5858 x 10 ⁻³ | 1.5461 x 10 ⁻³ | 6.0325 x 10 ⁻⁵ | 2.11 |

| Table 41 - Adsorption of TCNQ in dioxan on Dy₂O₃ activated at 800°C | | | |
|--|----------------------------------|----------------------------|------------------------|
| Initial concentration | Equilibrium Concentration | Amount adsorbed | Magnetic moment |
| mol.dm⁻³ | mol.dm⁻³ | mol.dm⁻² | BM |
| 9.8906 x 10 ⁻⁶ | 1.0091 x 10 ⁻⁷ | 6.6979 x 10 ⁻⁷ | 5.12 |
| 4.9953 x 10 ⁻⁵ | 3.0049 x 10 ⁻⁵ | 1.3480 x 10 ⁻⁶ | 4.78 |
| 9.8906 x 10 ⁻⁵ | 5.5004 x 10 ⁻⁵ | 3.0411 x 10 ⁻⁶ | 4.51 |
| 1.9981 x 10 ⁻⁴ | 1.3522 x 10 ⁻⁴ | 4.3576 x 10 ⁻⁵ | 3.98 |
| 3.9963 x 10 ⁻⁴ | 2.1999 x 10 ⁻⁴ | 1.2168 x 10 ⁻⁵ | 3.22 |
| 4.9953 x 10 ⁻⁴ | 2.9972 x 10 ⁻⁴ | 1.3525 x 10 ⁻⁵ | 3.18 |

| Table 42 - Adsorption of chloranil in acetonitrile on Dy₂O₃ activated at 800°C | | | |
|---|----------------------------------|---------------------------|------------------------|
| Initial concentration | Equilibrium Concentration | Amount adsorbed | Magnetic moment |
| mol.dm⁻³ | mol.dm⁻³ | mol.m⁻² | BM |
| 5.0594 x 10 ⁻⁵ | 2.0614 x 10 ⁻⁶ | 3.3706 x 10 ⁻⁶ | 4.86 |
| 2.5297 x 10 ⁻⁴ | 5.3776 x 10 ⁻⁵ | 1.3480 x 10 ⁻⁵ | 4.32 |
| 5.0594 x 10 ⁻⁴ | 5.6016 x 10 ⁻⁵ | 3.0411 x 10 ⁻⁵ | 3.72 |
| 1.0119 x 10 ⁻³ | 4.4211 x 10 ⁻⁴ | 4.1899 x 10 ⁻⁵ | 3.36 |
| 2.0238 x 10 ⁻³ | 1.3530 x 10 ⁻³ | 4.7432 x 10 ⁻⁵ | 2.79 |
| 2.5297 x 10 ⁻³ | 1.7948 x 10 ⁻³ | 4.9583 x 10 ⁻⁵ | 2.78 |

| Table 43 - Adsorption of chloranil in 1-4 dioxan on Dy₂O₃ activated at 800°C | | | |
|---|----------------------------------|---------------------------|------------------------|
| Initial concentration | Equilibrium Concentration | Amount adsorbed | Magnetic moment |
| mol.dm⁻³ | mol.dm⁻³ | mol.m⁻² | BM |
| 1.0493 x 10 ⁻⁵ | 4.213 x 10 ⁻⁶ | 4.2533 x 10 ⁻⁷ | 5.98 |
| 5.2465 x 10 ⁻⁵ | 4.0039 x 10 ⁻⁵ | 8.4158 x 10 ⁻⁷ | 4.42 |
| 2.0986 x 10 ⁻⁴ | 1.9290 x 10 ⁻⁴ | 1.1485 x 10 ⁻⁶ | 3.96 |
| 4.1972 x 10 ⁻⁴ | 3.9709 x 10 ⁻⁴ | 1.5328 x 10 ⁻⁶ | 3.51 |
| 5.2465 x 10 ⁻⁴ | 5.0107 x 10 ⁻⁴ | 1.5964 x 10 ⁻⁶ | 3.51 |

ELECTRON DONATING PROPERTIES OF TWO-COMPONENT SYSTEMS.

It is well known that two-component metal oxide systems exhibit characteristic surface properties which are not qualitatively predictable from consideration of the independent properties of the parent oxides. The mixed oxides of lanthanum and dysprosium with aluminum were prepared for different weight percentages of La_2O_3 & Dy_2O_3 by co-precipitation with aluminum nitrate solution. The following mixed oxides were prepared: 10,20,45,60 and 75% (by wt. of rare earth oxide) and were activated at a temperature of 500°C. The specific surface area of these oxides are given in Table 44.

| Table 44 - Surface area of $\text{La}_2\text{O}_3/\text{Al}_2\text{O}_3$ and $\text{Dy}_2\text{O}_3/\text{Al}_2\text{O}_3$ for various compositions. | | |
|---|---|---|
| Composition (% by wt. of rare earth oxide) | Surface area ($\text{m}^2.\text{g}^{-1}$) | |
| | $\text{La}_2\text{O}_3/\text{Al}_2\text{O}_3$ | $\text{Dy}_2\text{O}_3/\text{Al}_2\text{O}_3$ |
| 0 | 193.91 | 193.91 |
| 51 | 214.90 | 224.62 |
| 10 | 169.12 | 216.06 |
| 20 | 157.47 | 196.40 |
| 45 | 149.70 | 151.20 |
| 60 | 144.65 | 143.80 |
| 75 | 69.79 | 88.45 |
| 100 | 38.28 | 24.41 |

The electron donating properties of these mixed oxides were determined by using the same set of electron acceptors, given in Table 2 in acetonitrile and 1,4-dioxan. Data are given in Tables 45-88.

| Table 45 - Adsorption of TCNQ in acetonitrile on Al₂O₃ activated at 500°C | | |
|--|--|---|
| Initial concentration mol.dm ⁻³ | Equilibrium concentration mol.dm ⁻³ | Adsorbed amount mol.m ⁻² |
| 1.4604 x 10 ⁻³ | 4.0390 x 10 ⁻⁷ | 1.5052 x 10 ⁻⁵ |
| 2.9208 x 10 ⁻³ | 1.9746 x 10 ⁻⁶ | 3.0123 x 10 ⁻⁵ |
| 4.3812 x 10 ⁻³ | 7.1053 x 10 ⁻⁵ | 4.4437 x 10 ⁻⁵ |
| 7.3020 x 10 ⁻³ | 9.9474 x 10 ⁻⁴ | 6.5056 x 10 ⁻⁵ |
| 8.4815 x 10 ⁻³ | 2.0193 x 10 ⁻³ | 6.6593 x 10 ⁻⁵ |
| 9.4239 x 10 ⁻³ | 2.7785 x 10 ⁻³ | 6.8527 x 10 ⁻⁵ |

| Table 46 - Adsorption of TCNQ in dioxan on Al₂O₃ activated at 500°C | | |
|--|--|---|
| Initial concentration mol.dm ⁻³ | Equilibrium concentration mol.dm ⁻³ | Adsorbed amount mol.m ⁻² |
| 1.6163 x 10 ⁻³ | 7.9450 x 10 ⁻⁵ | 1.5835 x 10 ⁻⁵ |
| 3.2326 x 10 ⁻³ | 8.7493 x 10 ⁻⁴ | 2.4317 x 10 ⁻⁵ |
| 6.4652 x 10 ⁻³ | 3.6021 x 10 ⁻³ | 2.9518 x 10 ⁻⁵ |
| 8.0815 x 10 ⁻³ | 4.6647 x 10 ⁻³ | 3.5217 x 10 ⁻⁵ |
| 1.2015 x 10 ⁻² | 7.6715 x 10 ⁻³ | 4.4691 x 10 ⁻⁵ |
| 1.3348 x 10 ⁻² | 8.9502 x 10 ⁻³ | 4.5295 x 10 ⁻⁵ |

| Table 47 - Adsorption of chloranil in acetonitrile on Al₂O₃ activated at 500°C | | |
|---|--|---|
| Initial concentration mol.dm⁻³ | Equilibrium concentration mol.dm⁻³ | Adsorbed amount mol.m⁻² |
| 3.2642 x 10 ⁻⁴ | 2.0829 x 10 ⁻⁶ | 3.3416 x 10 ⁻⁶ |
| 1.3057 x 10 ⁻³ | 3.0276 x 10 ⁻⁴ | 1.0324 x 10 ⁻⁵ |
| 2.6113 x 10 ⁻³ | 1.3831 x 10 ⁻³ | 1.2648 x 10 ⁻⁵ |
| 6.5284 x 10 ⁻³ | 4.9296 x 10 ⁻³ | 1.6467 x 10 ⁻⁵ |
| 7.6577 x 10 ⁻³ | 5.5387 x 10 ⁻³ | 2.1837 x 10 ⁻⁵ |
| 8.5088 x 10 ⁻³ | 6.3569 x 10 ⁻³ | 2.2181 x 10 ⁻⁵ |

| Table 48 - Adsorption of chloranil in dioxan on Al₂O₃ activated at 500°C | | |
|---|--|---|
| Initial concentration mol.dm⁻³ | Equilibrium concentration mol.dm⁻³ | Adsorbed amount mol.m⁻² |
| 1.4511 x 10 ⁻⁴ | 9.4490 x 10 ⁻⁷ | 1.4861 x 10 ⁻⁶ |
| 7.2556 x 10 ⁻⁴ | 1.6840 x 10 ⁻⁴ | 5.7434 x 10 ⁻⁶ |
| 1.4511 x 10 ⁻³ | 6.9113 x 10 ⁻⁴ | 7.8366 x 10 ⁻⁶ |
| 2.9022 x 10 ⁻³ | 1.9033 x 10 ⁻³ | 1.0317 x 10 ⁻⁵ |
| 4.3533 x 10 ⁻³ | 3.2025 x 10 ⁻³ | 1.1864 x 10 ⁻⁵ |

| Table 49 - Adsorption of TCNQ in acetonitrile on 10% La₂O₃/Al₂O₃ activated at 500°C | | |
|--|--|---|
| Initial concentration mol.dm⁻³ | Equilibrium concentration mol.dm⁻³ | Adsorbed amount mol.m⁻² |
| 9.1523 x 10 ⁻⁴ | 1.0500 x 10 ⁻⁷ | 1.082 x 10 ⁻⁵ |
| 1.8306 x 10 ⁻³ | 5.8520 x 10 ⁻⁷ | 2.163 x 10 ⁻⁵ |
| 3.6613 x 10 ⁻³ | 2.1757 x 10 ⁻⁶ | 4.327 x 10 ⁻⁵ |
| 6.2240 x 10 ⁻³ | 4.2392 x 10 ⁻⁴ | 6.856 x 10 ⁻⁵ |
| 9.1532 x 10 ⁻³ | 1.9920 x 10 ⁻³ | 8.467 x 10 ⁻⁵ |
| 9.8680 x 10 ⁻³ | 2.6970 x 10 ⁻³ | 8.479 x 10 ⁻⁵ |

| Table 50 - Adsorption of TCNQ in dioxan on 10% La₂O₃/Al₂O₃ activated at 500°C | | |
|--|--|---|
| Initial concentration mol.dm⁻³ | Equilibrium concentration mol.dm⁻³ | Adsorbed amount mol.m⁻² |
| 1.7062 x 10 ⁻⁴ | 7.307 x 10 ⁻⁷ | 2.167 x 10 ⁻⁶ |
| 8.5312 x 10 ⁻⁴ | 3.731 x 10 ⁻⁶ | 1.0179 x 10 ⁻⁵ |
| 3.4124 x 10 ⁻³ | 6.5137 x 10 ⁻⁴ | 3.3083 x 10 ⁻⁵ |
| 5.0790 x 10 ⁻³ | 1.0528 x 10 ⁻³ | 4.7433 x 10 ⁻⁵ |
| 1.0158 x 10 ⁻² | 4.5428 x 10 ⁻³ | 6.6196 x 10 ⁻⁵ |
| 1.2697 x 10 ⁻² | 6.3558 x 10 ⁻³ | 6.7752 x 10 ⁻⁵ |

| Table 51 - Adsorption of chloranil in acetonitrile on 10% La₂O₃/Al₂O₃ activated at 500°C | | |
|---|--|---|
| Initial concentration mol.dm⁻³ | Equilibrium concentration mol.dm⁻³ | Adsorbed amount mol.m⁻² |
| 8.2113 x 10 ⁻⁴ | 2.436 x 10 ⁻⁶ | 9.685 x 10 ⁻⁶ |
| 1.6423 x 10 ⁻³ | 1.773 x 10 ⁻⁴ | 1.731 x 10 ⁻⁵ |
| 3.2845 x 10 ⁻³ | 1.325 x 10 ⁻³ | 2.316 x 10 ⁻⁵ |
| 5.7479 x 10 ⁻³ | 3.5461 x 10 ⁻³ | 2.602 x 10 ⁻⁵ |
| 8.2113 x 10 ⁻³ | 5.823 x 10 ⁻³ | 2.823 x 10 ⁻⁵ |
| 8.976 x 10 ⁻³ | 6.581 x 10 ⁻³ | 2.830 x 10 ⁻⁵ |

| Table 52 - Adsorption of chloranil in dioxan on 10 % La₂O₃/Al₂O₃ activated at 500°C | | |
|--|--|---|
| Initial concentration mol.dm⁻³ | Equilibrium concentration mol.dm⁻³ | Adsorbed amount mol.m⁻² |
| 2.7932 x 10 ⁻⁴ | 8.2113 x 10 ⁻⁶ | 2.4134 x 10 ⁻⁶ |
| 1.3966 x 10 ⁻³ | 1.6510 x 10 ⁻⁴ | 1.0941 x 10 ⁻⁵ |
| 2.7932 x 10 ⁻³ | 1.1896 x 10 ⁻³ | 1.4255 x 10 ⁻⁵ |
| 5.4222 x 10 ⁻³ | 3.6947 x 10 ⁻³ | 2.0413 x 10 ⁻⁵ |
| 1.0844 x 10 ⁻² | 8.7798 x 10 ⁻³ | 2.4402 x 10 ⁻⁵ |
| 1.3555 x 10 ⁻² | 1.1394 x 10 ⁻² | 2.5561 x 10 ⁻⁵ |

| Table 53 - Adsorption of TCNQ in acetonitrile on 20 % La₂O₃/Al₂O₃ activated at 500°C | | |
|---|--|---|
| Initial concentration mol.dm⁻³ | Equilibrium concentration mol.dm⁻³ | Adsorbed amount mol.m⁻² |
| 2.5848 x 10 ⁻³ | 1.8111 x 10 ⁻⁶ | 3.2767 x 10 ⁻⁵ |
| 5.1697 x 10 ⁻³ | 1.8505 x 10 ⁻⁴ | 6.3284 x 10 ⁻⁵ |
| 8.7855 x 10 ⁻³ | 2.1182 x 10 ⁻³ | 8.4715 x 10 ⁻⁵ |
| 1.2924 x 10 ⁻² | 5.1734 x 10 ⁻³ | 9.8381 x 10 ⁻⁵ |
| 1.3615 x 10 ⁻² | 5.7798 x 10 ⁻³ | 9.9276 x 10 ⁻⁵ |
| 1.4798 x 10 ⁻² | 6.8504 x 10 ⁻³ | 1.0089 x 10 ⁻⁴ |

| Table 54 - Adsorption of TCNQ in dioxan on 20% La₂O₃/Al₂O₃ activated at 500°C | | |
|--|--|---|
| Initial concentration mol.dm⁻³ | Equilibrium concentration mol.dm⁻³ | Adsorbed amount mol.m⁻² |
| 4.7407 x 10 ⁻⁴ | 1.9077 x 10 ⁻⁸ | 4.8252 x 10 ⁻⁶ |
| 9.4814 x 10 ⁻⁴ | 2.2893 x 10 ⁻⁷ | 9.6523 x 10 ⁻⁶ |
| 1.8963 x 10 ⁻³ | 4.0540 x 10 ⁻⁵ | 1.8893 x 10 ⁻⁵ |
| 5.0790 x 10 ⁻³ | 1.1455 X 10 ⁻³ | 4.9859 x 10 ⁻⁵ |
| 1.0115 x 10 ⁻² | 4.7232 x 10 ⁻³ | 6.8889 x 10 ⁻⁵ |
| 1.2697 x 10 ⁻² | 7.4427 x 10 ⁻³ | 6.6603 x 10 ⁻⁵ |

| Table 55 - Adsorption of chloranil in acetonitrile on 20 % La ₂ O ₃ /Al ₂ O ₃ activated at 500°C | | |
|---|---|--|
| Initial concentration mol.dm ⁻³ | Equilibrium concentration mol.dm ⁻³ | Adsorbed amount mol.m ⁻² |
| 2.6045 x 10 ⁻⁴ | 1.4197 x 10 ⁻⁶ | 3.2893 x 10 ⁻⁶ |
| 1.3023 x 10 ⁻³ | 9.5469 x 10 ⁻⁵ | 1.5330 x 10 ⁻⁵ |
| 2.6045 x 10 ⁻³ | 9.3507 x 10 ⁻⁴ | 2.1203 x 10 ⁻⁵ |
| 5.2090 x 10 ⁻³ | 3.2985 x 10 ⁻³ | 2.4236 x 10 ⁻⁵ |
| 7.8136 x 10 ⁻³ | 1.0844 x 10 ⁻² | 2.7659 x 10 ⁻⁵ |

| Table 56 - Adsorption of TCNQ in acetonitrile on 20 % La ₂ O ₃ /Al ₂ O ₃ activated at 500°C | | |
|--|---|--|
| Initial concentration mol.dm ⁻³ | Equilibrium concentration mol.dm ⁻³ | Adsorbed amount mol.m ⁻² |
| 2.6240 x 10 ⁻¹ | 4.9509 x 10 ⁻⁷ | 2.3241 x 10 ⁻⁶ |
| 1.3120 x 10 ⁻¹ | 7.8423 x 10 ⁻⁶ | 1.0979 x 10 ⁻⁵ |
| 2.6240 x 10 ⁻³ | 9.0105 x 10 ⁻⁴ | 1.5338 x 10 ⁻⁵ |
| 5.4222 x 10 ⁻³ | 3.7114 x 10 ⁻³ | 2.1663 x 10 ⁻⁵ |
| 1.0844 x 10 ⁻² | 8.7798 x 10 ⁻³ | 2.6155 x 10 ⁻⁵ |
| 1.3555 x 10 ⁻² | 1.1729 x 10 ⁻² | 2.3149 x 10 ⁻⁵ |

| Table 57 - Adsorption of TCNQ in acetonitrile on 45 % La ₂ O ₃ /Al ₂ O ₃ activated at 500°C | | |
|---|---|--|
| Initial concentration mol.dm ⁻³ | Equilibrium concentration mol.dm ⁻³ | Adsorbed amount mol.m ⁻² |
| 1.9688 x 10 ⁻⁴ | 2.100 x 10 ⁻⁷ | 2.6275 x 10 ⁻⁶ |
| 9.8440 x 10 ⁻⁴ | 1.0500 x 10 ⁻⁶ | 1.3137 x 10 ⁻⁵ |
| 1.9688 x 10 ⁻³ | 2.100 x 10 ⁻⁶ | 2.6275 x 10 ⁻⁵ |
| 3.9375 x 10 ⁻³ | 9.3306 x 10 ⁻⁶ | 5.2229 x 10 ⁻⁵ |
| 9.8436 x 10 ⁻³ | 2.5776 x 10 ⁻³ | 9.7074 x 10 ⁻⁵ |
| 1.3615 x 10 ⁻² | 5.7798 x 10 ⁻³ | 1.0189 x 10 ⁻⁴ |

| Table 58 - Adsorption of TCNQ in dioxan on 45 % La ₂ O ₃ /Al ₂ O ₃ activated at 500°C | | |
|---|---|--|
| Initial concentration mol.dm ⁻³ | Equilibrium concentration mol.dm ⁻³ | Adsorbed amount mol.m ⁻² |
| 3.6632 x 10 ⁻⁵ | 6.9408 x 10 ⁻⁶ | 3.9667 x 10 ⁻⁷ |
| 1.8316 x 10 ⁻⁴ | 3.1735 x 10 ⁻⁵ | 2.0230 x 10 ⁻⁶ |
| 3.6632 x 10 ⁻⁴ | 3.3184 x 10 ⁻⁵ | 4.4507 x 10 ⁻⁶ |
| 7.3264 x 10 ⁻⁴ | 1.3513 x 10 ⁻⁴ | 9.7916 x 10 ⁻⁶ |
| 1.4653 x 10 ⁻³ | 7.2396 x 10 ⁻⁴ | 1.9507 x 10 ⁻⁵ |
| 1.8316 x 10 ⁻³ | 1.7365 x 10 ⁻⁴ | 2.2150 x 10 ⁻⁵ |

| Table 61 - Adsorption of TCNQ in acetonitrile on 60% La₂O₃/Al₂O₃ activated at 500°C | | |
|--|--|---|
| Initial concentration mol.dm⁻³ | Equilibrium concentration mol.dm⁻³ | Adsorbed amount mol.m⁻² |
| 1.6681 x 10 ⁻³ | 4.3192 x 10 ⁻⁷ | 1.5505 x 10 ⁻⁵ |
| 3.3361 x 10 ⁻³ | 2.9340 x 10 ⁻⁶ | 3.1020 x 10 ⁻⁵ |
| 5.8382 x 10 ⁻³ | 4.0957 x 10 ⁻⁴ | 5.0469 x 10 ⁻⁵ |
| 8.3403 x 10 ⁻³ | 1.7965 x 10 ⁻³ | 6.0861 x 10 ⁻⁵ |
| 8.7889 x 10 ⁻³ | 2.0114 x 10 ⁻³ | 6.4244 x 10 ⁻⁵ |
| 9.7654 x 10 ⁻³ | 2.6868 x 10 ⁻³ | 6.5747 x 10 ⁻⁵ |

| Table 62 - Adsorption of TCNQ in dioxan on 60% La₂O₃/Al₂O₃ activated at 500°C | | |
|--|--|---|
| Initial concentration mol.dm⁻³ | Equilibrium concentration mol.dm⁻³ | Adsorbed amount mol.m⁻² |
| 3.6632 x 10 ⁻⁵ | 5.1200 x 10 ⁻⁷ | 4.9941 x 10 ⁻⁷ |
| 1.8316 x 10 ⁻⁴ | 2.7475 x 10 ⁻⁶ | 2.4945 x 10 ⁻⁶ |
| 3.6632 x 10 ⁻⁴ | 5.4950 x 10 ⁻⁶ | 4.9889 x 10 ⁻⁶ |
| 7.3264 x 10 ⁻⁴ | 9.6522 x 10 ⁻⁶ | 9.9778 x 10 ⁻⁶ |
| 1.4653 x 10 ⁻³ | 1.3514 x 10 ⁻⁴ | 1.8333 x 10 ⁻⁵ |
| 1.8316 x 10 ⁻³ | 2.6965 x 10 ⁻⁴ | 2.1596 x 10 ⁻⁵ |

| Table 63 - Adsorption of chloranil in acetonitrile on 60% La₂O₃/Al₂O₃ activated at 500°C | | |
|---|--|---|
| Initial concentration mol.dm⁻³ | Equilibrium concentration mol.dm⁻³ | Adsorbed amount mol.m⁻² |
| 8.3550 x 10 ⁻⁵ | 1.0831 x 10 ⁻⁷ | 1.1529 x 10 ⁻⁶ |
| 4.1775 x 10 ⁻⁴ | 1.0985 x 10 ⁻⁶ | 5.7585 x 10 ⁻⁶ |
| 8.3550 x 10 ⁻⁴ | 3.8681 x 10 ⁻⁶ | 1.1494 x 10 ⁻⁵ |
| 1.8041 x 10 ⁻³ | 4.8269 x 10 ⁻⁴ | 1.8252 x 10 ⁻⁵ |
| 1.8041 x 10 ⁻³ | 4.8269 x 10 ⁻⁴ | 1.8252 x 10 ⁻⁵ |
| 3.6083 x 10 ⁻³ | 1.7623 x 10 ⁻³ | 2.5518 x 10 ⁻⁵ |
| 4.5103 x 10 ⁻³ | 2.6105 x 10 ⁻³ | 2.6153 x 10 ⁻⁵ |

| Table 64 - Adsorption of chloranil in dioxan on 60 % La₂O₃/Al₂O₃ activated at 500°C | | |
|--|--|---|
| Initial concentration mol.dm⁻³ | Equilibrium concentration mol.dm⁻³ | Adsorbed amount mol.m⁻² |
| 1.8546 x 10 ⁻⁵ | 8.3100 x 10 ⁻⁷ | 2.4491 x 10 ⁻⁷ |
| 9.2728 x 10 ⁻⁵ | 4.1388 x 10 ⁻⁶ | 1.2246 x 10 ⁻⁶ |
| 1.8546 x 10 ⁻⁴ | 1.0088 x 10 ⁻⁵ | 2.4247 x 10 ⁻⁶ |
| 3.7091 x 10 ⁻⁴ | 2.8611 x 10 ⁻⁵ | 4.7283 x 10 ⁻⁶ |
| 7.4182 x 10 ⁻⁴ | 1.5511 x 10 ⁻⁴ | 8.1134 x 10 ⁻⁶ |
| 9.2728 x 10 ⁻⁴ | 2.7987 x 10 ⁻⁴ | 8.9457 x 10 ⁻⁶ |

| Table 65 - Adsorption of TCNQ in acetonitrile on 75 % La ₂ O ₃ /Al ₂ O ₃ activated at 500°C | | |
|---|---|--|
| Initial concentration mol.dm ⁻³ | Equilibrium concentration mol.dm ⁻³ | Adsorbed amount mol.m ⁻² |
| 9.8634 x 10 ⁻⁵ | 4.9308 x 10 ⁻⁵ | 1.4136 x 10 ⁻⁶ |
| 4.9137 x 10 ⁻⁴ | 2.4886 x 10 ⁻⁴ | 6.9971 x 10 ⁻⁶ |
| 9.8634 x 10 ⁻⁴ | 5.0280 x 10 ⁻⁴ | 1.3854 x 10 ⁻⁵ |
| 1.9727 x 10 ⁻³ | 1.0046 x 10 ⁻³ | 2.7708 x 10 ⁻⁵ |
| 3.9453 x 10 ⁻³ | 2.3051 x 10 ⁻³ | 4.6958 x 10 ⁻⁵ |
| 4.9317 x 10 ⁻³ | 3.2809 x 10 ⁻³ | 4.7309 x 10 ⁻⁵ |

| Table 66 - Adsorption of TCNQ in dioxan on 75 % La ₂ O ₃ /Al ₂ O ₃ activated at 500°C | | |
|---|---|--|
| Initial concentration mol.dm ⁻³ | Equilibrium concentration mol.dm ⁻³ | Adsorbed amount mol.m ⁻² |
| 2.7622 x 10 ⁻⁵ | 1.4945 x 10 ⁻⁵ | 3.6380 x 10 ⁻⁷ |
| 1.3811 x 10 ⁻⁴ | 7.4853 x 10 ⁻⁵ | 1.8129 x 10 ⁻⁶ |
| 2.7622 x 10 ⁻⁴ | 1.4971 x 10 ⁻⁴ | 3.6256 x 10 ⁻⁶ |
| 5.5244 x 10 ⁻⁴ | 2.9819 x 10 ⁻⁴ | 7.2510 x 10 ⁻⁶ |
| 1.1049 x 10 ⁻³ | 7.0226 x 10 ⁻⁴ | 1.1504 x 10 ⁻⁵ |
| 1.3811 x 10 ⁻³ | 9.5605 x 10 ⁻⁴ | 1.2181 x 10 ⁻⁵ |

| Table 69 - Adsorption of TCNQ in acetonitrile on 10% Dy ₂ O ₃ /Al ₂ O ₃ activated at 500°C | | |
|--|---|--|
| Initial concentration mol.dm ⁻³ | Equilibrium concentration mol.dm ⁻³ | Adsorbed amount mol.m ⁻² |
| 3.1539 x 10 ⁻¹ | 2.2267 x 10 ⁻⁶ | 2.9174 x 10 ⁻⁵ |
| 5.2040 x 10 ⁻³ | 1.0018 x 10 ⁻⁴ | 4.7246 x 10 ⁻⁵ |
| 7.8848 x 10 ⁻³ | 8.6825 x 10 ⁻⁴ | 6.4899 x 10 ⁻⁵ |
| 8.6009 x 10 ⁻³ | 1.3989 x 10 ⁻³ | 6.6616 x 10 ⁻⁵ |
| 9.5553 x 10 ⁻³ | 1.9925 x 10 ⁻³ | 6.9948 x 10 ⁻⁵ |
| 1.0078 x 10 ⁻² | 2.3117 x 10 ⁻³ | 7.1688 x 10 ⁻⁵ |

| Table 70 - Adsorption of TCNQ in dioxan on 10 % Dy ₂ O ₃ /Al ₂ O ₃ activated at 500°C | | |
|---|---|--|
| Initial concentration mol.dm ⁻³ | Equilibrium concentration mol.dm ⁻³ | Adsorbed amount mol.m ⁻² |
| 9.4814 x 10 ⁻⁴ | 2.2893 x 10 ⁻⁷ | 8.7744 x 10 ⁻⁶ |
| 1.8963 x 10 ⁻³ | 4.0540 x 10 ⁻⁵ | 1.7175 x 10 ⁻⁵ |
| 2.8444 x 10 ⁻³ | 2.5754 x 10 ⁻⁴ | 2.3946 x 10 ⁻⁵ |
| 4.7406 x 10 ⁻³ | 1.4880 x 10 ⁻³ | 3.0109 x 10 ⁻⁵ |
| 6.4672 x 10 ⁻³ | 2.2034 x 10 ⁻³ | 3.9343 x 10 ⁻⁵ |
| 9.2391 x 10 ⁻³ | 4.3115 x 10 ⁻³ | 4.5395 x 10 ⁻⁵ |

| Table 71 - Adsorption of chloranil in acetonitrile on 10 % Dy ₂ O ₃ /Al ₂ O ₃ activated at 500°C | | |
|--|---|--|
| Initial concentration mol.dm ⁻³ | Equilibrium concentration mol.dm ⁻³ | Adsorbed amount mol.m ⁻² |
| 2.6175 x 10 ⁻⁴ | 5.7633 x 10 ⁻⁷ | 2.4133 x 10 ⁻⁶ |
| 1.3088 x 10 ⁻³ | 4.0201 x 10 ⁻⁵ | 1.1736 x 10 ⁻⁵ |
| 2.6175 x 10 ⁻³ | 7.4683 x 10 ⁻⁴ | 1.7299 x 10 ⁻⁵ |
| 5.2351 x 10 ⁻³ | 2.7977 x 10 ⁻³ | 2.2535 x 10 ⁻⁵ |
| 8.5070 x 10 ⁻³ | 5.6143 x 10 ⁻³ | 2.6777 x 10 ⁻⁵ |
| 1.3088 x 10 ⁻² | 1.0014 x 10 ⁻² | 2.8397 x 10 ⁻⁵ |

| Table 72 - Adsorption of chloranil in dioxan on 10% Dy ₂ O ₃ /Al ₂ O ₃ activated at 500°C | | |
|---|---|--|
| Initial concentration mol.dm ⁻³ | Equilibrium concentration mol.dm ⁻³ | Adsorbed amount mol.m ⁻² |
| 1.2754 x 10 ⁻⁴ | 9.3485 x 10 ⁻⁷ | 1.1699 x 10 ⁻⁶ |
| 6.3771 x 10 ⁻⁴ | 2.8380 x 10 ⁻⁵ | 5.6392 x 10 ⁻⁶ |
| 1.2754 x 10 ⁻³ | 3.2252 x 10 ⁻⁴ | 8.8151 x 10 ⁻⁶ |
| 2.5508 x 10 ⁻³ | 1.2938 x 10 ⁻³ | 1.1629 x 10 ⁻⁵ |
| 4.0813 x 10 ⁻³ | 2.6243 x 10 ⁻³ | 1.3479 x 10 ⁻⁵ |
| 6.3771 x 10 ⁻³ | 4.7411 x 10 ⁻³ | 1.5141 x 10 ⁻⁵ |

| Table 73 - Adsorption of TCNQ in acetonitrile on 20% Dy ₂ O ₃ /Al ₂ O ₃ activated at 500°C | | |
|--|---|--|
| Initial concentration mol.dm ⁻³ | Equilibrium concentration mol.dm ⁻³ | Adsorbed amount mol.m ⁻² |
| 4.7407 x 10 ⁻⁴ | 1.9077 x 10 ⁻⁸ | 4.8252 x 10 ⁻⁶ |
| 9.4814 x 10 ⁻⁴ | 2.2893 x 10 ⁻⁷ | 9.6523 x 10 ⁻⁶ |
| 1.8963 x 10 ⁻³ | 4.0540 x 10 ⁻⁵ | 1.8893 x 10 ⁻⁵ |
| 4.8519 x 10 ⁻³ | 4.0630 x 10 ⁻⁴ | 4.5214 x 10 ⁻⁵ |
| 7.7312 x 10 ⁻³ | 1.9672 x 10 ⁻³ | 5.8668 x 10 ⁻⁵ |
| 1.1891 x 10 ⁻² | 5.6069 x 10 ⁻³ | 6.3861 x 10 ⁻⁵ |

| Table 74 - Adsorption of TCNQ in dioxan on 20% Dy ₂ O ₃ /Al ₂ O ₃ activated at 500°C | | |
|--|---|--|
| Initial concentration mol.dm ⁻³ | Equilibrium concentration mol.dm ⁻³ | Adsorbed amount mol.m ⁻² |
| 2.2714 x 10 ⁻⁴ | 9.7485 x 10 ⁻⁸ | 2.3147 x 10 ⁻⁶ |
| 2.2714 x 10 ⁻³ | 8.5787 x 10 ⁻⁵ | 2.2233 x 10 ⁻⁵ |
| 4.5428 x 10 ⁻³ | 1.1825 x 10 ⁻³ | 3.1469 x 10 ⁻⁵ |
| 7.9499 x 10 ⁻³ | 4.4551 x 10 ⁻³ | 3.5552 x 10 ⁻⁵ |
| 1.1415 x 10 ⁻² | 6.3947 x 10 ⁻³ | 5.1056 x 10 ⁻⁵ |
| 1.4267 x 10 ⁻² | 8.8309 x 10 ⁻³ | 5.5354 x 10 ⁻⁵ |

| Table 75 - Adsorption of chloranil in acetonitrile on 20 % Dy ₂ O ₃ /Al ₂ O ₃ activated at 500°C | | |
|--|---|--|
| Initial concentration mol.dm ⁻³ | Equilibrium concentration mol.dm ⁻³ | Adsorbed amount mol.m ⁻² |
| 2.8193 x 10 ⁻¹ | 1.0105 x 10 ⁻¹ | 2.8555 x 10 ⁻⁶ |
| 1.4096 x 10 ⁻³ | 1.5168 x 10 ⁻⁵ | 1.4159 x 10 ⁻⁵ |
| 2.8193 x 10 ⁻³ | 8.0645 x 10 ⁻⁴ | 2.0484 x 10 ⁻⁵ |
| 5.6385 x 10 ⁻³ | 3.2611 x 10 ⁻³ | 2.4159 x 10 ⁻⁵ |
| 7.8939 x 10 ⁻³ | 4.9685 x 10 ⁻³ | 2.9788 x 10 ⁻⁵ |
| 1.4096 x 10 ⁻² | 1.0950 x 10 ⁻² | 3.2035 x 10 ⁻⁵ |

| Table 76 - Adsorption of chloranil in dioxan on 20 % Dy ₂ O ₃ /Al ₂ O ₃ activated at 500°C | | |
|--|---|--|
| Initial concentration mol.dm ⁻³ | Equilibrium concentration mol.dm ⁻³ | Adsorbed amount mol.m ⁻² |
| 1.2754 x 10 ⁻¹ | 9.3485 x 10 ⁻⁷ | 1.2869 x 10 ⁻⁶ |
| 6.3771 x 10 ⁻¹ | 2.8380 x 10 ⁻⁵ | 6.2034 x 10 ⁻⁶ |
| 1.2754 x 10 ⁻³ | 3.2252 x 10 ⁻⁴ | 9.6971 x 10 ⁻⁶ |
| 2.5508 x 10 ⁻³ | 1.2938 x 10 ⁻³ | 1.2793 x 10 ⁻⁵ |
| 4.0813 x 10 ⁻³ | 2.6243 x 10 ⁻³ | 1.4828 x 10 ⁻⁵ |
| 6.3771 x 10 ⁻³ | 4.7411 x 10 ⁻³ | 1.6656 x 10 ⁻⁵ |

| Table 77 - Adsorption of TCNQ in acetonitrile on 45% Dy ₂ O ₃ /Al ₂ O ₃ activated at 500°C | | |
|--|---|--|
| Initial concentration mol.dm ⁻³ | Equilibrium concentration mol.dm ⁻³ | Adsorbed amount mol.m ⁻² |
| 2.0794 x 10 ⁻⁴ | 3.1013 x 10 ⁻⁸ | 2.7485 x 10 ⁻⁶ |
| 1.0397 x 10 ⁻³ | 3.7209 x 10 ⁻⁷ | 1.3737 x 10 ⁻⁵ |
| 2.0794 x 10 ⁻³ | 1.4883 x 10 ⁻⁶ | 2.7485 x 10 ⁻⁵ |
| 4.1589 x 10 ⁻³ | 4.8837 x 10 ⁻⁵ | 5.4301 x 10 ⁻⁵ |
| 8.3177 x 10 ⁻³ | 1.4980 x 10 ⁻³ | 9.0147 x 10 ⁻⁵ |
| 1.0397 x 10 ⁻² | 2.8875 x 10 ⁻³ | 9.2173 x 10 ⁻⁵ |

| Table 78 - Adsorption of TCNQ in dioxan on 45 % Dy ₂ O ₃ /Al ₂ O ₃ activated at 500°C | | |
|---|---|--|
| Initial concentration mol.dm ⁻³ | Equilibrium concentration mol.dm ⁻³ | Adsorbed amount mol.m ⁻² |
| 2.0324 x 10 ⁻⁴ | 9.7244 x 10 ⁻⁸ | 2.6823 x 10 ⁻⁶ |
| 1.0162 x 10 ⁻³ | 3.1896 x 10 ⁻⁶ | 1.3386 x 10 ⁻⁵ |
| 2.0324 x 10 ⁻³ | 8.5574 x 10 ⁻⁵ | 2.5746 x 10 ⁻⁵ |
| 4.0648 x 10 ⁻³ | 6.0291 x 10 ⁻⁴ | 4.5755 x 10 ⁻⁵ |
| 8.1297 x 10 ⁻³ | 3.3501 x 10 ⁻³ | 6.3209 x 10 ⁻⁵ |
| 1.0162 x 10 ⁻² | 4.8914 x 10 ⁻³ | 6.9702 x 10 ⁻⁵ |

| Table 79 - Adsorption of chloronil in acetonitrile on 45 % Dy₂O₃/Al₂O₃ activated at 500°C | | |
|--|--|---|
| Initial concentration mol.dm⁻³ | Equilibrium concentration mol.dm⁻³ | Adsorbed amount mol.m⁻² |
| 2.6094 x 10 ⁻⁴ | 6.3052 x 10 ⁻⁷ | 3.4357 x 10 ⁻⁶ |
| 1.3047 x 10 ⁻³ | 3.9228 x 10 ⁻⁶ | 1.7196 x 10 ⁻⁵ |
| 2.6094 x 10 ⁻³ | 2.1802 x 10 ⁻⁴ | 3.1639 x 10 ⁻⁵ |
| 5.2188 x 10 ⁻³ | 2.0100 x 10 ⁻³ | 4.2385 x 10 ⁻⁵ |
| 9.1329 x 10 ⁻³ | 5.3399 x 10 ⁻³ | 5.0071 x 10 ⁻⁵ |
| 1.3047 x 10 ⁻² | 8.7907 x 10 ⁻³ | 5.6177 x 10 ⁻⁵ |

| Table 80 - Adsorption of chloronil in dioxan on 45 % Dy₂O₃/Al₂O₃ activated at 500°C | | |
|--|--|---|
| Initial concentration mol.dm⁻³ | Equilibrium concentration mol.dm⁻³ | Adsorbed amount mol.m⁻² |
| 2.6289 x 10 ⁻⁴ | 2.9342 x 10 ⁻⁶ | 3.4379 x 10 ⁻⁶ |
| 1.3145 x 10 ⁻³ | 4.8910 x 10 ⁻⁵ | 1.6721 x 10 ⁻⁵ |
| 2.6289 x 10 ⁻³ | 6.5146 x 10 ⁻⁴ | 2.6136 x 10 ⁻⁵ |
| 5.2578 x 10 ⁻³ | 2.6411 x 10 ⁻³ | 3.4576 x 10 ⁻⁵ |
| 1.0516 x 10 ⁻² | 7.5988 x 10 ⁻³ | 3.8557 x 10 ⁻⁵ |
| 1.3145 x 10 ⁻² | 9.8781 x 10 ⁻³ | 4.3091 x 10 ⁻⁵ |

| Table 81 - Adsorption of TCNQ in acetonitrile on 60 % Dy₂O₃/Al₂O₃ activated at 500°C | | |
|---|--|---|
| Initial concentration mol.dm⁻³ | Equilibrium concentration mol.dm⁻³ | Adsorbed amount mol.m⁻² |
| 2.0843 x 10 ⁻⁴ | 1.2374 x 10 ⁻⁷ | 2.6006 x 10 ⁻⁶ |
| 1.0422 x 10 ⁻³ | 3.4030 x 10 ⁻⁷ | 9.2650 x 10 ⁻⁶ |
| 2.0843 x 10 ⁻³ | 9.5901 x 10 ⁻⁷ | 1.8542 x 10 ⁻⁵ |
| 4.1687 x 10 ⁻³ | 1.0828 x 10 ⁻⁵ | 3.7021 x 10 ⁻⁵ |
| 8.3373 x 10 ⁻³ | 7.073 x 10 ⁻⁴ | 6.7937 x 10 ⁻⁵ |
| 1.0422 x 10 ⁻² | 2.5145 x 10 ⁻³ | 7.0408 x 10 ⁻⁵ |

| Table 82 - Adsorption of TCNQ in dioxan on 60 % Dy₂O₃/Al₂O₃ activated at 500°C | | |
|---|--|---|
| Initial concentration mol.dm⁻³ | Equilibrium concentration mol.dm⁻³ | Adsorbed amount mol.m⁻² |
| 1.1768 x 10 ⁻³ | 4.0706 x 10 ⁻⁵ | 1.0464 x 10 ⁻⁵ |
| 2.3537 x 10 ⁻³ | 1.1705 x 10 ⁻⁴ | 1.9863 x 10 ⁻⁵ |
| 4.7074 x 10 ⁻³ | 1.3459 x 10 ⁻³ | 2.9918 x 10 ⁻⁵ |
| 9.4148 x 10 ⁻³ | 5.7692 x 10 ⁻³ | 3.2421 x 10 ⁻⁵ |
| 1.1768 x 10 ⁻² | 7.9265 x 10 ⁻³ | 3.4172 x 10 ⁻⁵ |

| Table 83 - Adsorption of chloronil in acetonitrile on 60 % Dy ₂ O ₃ /Al ₂ O ₃ activated at 500°C | | |
|---|---|--|
| Initial concentration mol.dm ⁻³ | Equilibrium concentration mol.dm ⁻³ | Adsorbed amount mol.m ⁻² |
| 2.6240 x 10 ⁻⁴ | 4.9509 x 10 ⁻⁷ | 2.3241 x 10 ⁻⁶ |
| 1.3120 x 10 ⁻³ | 7.8423 x 10 ⁻⁵ | 1.0979 x 10 ⁻⁵ |
| 2.6240 x 10 ⁻³ | 9.0107 x 10 ⁻⁴ | 1.5338 x 10 ⁻⁵ |
| 5.2481 x 10 ⁻³ | 3.0885 x 10 ⁻³ | 1.9213 x 10 ⁻⁵ |
| 7.8721 x 10 ⁻³ | 5.5763 x 10 ⁻³ | 2.0433 x 10 ⁻⁵ |
| 1.3120 x 10 ⁻² | 1.0446 x 10 ⁻² | 2.3799 x 10 ⁻⁵ |

| Table 84 - Adsorption of chloronil in dioxan on 60 % Dy ₂ O ₃ /Al ₂ O ₃ activated at 500°C | | |
|---|---|--|
| Initial concentration mol.dm ⁻³ | Equilibrium concentration mol.dm ⁻³ | Adsorbed amount mol.m ⁻² |
| 2.7932 x 10 ⁻⁴ | 8.2113 x 10 ⁻⁶ | 2.4134 x 10 ⁻⁶ |
| 1.3966 x 10 ⁻³ | 1.6510 x 10 ⁻⁴ | 1.0941 x 10 ⁻⁵ |
| 2.7932 x 10 ⁻³ | 1.1896 x 10 ⁻³ | 1.4255 x 10 ⁻⁵ |
| 5.5863 x 10 ⁻³ | 3.5504 x 10 ⁻³ | 1.8107 x 10 ⁻⁵ |
| 1.1173 x 10 ⁻² | 8.6995 x 10 ⁻³ | 2.2020 x 10 ⁻⁵ |
| 1.3966 x 10 ⁻² | 1.1343 x 10 ⁻² | 2.4242 x 10 ⁻⁵ |

| Table 85 - Adsorption of TCNQ in acetonitrile on 75% Dy ₂ O ₃ /Al ₂ O ₃ activated at 500°C | | |
|--|---|--|
| Initial concentration mol.dm ⁻³ | Equilibrium concentration mol.dm ⁻³ | Adsorbed amount mol.m ⁻² |
| 8.3550 x 10 ⁻⁵ | 1.0831 x 10 ⁻⁷ | 1.8852 x 10 ⁻⁶ |
| 4.1775 x 10 ⁻⁴ | 1.0985 x 10 ⁻⁶ | 9.4174 x 10 ⁻⁶ |
| 8.3550 x 10 ⁻⁴ | 3.8681 x 10 ⁻⁶ | 1.8797 x 10 ⁻⁵ |
| 1.6710 x 10 ⁻³ | 9.6701 x 10 ⁻⁶ | 3.7542 x 10 ⁻⁵ |
| 2.9242 x 10 ⁻³ | 1.9339 x 10 ⁻⁴ | 6.1711 x 10 ⁻⁵ |
| 4.1775 x 10 ⁻³ | 1.0289 x 10 ⁻³ | 7.1223 x 10 ⁻⁵ |

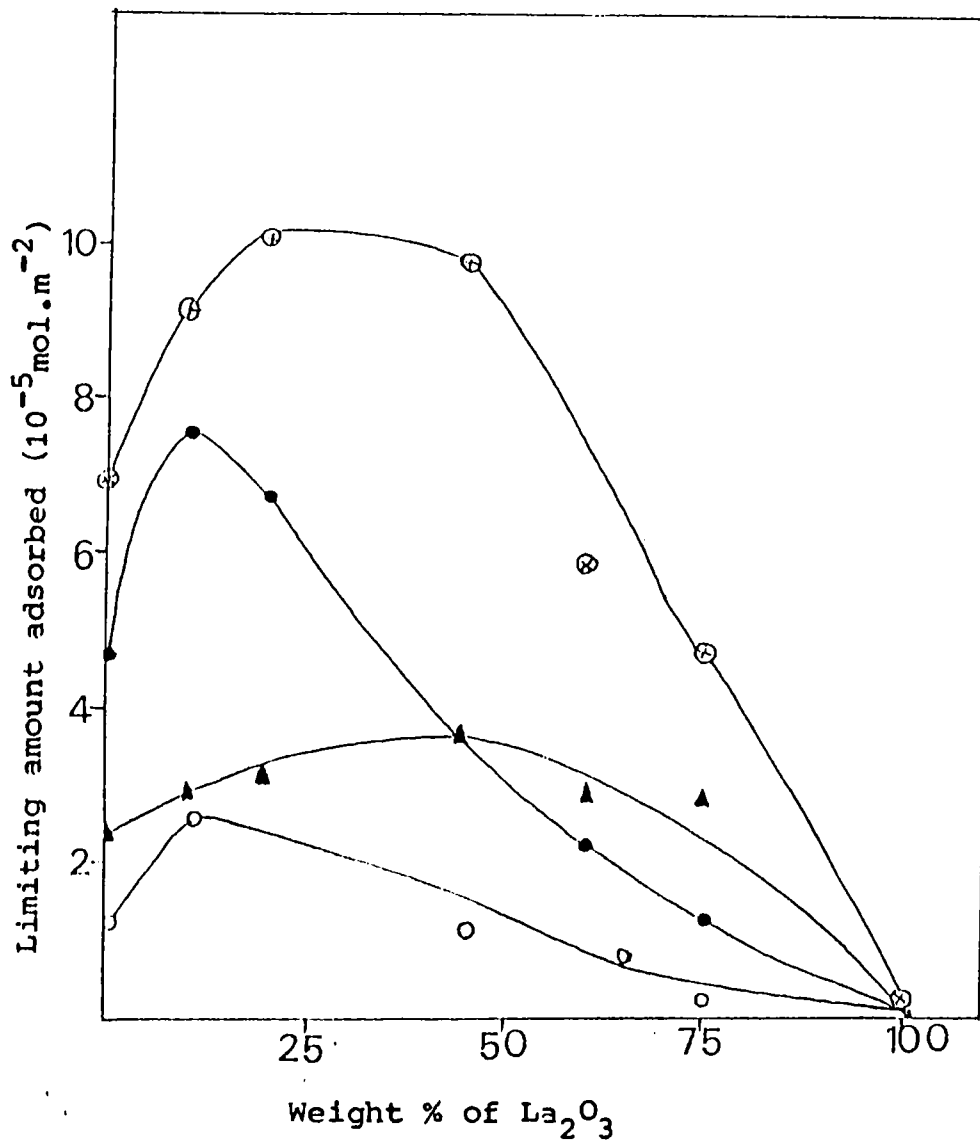
| Table 86 - Adsorption of TCNQ in dioxan on 75 % Dy ₂ O ₃ /Al ₂ O ₃ activated at 500°C | | |
|---|---|--|
| Initial concentration mol.dm ⁻³ | Equilibrium concentration mol.dm ⁻³ | Adsorbed amount mol.m ⁻² |
| 4.9366 x 10 ⁻⁵ | 3.1913 x 10 ⁻⁷ | 1.1077 x 10 ⁻⁶ |
| 2.4683 x 10 ⁻⁴ | 6.1832 x 10 ⁻⁷ | 5.5617 x 10 ⁻⁶ |
| 4.9366 x 10 ⁻⁴ | 5.3255 x 10 ⁻⁶ | 1.1053 x 10 ⁻⁵ |
| 9.8732 x 10 ⁻⁴ | 3.2507 x 10 ⁻⁴ | 1.4975 x 10 ⁻⁵ |
| 1.9746 x 10 ⁻³ | 5.3105 x 10 ⁻⁴ | 3.2575 x 10 ⁻⁵ |
| 2.4683 x 10 ⁻³ | 8.5269 x 10 ⁻⁴ | 3.6436 x 10 ⁻⁵ |

| Table 87 - Adsorption of chloranil in acetonitrile on 75 % Dy ₂ O ₃ /Al ₂ O ₃ activated at 500°C | | |
|--|---|--|
| Initial concentration mol.dm ⁻³ | Equilibrium concentration mol.dm ⁻³ | Adsorbed amount mol.m ⁻² |
| 7.0685 x 10 ⁻⁵ | 1.4977 x 10 ⁻⁶ | 1.5638 x 10 ⁻⁶ |
| 3.5342 x 10 ⁻⁴ | 2.6097 x 10 ⁻⁶ | 7.9134 x 10 ⁻⁶ |
| 7.0685 x 10 ⁻⁴ | 4.7107 x 10 ⁻⁵ | 1.4906 x 10 ⁻⁵ |
| 1.4137 x 10 ⁻³ | 2.1145 x 10 ⁻⁴ | 2.7152 x 10 ⁻⁵ |
| 2.4739 x 10 ⁻³ | 1.2193 x 10 ⁻³ | 2.8369 x 10 ⁻⁵ |
| 3.5342 x 10 ⁻³ | 2.2714 x 10 ⁻³ | 2.8530 x 10 ⁻⁵ |

| Table 88 - Adsorption of chloranil on 75 % Dy ₂ O ₃ /Al ₂ O ₃ activated at 500°C | | |
|--|---|--|
| Initial concentration mol.dm ⁻³ | Equilibrium concentration mol.dm ⁻³ | Adsorbed amount mol.m ⁻² |
| 1.0493 x 10 ⁻⁴ | 1.8103 x 10 ⁻⁶ | 2.3293 x 10 ⁻⁶ |
| 2.0986 x 10 ⁻⁴ | 1.1833 x 10 ⁻⁵ | 4.4750 x 10 ⁻⁶ |
| 4.1972 x 10 ⁻⁴ | 2.7146 x 10 ⁻⁵ | 8.8731 x 10 ⁻⁶ |
| 8.3943 x 10 ⁻⁴ | 2.6171 x 10 ⁻⁴ | 1.3050 x 10 ⁻⁵ |
| 1.0493 x 10 ⁻³ | 3.4443 x 10 ⁻⁴ | 1.5938 x 10 ⁻⁵ |
| 1.3966 x 10 ⁻³ | 6.7000 x 10 ⁻⁴ | 1.6430 x 10 ⁻⁵ |

Fig. 15&16 show the increase in limiting amount of electron acceptor adsorbed as a function of the composition of the mixed oxides. Surface hydroxyls may exist on all the oxides. However, surface hydroxyls on metal oxides are shown to differ in their chemical properties and the difference in acidity among the hydroxyl groups of several oxide surfaces have been reported [20]. These results suggest that the hydroxyl ions on the metal oxide surfaces have different electron donor properties. In the mixed oxides $\text{La}_2\text{O}_3/\text{Al}_2\text{O}_3$ & $\text{Dy}_2\text{O}_3/\text{Al}_2\text{O}_3$ the limiting amount of the electron acceptors adsorbed increases with increase in percentage of La_2O_3 or Dy_2O_3 as a consequence of the increase in concentration of Al-O-La or Al-O-Dy bonds. Further addition of rare earth oxides decrease the limiting amount without changing the limit of electron transfer may be due to the increase in concentration of rare earth oxide in the mixed oxide lattice because rare earth oxides have lower electron donocity than Al_2O_3 . The surface electron properties of alumina are promoted by the rare earth oxides in the mixed oxides without changing the limit of electron transfer.

The concentration and strength of acidic and basic sites on the surface of these mixed oxides were measured by titration method using Hammett indicators. Data are given in Tables 89 & 90. H_0, max values obtained from Fig.17 & 18 parallel the electron donating properties of the mixed oxides.



Electron acceptor/Solvent
 Δ CA/AN \odot TC/AN \circ CA/D \bullet TC/D

Fig.15 Limiting amount of electron acceptors adsorbed as a function of composition of La_2O_3 Al_2O_3

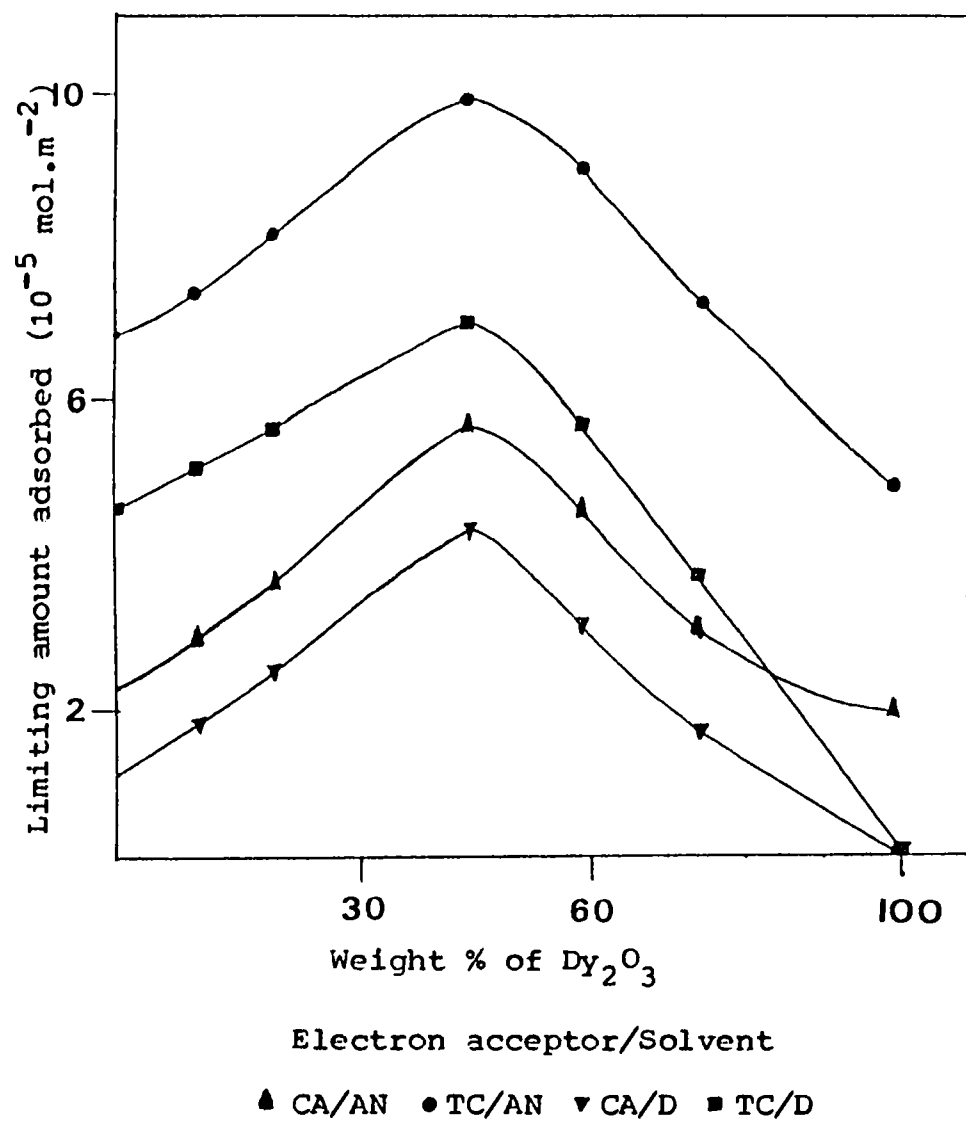


Fig.16 Limiting amount of electron acceptors adsorbed as a function of composition of Dy_2O_3 Al_2O_3

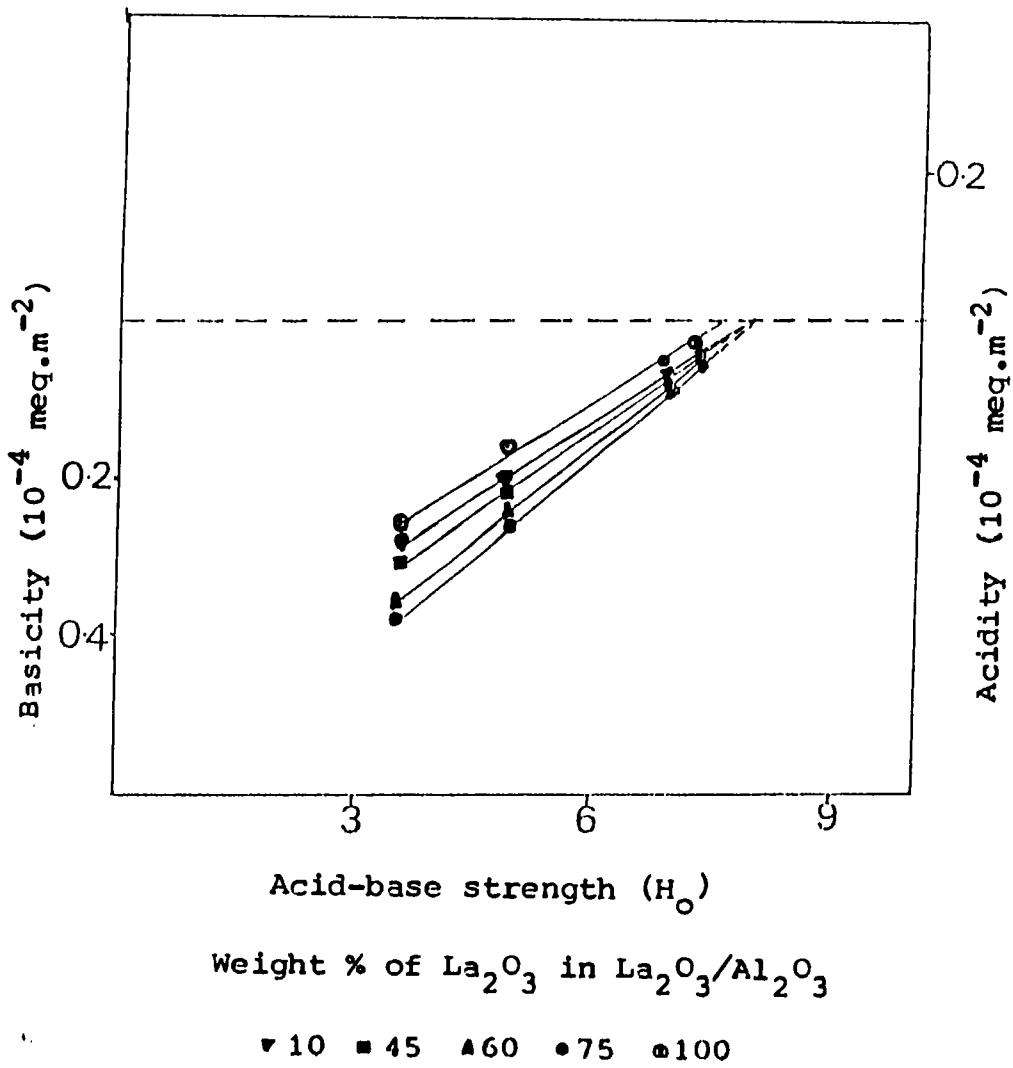


Fig.17 Acid-base strength distribution of $\text{La}_2\text{O}_3/\text{Al}_2\text{O}_3$

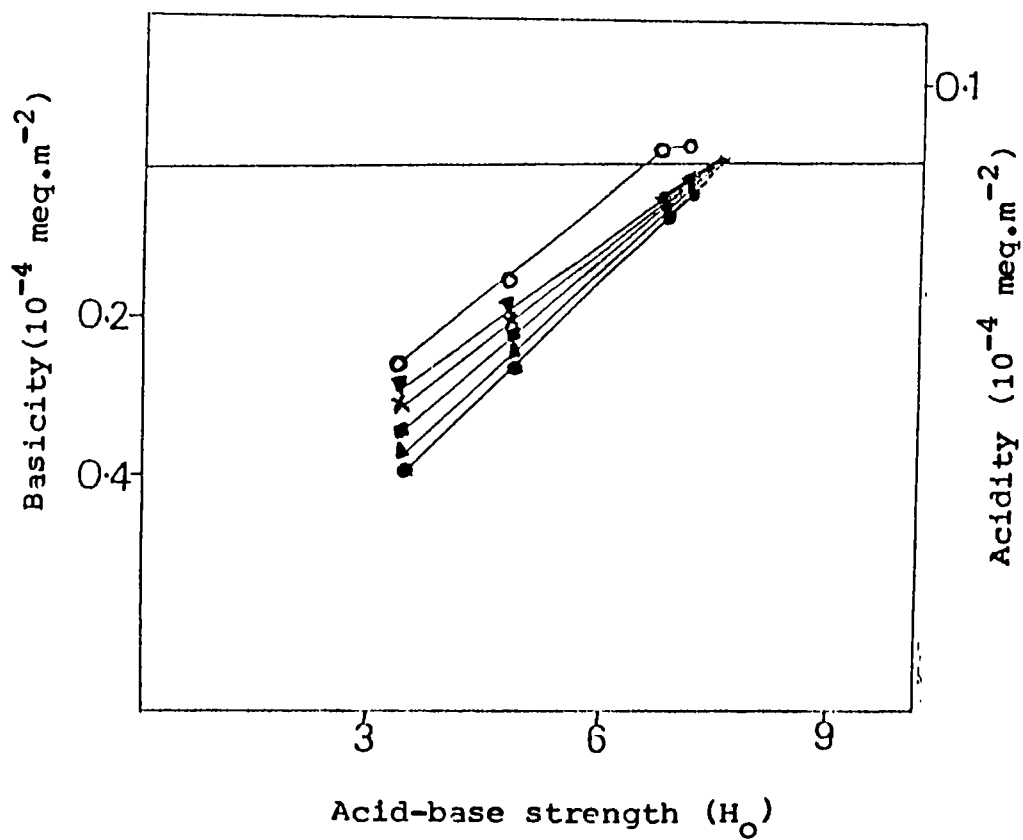


Fig.18 Acid-base strength distribution of Dy_2O_3/Al_2O_3

| Table 89 - Basicity and Ho,max. of La ₂ O ₃ and its mixed oxides | | | | | |
|---|---|-------------|-------------|-------------|---------|
| % by wt. of La ₂ O ₃ in La ₂ O ₃ /Al ₂ O ₃ | Basicity (10 ⁻⁴ meq. m ⁻²) | | | | Ho,max. |
| | Ho ≥ 3.3 | Ho ≥ 4.8 | Ho ≥ 6.8 | Ho ≥ 7.2 | |
| 0 | 0.38 | 0.25 | 0.07 | 0.05 | 7.5 |
| 10 | 0.38 | 0.25 | 0.07 | 0.05 | 7.5 |
| 20 | 0.36 | 0.24 | 0.07 | 0.05 | 7.8 |
| 45 | 0.30 | 0.21 | 0.07 | 0.05 | 7.8 |
| 60 | 0.29 | 0.20 | 0.07 | 0.05 | 7.8 |
| 75 | 0.27 | 0.20 | 0.07 | 0.05 | 7.4 |
| 100 | 0.26 | 0.15 | 0.07 | 0.05 | 7.2 |

| Table 90 - Basicity and Ho,max of Dy ₂ O ₃ and its mixed oxides | | | | | |
|---|---|-------------|-------------|-------------|---------|
| % by wt. of Dy ₂ O ₃ in Dy ₂ O ₃ /Al ₂ O ₃ | Basicity (10 ⁻⁴ meq. m ⁻²) | | | | Ho,max. |
| | Ho ≥ 3.3 | Ho ≥ 4.8 | Ho ≥ 6.8 | Ho ≥ 7.2 | |
| 0 | 0.38 | 0.25 | 0.07 | 0.05 | 7.5 |
| 10 | 0.36 | 0.23 | 0.07 | 0.05 | 7.6 |
| 20 | 0.33 | 0.21 | 0.07 | 0.05 | 7.8 |
| 45 | 0.32 | 0.21 | 0.07 | 0.05 | 7.8 |
| 60 | 0.29 | 0.20 | 0.07 | 0.05 | 7.8 |
| 75 | 0.27 | 0.18 | 0.07 | 0.05 | 7.2 |
| 100 | 0.25 | 0.15 | ---- | ---- | 6.5 |

CATALYTIC ACTIVITY

In an attempt to correlate the electron donating properties of rare earth oxides with their catalytic activities, the reduction of cyclohexanone with 2-propanol using La_2O_3 and Dy_2O_3 activated at 300, 500 and 800°C and its mixed oxides with alumina as catalyst have been studied.

The reduction of multiple bonds using an organic molecule as a hydrogen donor in place of hydrogen gas or metal hydride is known as hydrogen transfer reaction [21]. One example is the reduction of aldehydes and ketones with metal alkoxide and alcohol. This is called the Meerwein-Ponndorf-Verley reduction. It was discovered in 1925 and has been used successfully in a number of instances [22]. Aluminum isopropoxide has been found to be the best reagent for this reduction. However, this method calls for both addition of at least 100 to 200 % excess aluminum isopropoxide and the neutralisation of alkoxide salt with strong acid. As other catalysts for this reduction, complexes of cobalt, iridium, rhodium, ruthenium, indium, molybdenum and zirconium have been reported [23-29]. Although these catalysts have many advantages over conventional metal alkoxides, the isolation of products is always attended by tedious workup.

Heterogeneous methods for the reduction are known, and zeolites and oxides of aluminum, magnesium, silicon, calcium, barium, strontium, zirconium, titanium, vanadium, molybdenum, zinc and thorium have been reported to be successful catalysts [30-33]. These methods have several advantages in the isolation of products. However, they need to be carried out in the vapour phase, and require high reaction temperatures in flow reactor systems.

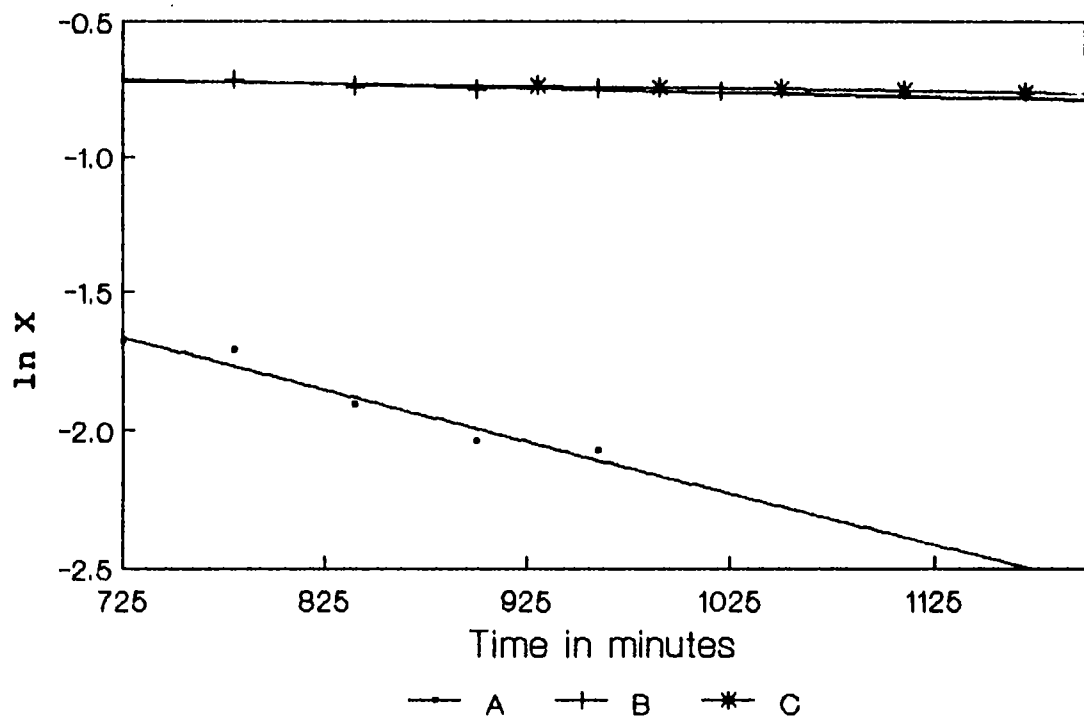
Posuer *et al* [34] reported that dried chromatographic alumina served as a catalyst in the liquid phase. Several aldehydes and ketones could be reduced by use of this catalyst and products were easily isolated by filtering of catalyst and subsequent evaporation of solvent. However, this reduction requires water free conditions. The reduction of aldehydes and ketones with 2-propanol proceeded efficiently over hydrous zirconium oxide in the liquid phase [35].

La_2O_3 activated between 300-800°C, Dy_2O_3 activated at 800°C and mixed oxides of lanthanum and dysprosium with aluminum has been found to be effective catalysts for the liquid phase reduction of cyclohexanone. The reaction was followed by product analysis by means of a gas chromatograph. No by-products were detected. The reaction showed a first order dependence on the concentration of ketone. The activity is reported as the first order rate coefficient for the formation of cyclohexanol per gram of the catalyst. Data are given in Tables 91-93 and in Fig.19 & 21.

| Table 91 - Catalytic activity of La_2O_3 activated at various temperatures for the reduction of cyclohexanone to cyclohexanol | |
|---|---|
| Activation Temperature (°C) | Rate Constant (10^5 s^{-1}) |
| 300 | 0.1476 |
| 500 | 0.3516 |
| 800 | 2.7295 |

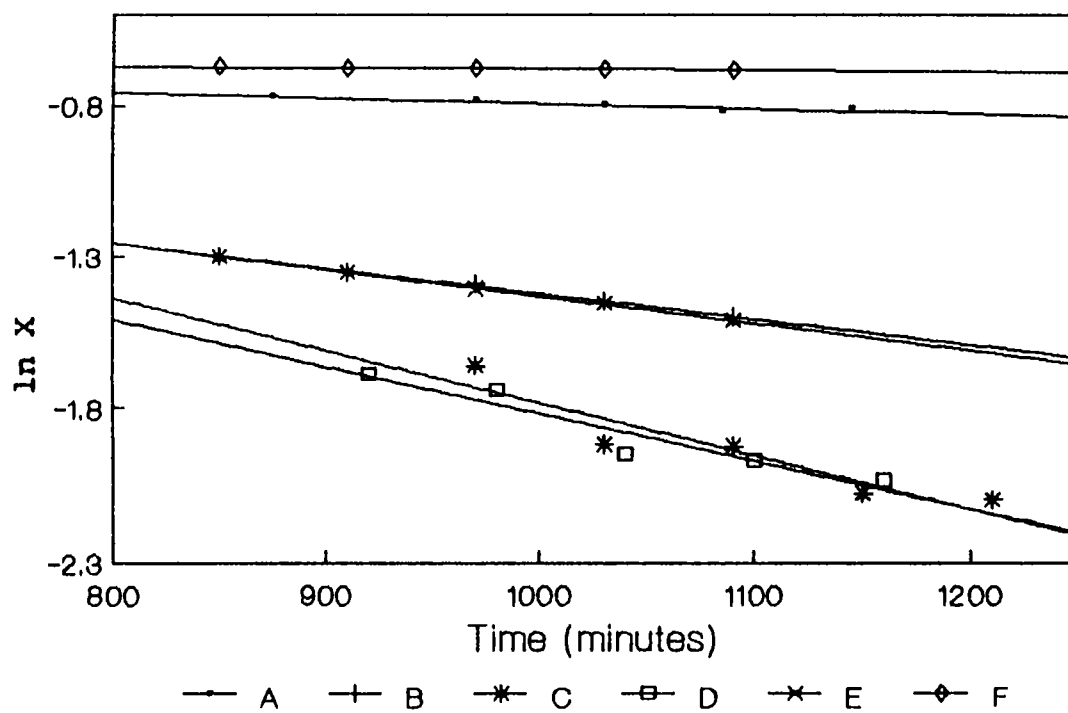
| Table 92 - Catalytic activity of $\text{La}_2\text{O}_3/\text{Al}_2\text{O}_3$ for various compositions activated at 500°C | |
|--|--|
| % by wt. of La_2O_3 in $\text{La}_2\text{O}_3/\text{Al}_2\text{O}_3$ | Rate Constant (10^{-5} s^{-1}) |
| 0 | 0.07531 |
| 10 | 0.0944 |
| 20 | 0.2328 |
| 45 | 0.5871 |
| 60 | 1.3725 |
| 75 | 0.3809 |
| 100 | 0.3516 |

| Table 93 - Catalytic activity of $\text{Dy}_2\text{O}_3/\text{Al}_2\text{O}_3$ for various compositions activated at 500°C | |
|--|--|
| % by wt. of Dy_2O_3 in $\text{Dy}_2\text{O}_3/\text{Al}_2\text{O}_3$ | Rate Constant (10^{-5} s^{-1}) |
| 0 | 0.0753 |
| 10 | 0.2412 |
| 20 | 1.3534 |
| 45 | 2.2122 |
| 60 | 2.1441 |
| 75 | 0.3516 |
| 100 | 0 |



A La_2O_3 (300°C) B La_2O_3 (500°C) C La_2O_3 (800°C)
 X Concentration of ketone

Fig.19 Kinetics of reduction of cyclohexanone on La_2O_3 catalyst activated at different temperatures

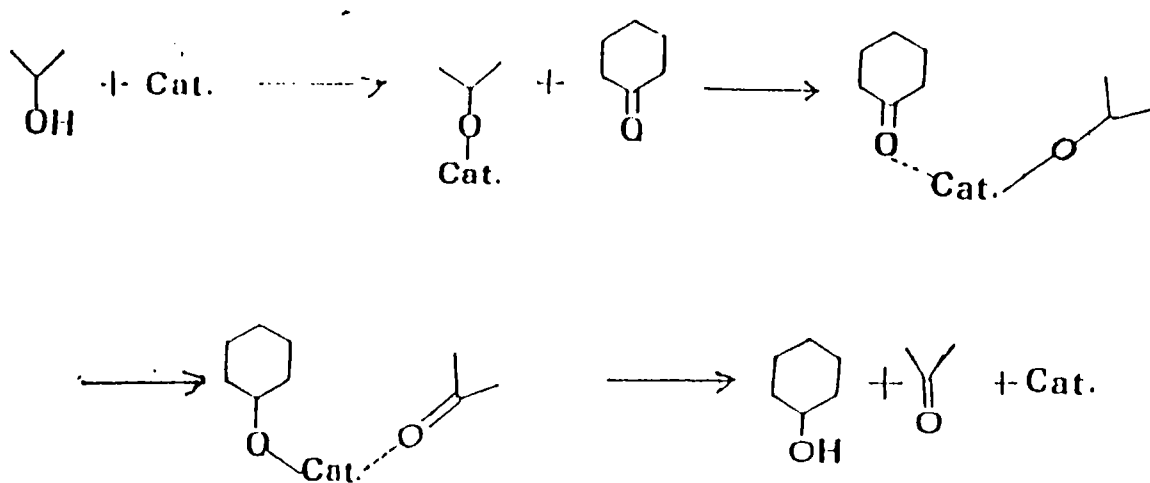


| | | | |
|---|---|---|---|
| A | 10% $\text{La}_2\text{O}_3/\text{Al}_2\text{O}_3$ | D | 60% $\text{La}_2\text{O}_3/\text{Al}_2\text{O}_3$ |
| B | 20% $\text{La}_2\text{O}_3/\text{Al}_2\text{O}_3$ | E | 75% $\text{La}_2\text{O}_3/\text{Al}_2\text{O}_3$ |
| C | 45% $\text{La}_2\text{O}_3/\text{Al}_2\text{O}_3$ | F | Al_2O_3 |

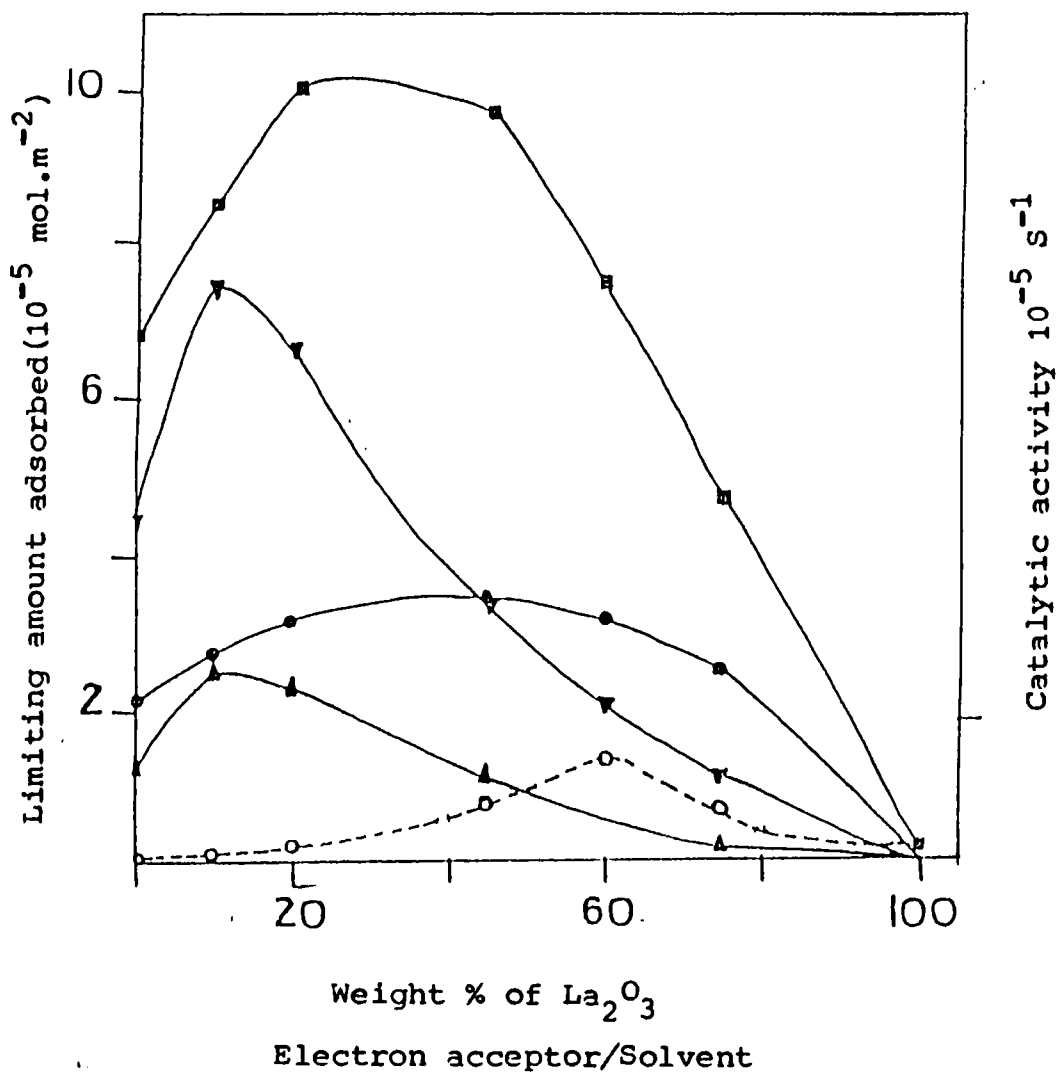
X Concentration of ketone

Fig. 20 Kinetics of reduction of cyclohexanone on $\text{La}_2\text{O}_3/\text{Al}_2\text{O}_3$ catalyst at different compositions.

An MPV type mechanism has been proposed. A similar mechanism has been proposed for the reduction of aldehydes and ketones with 2 - propanol over hydrous zirconium oxide from kinetic studies and kinetic isotopic effect studies [32].



The catalytic activity data can be correlated with the electron donating properties of the catalysts. The change in catalytic activity as a function of activation temperature and composition of the catalyst, (Fig.22 &24) can be understood in terms of the electron donocity of the oxide surface. A weak electron acceptor like PDNB (1.77 eV) can accept electrons from only strong electron donor sites whereas a strong electron acceptor like TCNQ (2.84 eV) can accept electrons from both weak and strong sites. The strength of an electron donor site can be expressed in terms of the electron affinity of the acceptor which can form anion radical on the adsorption site. Hence the limit of electron transfer of lanthana, dysprosia and its mixed oxides with alumina is between 2.40 and 1.77 eV. The change in catalytic activity of these oxides as a function of activation temperature and composition is comparable with the plots of limiting amount of chloranil adsorbed implying that all the electron donor sites available on the oxide surface are not effective in bringing out this reaction and those sites which can form chloranil anion radicals (2.40 eV) are effective in catalysing this reaction. Information on the base-strength distribution of catalyst surfaces will be essentially important for quantitative investigation of solid-base catalysts.

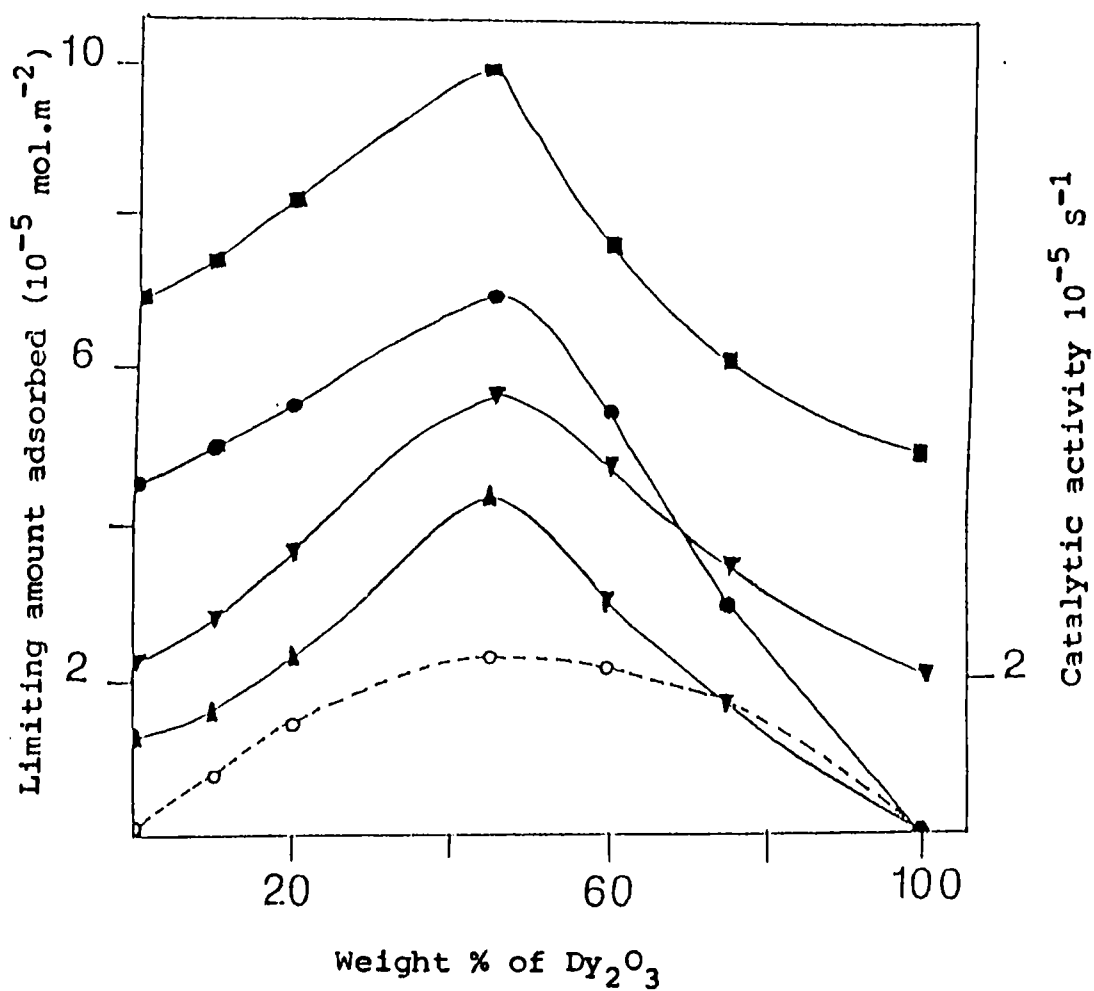


(CA - Chloranil; AN - acetonitrile; D-1,4 dioxan; TC-TCNQ)

● CA/AN ▲ CA/D ■ TC/AN ▼ TC/D

○ Rate constant

Fig.23 Limiting amount of electron acceptors adsorbed and the catalytic activity vs. composition of $\text{La}_2\text{O}_3/\text{Al}_2\text{O}_3$.



Electron acceptor/Solvent

(CA - Chloranil; AN - acetonitrile; D-1,4 dioxan; TC - TCNQ)

▼ CA/AN ■ TC/AN ▲ CA/D ● TC/D

○ Rate constant

Fig.24 Limiting amount of electron acceptors adsorbed and the catalytic activity vs. composition of Dy_2O_3/Al_2O_3 .

REFERENCES

1. S.Sugunan, G.Devika Rani, K.B.Sherly, *React.Kinet. Catal.Lett.*, **43** 375 (1991)
2. S.Sugunan, G.Devika Rani, *J.Mat.Sci.Lett.*, **10** 887 (1991)
3. S.Sugunan, G.Devika Rani, *J.Mat.Sci.Lett.*, **11** 1269 (1992)
4. S.Sugunan, G.Devika Rani, *J.Mat.Sci.*, (in press)
5. S.Sugunan, G.Devika Rani, *Indian.J.Chem.* (in Press).
6. K.Meguro and K.Esumi, *J.Colloid Interface Sci.*, **59** 93 (1977).
7. A.J.Tench and R.L.Nelson, *Trans.Faraday Soc.*, **63** 2254 (1967).
8. R.H.Boyd and W.D.Philips, *J.Chem.Phys.*, **43** 2927 (1965)
9. R.G.Kepler,P.E.Bierstedt and R.E.Merrifield, *Phys.Rev.Lett.*, **5**,503 (1960).
10. D.B.Chesnut, H.Foster and W.D.Philips, *J.Chem.Phys.*,**34** 684 (1961)
11. M.P.Rosynek and D.T.Magnuson, *J.Catal.*, **46** 402 (1977)
12. V.M.Vedeneer,"Cleavage Energies of Chemical Bonds, Ionization Potentials and Electron Affinity" Handbook, Izd AN USSR (1960)
13. G.V.Fomin, L.A.Blyumenfeld and V.I.Sukhorukov,Proc. Acad.Sci., USSR **157** 819 (1964)
14. R.S.Drago, L.B.Parr and C.S.Chamberlain, *J.Am.Chem.Soc.*, **99** 3203 (1977)
15. R.S.Drago, G.E.Vogel and T.E.Needham, *J.Am.Chem.Soc.*, **93** 6014 (1971)
16. G.Briegleb, J.Czekalla and G.Reuss, *J.Phy.Chem.*, **30** 333 (1961)
17. G.Briegleb and J.Czekalla, *J.Electrochem.*, **58** 249 (1954)

18. T.Yamanaka and K.Tanabe, *J.Phys.Chem.*, **79** 2049 (1975)
19. T.Yamanaka and K.Tanabe, *J.Phys.Chem.*, **80** 1723 (1976)
20. M.L.Hair and W.Hertl, *J.Phys.Chem* **74** 91 (1970)
21. G.Brieger and T.J.Nestrick, *Chem.Rev.* **74** 567 (1974)
22. A.L.Wilds, *Org.React.*, **2** 178 (1944)
23. M.Onishi, M.Matsuda and K.Hiraki, *Chem.Lett.*, 1157 (1984)
24. F.Martinelli, G.Mestroni, A.Camus and G.Zassinovich, *J.Organomet.Chem.*, **220** 383 (1981)
25. E.Farnetti, F.Vinzi and G.Mestroni, *J.Mol.Catal.*, **24** 147 (1984)
26. J.Blum, S.Shtelzer, D.Albin and Y.Sasson, *J.Mol.Catal.*, **16** 167 (1982)
27. A.Miyamoto and Y.Ocino, *J.Catal.*, **43** 143 (1976)
28. T.Tatsumi, M.Shibagaki and H.Tominaga, *J.Mol.Catal.*, **13** 331 (1981)
29. Y.Ishil, T.Nakano, A.Inada, Y.Kishigani, K.Sakurai and M.Ogawa, *J.Org.Chem.*, **51** 240 (1986)
30. L.H.Klemm and D.R.Taylor, *J.Org.Chem.*, **35** 3216 (1970)
31. H.Niiyama and E.Echigoya, *Bull.Jpn.Petrol.Inst.*, **14** 83 (1972)
32. H.Niiyama and E.Echigoya, *Bull.Chem.Soc.Jpn.*, **45** 938 (1972)
33. C.L.Kibby and W.Keith Lall, *J.Catal.*, **31** 65 (1973)
34. G.H.Posuer, A.W.Runquist and M.J.Chapdelaine, *J.Org.Chem.*, **42** 1202 (1977)
35. H. Matsushita, S.Ishiguro, H.Ichinose, A.Izumi and S.Mizusaki, *Chem.Lett.*, **731** (1985)

CONCLUSION

The experimental investigations carried out to study the electron donor properties and catalytic activity of rare earth oxides revealed the following interesting results.

The amount of electron acceptors adsorbed on the rare earth oxide surface depend on the activation temperature of the oxide, basicity of the solvent and the electron affinity of the electron acceptors. The limiting amount of electron acceptors adsorbed on the oxide surface increases with increase in activation temperature of the oxide, increase in electron affinity of the electron acceptor and decrease in basicity of the solvent.

The limit of electron transfer from the electron donor site of lanthana and dysprosia is located between 1.77 and 2.40 eV in terms of the electron affinity of the acceptor.

In the case of mixed oxides with alumina, surface electron properties of alumina gets modified by the rare earth oxide without changing the limit of electron transfer.

For the paramagnetic oxide, dysprosia, the magnetic moment changes during adsorption indicating the extent of electron transfer from the oxide surface to the electron acceptor.

The basic sites were estimated by two methods, ie the adsorption and the titration method gave a similar tendency towards the basicity of the rare earth oxide.

La_2O_3 activated between 300-800°C, Dy_2O_3 activated at 800°C and mixed oxides of lanthanum and dysprosium with aluminum are effective catalysts for the liquid phase reduction of cyclohexanone. The reaction showed a first order dependence on the concentration of ketone. The change in catalytic activity of these oxides with temperature and composition implied that all the electron donor sites available on the oxide surface are not effective in bringing out this reaction and those sites which can form chloranil anion radicals (2.40 eV) are effective in catalysing this reaction.

For the paramagnetic oxide, dysprosia, the magnetic moment changes during adsorption indicating the extent of electron transfer from the oxide surface to the electron acceptor.

The basic sites were estimated by two methods, ie the adsorption and the titration method gave a similar tendency towards the basicity of the rare earth oxide.

La_2O_3 activated between 300-800°C, Dy_2O_3 activated at 800°C and mixed oxides of lanthanum and dysprosium with aluminum are effective catalysts for the liquid phase reduction of cyclohexanone. The reaction showed a first order dependence on the concentration of ketone. The change in catalytic activity of these oxides with temperature and composition implied that all the electron donor sites available on the oxide surface are not effective in bringing out this reaction and those sites which can form chloranil anion radicals (2.40 eV) are effective in catalysing this reaction.

- G 5364 -

LIST OF PAPERS ACCEPTED/COMMUNICATED FOR PUBLICATION

1. Basicity and electron donor properties of lanthanum oxide and its mixed oxides with alumina.
S.Sugunan and K.B.Sherly, Indian Journal of Chemistry (in press).
2. The surface electron donor properties of Dy_2O_3 , Y_2O_3 and their mixed oxides with alumina catalyst.
S. Sugunan, K.B.Sherly and G.Devika Rani, Reaction Kinetics and Catalysis Letters (in press).
3. Dy_2O_3 as a catalyst for a Meerwein-Ponndorf Verley reaction.
S.Sugunan and K.B.Sherly, Reaction Kinetics and Catalysis Letters (in press).
4. Electron donor properties and catalytic activity of dysprosium oxide.
S.Sugunan and K.B.Sherly, 20th Rare Earth Research Conference, Monterey, USA, September 12-17, 1993.
5. Catalytic activity of La_2O_3 for the reduction of a ketone.
S.Sugunan and K.B. Sherly, Communicated to Catalysis Letters.